Hydrophobic core/shell particles via miniemulsion polymerization

By

Hussein Mohamed Etmimi

Thesis presented in partial fulfilment of the requirement for the degree of

Master of Science (Polymer Science)

at the

University of Stellenbosch

Promoter: Prof. R. D. Sanderson

Mentor: Dr. M. Tonge

Stellenbosch

December 2006

Declaration

I, the undersigned, hereby declare that the work presented in this thesis is my own original work and that I have not previously in its entirely or in part submitted it at any university for a degree.

Signature: ……... Date: ……

ABSTRACT

Hydrophobic core/shell latex particles were synthesized for use in barrier coatings using the miniemulsion polymerization process. Particles with liquid or with hard cores were successfully synthesized using miniemulsion as a one-step nanoencapsulation technique. Different materials, including an oil (hexadecane, HD) and two different waxes (paraffin and microcrystalline wax), were used as the core of the particles. The shell of the particles was mainly made from a copolymer containing three relatively hydrophobic monomers, namely methyl methacrylate (MMA), butyl acrylate (BA) and vinyl neodecanoate (Veova-10).

Before any further investigations could be carried out, it was important to determine the morphology of the synthesized core/shell particles at the nanometer level. Particle morphology was mainly determined by two different techniques: transmission electron microscopy (TEM) and atomic force microscopy (AFM). TEM was used to directly visualize the morphology of the investigated core/shell particles at the nanometer level, while AFM was used to confirm the formation of these core/shell particles. AFM was a powerful technique with which to study the particle morphology of the core/shell latices during the film formation process.

As a second part of the study, the effect of various factors on the hydrophobicity and barrier properties of the resulting films produced from the synthesized core/shell latices to water and water vapour was investigated. This included the effect of: (i) the surfactant concentration, (ii) the wax/polymer ratio for both waxes, (iii) the molecular weight of the polymeric shell, (iv) the amount of the most hydrophobic monomer used (Veova-10), and (v) the degree of crosslinking in the polymeric shell.

Results showed that all the above-mentioned factors had a significant impact on the water sensitivity of the resultant films prepared from the synthesized core/shell latices. It was found that the presence of wax materials as the cosurfactant, instead of HD, in the miniemulsion formulation could significantly improve the hydrophobicity and barrier properties of the final films to water and water vapour. In addition, increasing the amount of wax, Veova-10, and the molecular weight of the resultant polymeric shell, led to a significant increase in the hydrophobicity and barrier properties of the resultant latex films. In contrast, hydrophobicity and water barrier properties decreased drastically as the quantity of surfactant and degree of crosslinking increased in the final latex films.

OPSOMMING

Hidrofobiese kern/skil lateks-partikels is berei vir gebruik in deklae (barrier coatings) deur gebruik te maak van die mini-emulsiepolimerisasieproses. Partikels met vloeibare of harde kerne is suksesvol berei deur gebruik te maak van mini-emulsies, as ‘n een-stap nanokapseleringstegniek. Verskillende materiale, insluitend heksadekeen (HD, ‘n olie), en twee verskillende wasse (paraffien en mikrokristallyne was) is vir die partikelkern gebruik. Die skil van die partikels is hoofsaaklik gemaak van ‘n kopolimeer wat drie relatief hidrofobiese monomere bevat het, naamlik metielmetakrilaat (MMA), butielakrilaat (BA) en vinielneodekanoaat (Veova-10).

Voordat enige verdere ondersoeke uitgevoer kon word, was dit belangrik om die morfologie van die bereide kern/skil-partikels op nanometervlak te bepaal. Partikelmorfologie is hoofsaaklik bepaal m.b.v. twee verskillende tegnieke: TEM en AFM. TEM is gebruik om die morfologie van die kern/skil-partikels op nanometervlak direk te ondersoek, terwyl AFM gebruik is om die vorming van die kern/skil-partikels te bevestig. AFM is ‘n baie goeie tegniek om die partikelmorfologie van die kern/skil-netwerke gedurende die filmvormingsproses te bestudeer.

In die tweede deel van hierdie studie is die invloed van verskeie faktore op die hidrofobisiteit en intervlakeienskappe van die films gemaak om die kern/skil-netwerke op water en waterdamp ondersoek. Dit het die invloed van die volgende ingesluit: (i) die seepkonsentrasie, (ii) die was/polimeer-verhouding vir beide wasse, (iii) die molekulerê massa van die polimeerskil, (iv) die hoeveelheid van die mees hidrofobiese monomeer wat gebruik is (Veova-10), en (v) die graad van kruisbinding in die polimeerskil.

Resultate het getoon dat al bogenoemde faktore ‘n noemenswaardinge invloed gehad het op die vogsensitiwiteit van die films wat van die kern/skil-netwerke berei is. Daar is bevind dat die teenwoordigheid van was-verbindings, in plaas van HD as die hulp-seep in die mini-emulsieformulering, die hidrofobisiteit en intervlakeienskappe van die finale films teenoor water en waterdamp kon verbeter. Verder het ‘n verhoging in die hoeveelheid was en Veova-10 en die molekulêre massa van die verkreë polimeerskil, ‘n noemenswaardige toename in die hidrofobisiteit en intervlakeienskappe van die lateks films tot gevolg gehad. In teenstelling hiermee het die hidrofobisiteit en waterspereienskappe drasties afgeneem namate die hoeveelheid seep en die graad van kruisbinding in die finale lateksfilm toegeneem het.

ACKNOWLEDGEMENTS

I would first like to thank Allah (God) who gave me the strength, health and opportunity to carry out this study in a proper way.

My appreciation and gratitude go to my parents, for providing me with all the opportunities and guidance throughout my life. My father is gratefully thanked for his continuous encouragement and support. Since I was a child I could feel his real desire to let me study and learn something new every day and to be a successful person in my life. My mother is especially thanked for her love, worrying, patience and praying to make this success possible. I would also like to extend my sincere thanks to all my brothers and sisters for their thinking about me and for being who they are.

On a more personal note, and from my heart, I would like to say a very big thank you to my wife, Gamra, for her love, help and support during my study in South Africa. She continuously provided me with all the love and the necessary care to finish my honours and master degrees.

I would also like to express my thanks to my promoter, Prof. R. Sanderson, for his help and support, and the opportunity to carry out this MSc project in his group. I am also sincerely grateful to Dr. M. Tonge for his advice, and for taking the time to read my thesis. The help and assistance I received from Dr. M. Hurndall in writing my thesis is also appreciated and thankfully acknowledged.

For providing most of the chemicals and instruments used in this study, Valeska Cloete is acknowledged. Mohamed Jaffer (University of Cape Town) is thanked for doing TEM analysis. Dr. M. Meincken (University of Stellenbosch) is also thanked for doing AFM analysis and interpreting the results.

Finally I would like to say thank you to all my colleges and friends, without whom my experience in South Africa would not have been the same.

The International Center for Macromolecular Chemistry and Technology in Libya is gratefully acknowledged for the financial support to make this study possible.

Dedicated to my father

LIST OF CONTENTS

Pectora roborant cultus recti

LIST OF FIGURES

LIST OF TABLES

Pectora roborant cultus recti

LIST OF ABBREVIATIONS

ABCVA	4,4´-azobis-(4-cyanovaleric acid)
AFM	Atomic force microscopy
AIBN	2,2'-azobis(isobutyronitrile)
AMBN	2,2'-azobis(2-methyl-butyronitrile)
BA	Butyl acrylate
BPO	Benzoyl peroxide
CA	Cetyl alcohol
cmc	Critical micelle concentration
DDI	Distilled deionized
DLS	Dynamic light scattering
DMA	Dynamic mechanical analysis
DSC	Differential scanning calorimetry
EGDMA	Ethylene glycol dimethacrylate
ESCA	Electron spectroscopy for chemical analysis
HD	Hexadecane
HPLC	High performance liquid chromatography
KOH	Potassium hydroxide
KPS	Potassium persulfate
LMA	Lauryl methacrylate
LPO	Lauroyl peroxide
m	Mass
MAA	Methacrylic acid
MFFT	Minimum film-forming temperature
Micro wax	Microcrystalline wax
MMA	Methyl methacrylate
MVTR	Moisture vapour transmission rate
NMR	Nuclear magnetic resonance
PAH	Poly(allylamine hydrochloride)
PAN	Polyacrylonitrile
PE	Polyethylene
PLLA	Poly(L-lactic acid)

PMMA	Poly methyl methacrylate
PSS	Poly(styrene sulfonate)
PSD	Particle size distribution
PS	Polystyrene
PVP	Poly(vinylpyrrolidone)
PW	Paraffin wax
RH	Relative humidity
Sty	Styrene
SAXS	Small angle X-ray scattering
SDBS	Sodium dodecylbenzene sulfonate
SDS	Sodium lauryl (dodecyl) sulfate
SEC	Size exclusion chromatography
SEM	Scanning electron microscopy
TEM	Transmission electron microscopy
THF	Tetrahydrofuran
UAc	Uranyl acetate
Veova-9	Vinyl neononanoate
Veova-10	Vinyl neodecanoate
w.u.	Water uptake
WVTR	Water vapour transmission rate

LIST OF SYMBOLS

D	Diffusion coefficient
S	Solubility coefficient
E_p	Activation energy for permeation
R	Gas constant
T	Temperature
E_d	The activation energy for diffusion
ΔH_{sol}	The heat of solution for the permeant in a polymer
w_i	Weight fraction
θ	Contact angle
R_p	Rate of polymerization
k_p	The propagation rate coefficient
$[M]_p$	Monomer concentration in the particles
$\bar{n}$	The average number of free radicals per particle
N_p	Number of particles
N_A	Avogadro's number
[S]	Surfactant concentration
[I]	Initiator concentration
$\overline{M}_w$	Weight average molecular weight
$\overline{M}_n$	Number average molecular weight

CHAPTER 1

INTRODUCTION AND OBJECTIVES

1.1 Introduction

The ability to synthesize composite latex particles with well-defined geometries such as core/shell morphology can be of great scientific and industrial importance due to their potential applications. The synthesis of such multiphase composite particles provides an opportunity to tailor properties for a range of desired applications. These include applications such as paints, coatings, and adhesives,[1,2] where these composite latices can be used in order to create latex films with properties that can not be achieved by a physical blend of two or more different polymer components.

For instance, binders used in coatings need to fulfill contradictory demands, such as excellent film formation and appearance as well as good blocking resistance (blocking is the tendency of a polymer film to stick to itself by physical contact[3]) and hardness. By using core/shell particles, which have hard domains (formed from a high glass transition temperature (T_g) polymer) and soft domains (formed from a lower T_g polymer), it is possible to produce binders with a high blocking resistance and a low minimum film-forming temperature (MFFT).[4] The low T_g shells lead to film formation while the hard cores improve the blocking resistance and mechanical properties, and stabilize the film.

Wax emulsions are widely used in aqueous formulations such as coatings to reduce the unwanted penetration of water and water vapour molecules through a permeable material.[5-7] However, wax is hard to emulsify, and a single surfactant system is not sufficient to achieve proper emulsification.[8] For example, mixed emulsifiers comprising nonionic surfactant and anionic surfactant are used to achieve highly stable wax emulsions.[9] In addition, waxes such as petroleum wax must be modified by different methods, of which oxidation is the earliest and most widely used.

Through oxidation, the petroleum waxes can obtain high acid numbers, which makes them suitable for emulsification.[9] One solution is to combine a wax emulsion with a polymer emulsion. However, in such a case there is the problem of surfactant compatibility, which can be a limiting issue when different surfactant systems are used in each emulsion.

By using the core/shell concept, it is possible to prepare latex particles that consist of a hydrophobic core formed from highly hydrophobic materials such as waxes, surrounded by a less hydrophobic shell composed of a relatively hydrophobic polymer(s).[10] This study describes the synthesis of highly hydrophobic wax-polymer core/shell particles for use in barrier coatings using miniemulsion as a one-step nanoencapsulation process.

In the past, many different techniques have been used to prepare core/shell particles, including suspension cross-linking,[11] coacervation,[12] solvent evaporation[13] and interfacial polymerization.[14] However, the most common process by which to synthesize these core/shell latex particles is seeded emulsion polymerization, which was the first general method used to prepare polymer latices having such unique structures.[15-18] This technique allows one to prepare particles with a well-defined structure regarding the resulting particle morphology. By using different monomer compositions at different stages in a seeded emulsion polymerization, it is possible to achieve many desired particle morphologies. In the case of core/shell particles, the second stage monomer is polymerized in the presence of the core seed latex, leading to particles with the desired core/shell morphology.

The preparation of core/shell particles with hydrophobic cores is difficult to achieve by conventional emulsion polymerization.[19] This is due to the high hydrophobicity and low water solubility of the core. In conventional emulsion systems, no transport of the hydrophobic core component into micelles can take place, leading to phase separation. However, miniemulsion polymerization, due to the initial dispersion of the hydrophobic components, can be a powerful technique for the preparation of latex particles with very hydrophobic cores. It allows the encapsulation of hydrophobic compounds such as hexadecane[19] or wax[10] within a polymeric shell in a convenient one-step polymerization process. In addition, miniemulsion allows for the polymerization of hydrophobic monomers with low water solubility, which often can only be polymerized in emulsion polymerization with difficulty.[20,21]

In comparison with emulsion polymerization, in miniemulsion most monomer droplets are in principle directly converted into particles, since the droplets are regarded as the locus of the initiation and propagation site for the polymerization.[22] Therefore, the transport of the monomer or other hydrophobic compounds from a reservoir to the polymerization locus, as in the case for emulsion polymerization, is unnecessary. This feature makes miniemulsion polymerization quite efficient as a convenient one-step nanoencapsulation technique for hydrophobic compounds. In this process, the oil phase, which consists of the monomer and the hydrophobe, is dispersed in the water phase, which consists of the surfactant, by a high shear device.[23] This will lead to the formation of droplets, containing the hydrophobic compounds and stabilized by the surfactant, from which polymer particles will develop during the polymerization step. In addition, phase separation within the minidroplets dispersed in the aqueous phase can take place, leading to the formation of the structured particles with the desired morphology.

Many analytical techniques such as scanning electron microscopy (SEM),[24] solid-state NMR[25,26] and small angle X-ray scattering (SAXS)[27] have been used to determine and characterize the morphology of core/shell particles. Transmission electron microscopy (TEM) has been classically used in the characterization of these composite particles at a high level of resolution.[10,25,28] Atomic force microscopy (AFM)[29,30] has also proven itself as a promising technique to qualify the morphology of single latex particles and to study latex dispersion films. AFM,[30] due to its resolution at the nanometer level and its non-destructive operation mode, and the ability to operate in a non-vacuum system in an aqueous environment, makes it a powerful tool with which to monitor the drying and film formation process in a core/shell latex. This study focuses on the use of TEM and AFM for the determination of particle morphology.

1.2 Objectives

The overall aim of this project was twofold. The first objective was the preparation of hydrophobic core/shell latex particles for barrier coating applications, using a miniemulsion polymerization process. The emphasis was on the synthesis of latices with hydrophobic cores made with different soft (hexadecane) and hard (paraffin and microcrystalline wax) materials in a one-step nanoencapsulation technique.

The particle morphology of the synthesized core/shell latices was to be investigated by two different techniques: transmission electron microscopy and atomic force microscopy. TEM was used to determine the particle morphology by directly visualizing the particles at the nanometer level, while AFM was used to determine the particle morphology by probing the drying films produced from the prepared core/shell latices during the film formation process.

The second aim of the project was to investigate the effect of various factors on the hydrophobicity and barrier properties of the final films produced from the synthesized core/shell latices to water and water vapour. These factors included: the amount of surfactant used in the miniemulsion formulation, the type of wax used in the core, wax/polymer ratios, the amount of the most hydrophobic monomer used (vinyl neodecanoate (Veova-10), referred to also as vinyl versatate), the degree of crosslinking in the polymeric shell, and the molecular weight of the polymeric shell.

1.3 Thesis layout

This thesis consists of six chapters, three of which describe experimental procedures. Chapter 1 provides a general introduction to the research, followed by the objectives and thesis layout. Chapter 2 describes, in detail, miniemulsion polymerization and the preparation of core/shell particles. The preparations of miniemulsions as well as the properties of these miniemulsions, including the differences between emulsion and miniemulsion systems are discussed. The prediction of particle morphology using two theories is also presented. In addition, this chapter provides a short overview on the barrier properties of polymers used in coatings. The permeability of low molecular weight molecules, such as water, through polymers is discussed. Chapter 3 gives detailed information about the synthesis of the investigated core/shell latices as well as the experimental methods used for the characterization of these latices.

The results are presented in two chapters, namely Chapters 4 and 5. Chapter 4 describes the determination of the particle morphology of the synthesized core/shell latex particles. Here TEM was used to visualize the particles at the nanometer level while AFM was used to determine their morphology by imaging the surface of the latex films and providing information about their film formation.

TEM micrographs of the core/shell latex particles as well as AFM images of the film formation process at different temperatures and times, revealing the morphology of the synthesized core/shell particles are presented.

Chapter 5 shows the results obtained from hydrophobicity, water uptake, conductivity and moisture vapour transmission rate (MVTR) measurements. Here the effects of different factors on the hydrophobicity and barrier properties, in terms of water and water vapour, of the resultant films produced from the synthesized core/shell latices, are described.

Chapter 6 summarizes the main conclusions drawn from the results and mentions some recommendations and future work.

1.4 References

(1) Dimonie, V.; Daniels, E.; Shaffer, O.; El-Aasser, M. *Control of Particle Morphology*, In *Emulsion Polymerization and Emulsion Polymers*, Lovell, P.; El-Aasser, M., Eds.; John Wiley & Sons Ltd.: New York, 1997; pp 293-326.

(2) Stubbs, J.; Sundberg, D. *Journal of Coatings Technology* **2003**, *75*, 59-67.

(3) Hernandez, R. *Polymer Properties*, In *The Wiley Encyclopedia of Packaging Technology*, Brody, A.; Marsh, K., Eds.; John Wiley & Sons, Inc.: New York, 1997; pp 758-765.

(4) Schuler, B.; Baumstark, R.; Kirsch, S.; Pfau, A.; Sandor, M.; Zosel, A. *Progress in Organic Coatings* **2000**, *40*, 139-150.

(5) Wang, S.; Schork, F. *Journal of Applied Polymer Science* **1994**, *54*, 2157-2164.

(6) Hagenmaier, R.; Baker, R. *Journal of Agricultural and Food Chemistry* **1994**, *42*, 899-902.

(7) Hagenmaier, R.; Shaw, P. *Journal of Agricultural and Food Chemistry* **1991**, *39*, 1705-1708.

(8) Eccleston, G. *Colloids and Surfaces A: Physicochemical and Engineering Aspects* **1997**, *123-124*, 169-182.

(9) Pang, H.; Zhang, J.; Yan, Y.; Xu, B.; Zhang, Z.; Pan, J.; Deng, J.; Du, L. *Petroleum Science & Technology* **2004**, *22*, 439-445.

(10) Luo, Y.; Zhou, X. *Journal of Polymer Science: Part A: Polymer Chemistry* **2004**, *42*, 2145-2154.

(11) Arshady, R. *Polymer Engineering and Science* **1989**, *29*, 1746-1758.

(12) Arshady, R. *Polymer Engineering and Science* **1990**, *30*, 905-914.

(13) Arshady, R. *Polymer Engineering and Science* **1990**, *30*, 915-924.

(14) Frere, Y.; Danicher, L.; Gramain, P. *European Polymer Journal* **1998**, *34*, 193-199.

(15) Winnik, M.; Zhao, C.; Shaffer, O.; Shivers, R. *Langmuir* **1993**, *9*, 2053-2066.

(16) Stutman, D.; Klein, A.; El-Aasser, M.; Vanderhoff, J. *Industrial & Engineering Chemistry Product Research and Development* **1985**, *24*, 404-412.

(17) Hughes, L.; Brown, G. *Journal of Applied Polymer Science* **1961**, *5*, 580-588.

(18) Grancio, M.; Williams, D. *Journal of Polymer Science: Part A-1* **1970**, *8*, 2617-2629.

(19) van Zyl, A.; Sanderson, R.; de Wet-Roos, D. ; Klumperman, B. *Macromolecules* **2003**, *36*, (23), 8621-8629.

(20) Wu, X.; Schork, F. *Industrial & Engineering Chemistry Research* **2000**, *39*, 2855-2865.

(21) Asua, J. *Progress in Polymer Science* **2002**, *27*, 1283-1346.

(22) Antonietti, M.; Landfester, K. *Progress in Polymer Science* **2002**, *27*, 689-757.

(23) Sudol, E.; El-Aasser, M. *Miniemulsion Polymerization*, In *Emulsion Polymerization and Emulsion Polymers*, Lovell, P.; El-Aasser, M., Eds.; John Wiley & Sons Ltd.: New York, 1997; pp 699-722.

(24) Loxley, A.; Vincent, B. *Journal of Colloid and Interface Science* **1998**, *208*, 49-62.

(25) Kirsch, S.; Doerk, A.; Bartsch, E.; Sillescu, H.; Landfester, K.; Spiess, H.; Maechtle, W. *Macromolecules* **1999**, *32*, 4508-4518.

(26) Landfester, K.; Boeffel, C.; Lambla, M.; Spiess, H. *Macromolecules* **1996**, *29*, 5972-5980.

(27) Dobashi, T.; Yeh, J.; Ying, Q.; Ichikawa, K.; Chu, B. *Langmuir* **1995**, *11*, 4278-4282.

(28) Chen, W.; Zhu, M.; Song, S.; Sun, B.; Chen, Y.; Adler, H. *Macromolecular Materials and Engineering* **2005**, *290*, 669-674.

(29) Schellenberg, C.; Akari, S.; Regenbrecht, M.; Tauer, K.; Petrat, F.; Antonietti, M. *Langmuir* **1999**, *15*, 1283-1290.

(30) Sommer, F.; Duc, T.; Pirri, R.; Meunier, G.; Quet, C. *Langmuir* **1995**, *11*, 440-448.

Pectora roborant cultus recti

CHAPTER 2

HISTORICAL AND THEORETICAL BACKGROUND

2.1 Miniemulsion polymerization

2.1.1 Introduction

Miniemulsion polymerization is a convenient one-step technique for the encapsulation of hydrophobic compounds and the polymerization of monomers with low water solubility. It offers several advantages over other dispersion polymerization techniques, such as: small particle size of the final latex particles, efficient use of surfactant, production of latices with high solids content, and particles that are a 1:1 copy of the miniemulsion droplets can be produced.[1,2] The latter can be attributed to the fact that the miniemulsion droplets are directly polymerized, thus the resulting polymer particles are often one-to-one copies of the monomer droplets.[1]

Miniemulsions contain submicron-sized monomer droplets ranging from 50-500 nm.[3] The droplets are formed by shearing a pre-mixed system comprising water, monomer, surfactant and a cosurfactant (also referred to as a hydrophobe or a costabilizer). The surfactant prevents the droplets from coalescence, and the hydrophobe prevents Ostwald ripening. Coalescence occurs upon the collision of droplets while Ostwald ripening is caused by the diffusion degradation of the droplets. In a system susceptible to Ostwald ripening larger monomer droplets will grow in size at the expense of the smaller ones due to the difference in the chemical potential between droplets of different radii.[4] The low molecular weight molecules of the hydrophobe can diffuse only very slowly from one droplet to the other due to their highly hydrophobic nature, therefore they are trapped in the droplet. This will lead to the creation of an osmotic pressure in every droplet, which will suppress monomer diffusion from smaller to bigger droplets.

A well designed miniemulsion formulation would therefore greatly rely on a suitable choice of surfactant(s) and hydrophobe. Furthermore, the amount of surfactant used allows control over particle size of the final latex particles.[5]

An increase in the surfactant concentration will lead to a decrease in the particle size. Different surfactant/cosurfactant (hydrophobe) systems can be used for miniemulsion formulations. The most common model systems employ sodium lauryl (dodecyl) sulfate (SDS) in combination with cetyl alcohol (CA) or hexadecane (HD).

A characteristic feature of miniemulsion polymerization is that droplet nucleation is the predominant mechanism of particle formation.[6] The nanometer-sized monomer droplets formed by the application of high shear to the system have a sufficiently large surface area to effectively compete with the micelles or particles for radical capture.[7] The large droplet surface area is stabilized with the adsorption of an additional amount of surfactant from the water phase, which leads to a decrease in surfactant concentration in the water phase. Thus there are usually no micelles present in a well prepared miniemulsion. The size of the droplets can be controlled through changes in the surfactant concentration, the shear rate, and time.[8]

The first report on miniemulsion polymerization dates back to 1973, when Ugelstad *et al.*[6] reported the polymerization of styrene in the presence of a mixed emulsifier system of SDS and CA. For comparison, styrene emulsions made with SDS alone were also prepared. Results showed that these emulsions were unstable and phase separated within a few minutes when the stirring was stopped. On the other hand, when the CA was used in addition to SDS, the stability of the styrene emulsions was very good and the average droplet size was very small. At that time the term miniemulsion had not been used, however the polymerization features fit the general definition of miniemulsion polymerization where monomer droplets smaller than 1 micron were obtained by simple mixing of the monomer into an aqueous solution of a surfactant and a cosurfactant. The reduction in average size makes the monomer droplets more competitive in capturing radicals generated in the aqueous phase, which provides the basis of miniemulsion polymerization, i.e., monomer droplet nucleation. Furthermore, due to the reduction in average size, droplets have a very high total surface area, therefore the particle number is also very high.

2.1.2 Emulsion vs. miniemulsion polymerization

In a number of publications authors have studied the differences between conventional emulsion and miniemulsion polymerization.[9,10] The difference in size of the monomer

droplets in emulsion and miniemulsion polymerization is the key factor to distinguish between the two systems. The size of the dispersed droplets in miniemulsion is quite small (between 50 and 500 nm) relative to the size of monomer droplets in an emulsion system (ranging from 1 to 100 µm).[3] This significant difference in the droplet size is liable for the different mechanisms of particle nucleation operating in the two systems.

Emulsion polymerization normally consists of water-insoluble monomer(s), a dispersing medium (usually water), a suitable surfactant, and a water-soluble initiator. The role of surfactant is to facilitate micelle formation. In addition, surfactant plays an important role in the stability, rheology, and control of particle size of the resulting latices. The action of the surfactant is due to its molecules having both hydrophobic and hydrophilic segments. When the concentration of the surfactant is above its critical micelle concentration (cmc), the unabsorbed surfactant molecules remain in the aqueous phase and form micelles. The hydrophobic tail region of the aggregates will then be swollen by monomer, forming what is usually referred to as monomer-swollen micelles. The locus of initiation in an emulsion system is generally accepted to be in the aqueous phase.

The polymerization process commences with radicals, generated by the thermal decomposition (or otherwise) of the initiator, reacting with the monomer in the aqueous phase to form oligomeric radical chains. In an emulsion system, there are three possible nucleation mechanisms for the growing oligomeric radical species. These are micellar, homogeneous (water phase) and less often droplet nucleation.[11] Droplet nucleation occurs when radicals formed in the aqueous phase enter monomer droplets and propagate to form polymer particles.

In homogenous nucleation, oligomers growing in the aqueous phase, if they have not entered a polymer particle, begin to precipitate from solution as they reach a degree of polymerization that exceeds their solubility limit. This will happen as these oligomers reach a critical length, at which they will become insoluble in the aqueous phase, and consequently precipitation will occur. The oligomeric radicals will then form precursor particles stabilized by adsorbing surfactant molecules. These primary particles can then absorb monomer for further propagation, to form polymer particles.

Micellar nucleation, on the other hand, occurs when sufficient surfactant is present in the system to exceed the cmc. As a result of Ostwald ripening in the emulsion system, monomer molecules tend to diffuse from smaller monomer droplets to larger ones to minimize the total interfacial energy of the system. The droplets are consequently large and the total interfacial area is unable to accommodate all of the surfactant molecules. The desorbed surfactant molecules remain in the aqueous phase and form micelles if the concentration of the surfactant is above the cmc. The hydrophobic tail of the aggregates will then be swollen by monomer, forming monomer-swollen micelles. Initiator radicals (or oligomeric radicals) generated in the aqueous phase can then enter the monomer-swollen micelles to form monomer-swollen polymeric particles. These swollen polymeric particles will grow further by propagation reactions until monomer and surfactant are depleted from unentered micelles. Growth will then cease, with the disappearance of the micelles, at a point where a constant number of particles will be present.

All three of the above-mentioned mechanisms can occur in classical emulsion polymerization. However, due to the large size (small surface area) of the monomer droplets, they cannot effectively compete with micellar and homogeneous nucleation. Droplets merely act as reservoirs for monomer that diffuses through the water phase to the growing latex particles. Therefore, droplet nucleation is insignificant for most emulsion polymerizations.

Pectora roborant cultus recti

On the other hand, in miniemulsion polymerization, droplet nucleation is the predominant mechanism of particle formation due to the small size of monomer droplets and the presence of little or no micelles in the system.[12] These submicron droplets have a large interfacial area and are capable of capturing most of the oligomeric free radicals; thus the droplets become the locus of nucleation.

2.1.3 Miniemulsion formulations

A typical miniemulsion formulation includes water, a monomer (or monomer mixture), a surfactant, a cosurfactant and a suitable initiator system. Different monomers, with a wide range of water solubilities, including vinyl acetate (VAc),[13] methyl methacrylate (MMA),[14,15] butyl acrylate (BA)[16] and styrene (Sty),[17,18] have been polymerized by means of this technique. In other cases, formulations that contain more than one monomer have also been

prepared, including miniemulsions in which quantities of very water-soluble monomers, such as acrylic acid (AA)[19] and methacrylic acid (MAA),[20] have been used.

A very important factor for the formulation of a stable miniemulsion is the choice of an appropriate water-insoluble compound, or so-called hydrophobe. In most of the early work, authors investigated the miniemulsion polymerization of Sty stabilized with CA as a hydrophobe.[2] It was found that although the nucleation period was rather long, most of the particles were nucleated at low conversion. As proposed by Landfester *et al.*,[21] the most efficient hydrophobes are very water-insoluble, surface-inactive reagents. The authors found that the predominant requirement for the hydrophobe is an extremely low water solubility (less than 10^{-7} mL mL^{-1}) independent of its chemical nature. It was also found that regardless of the amount and type of the hydrophobe, stable miniemulsions with similar structural characteristics were obtained. The water-insoluble compound is usually a fatty alcohol or a long-chain alkane. The addition of the hydrophobe, such as a long-chain alkane (*e.g.* hexadecane)[22,23] or a long chain alcohol (*e.g.* cetyl alcohol),[6,15,18] can efficiently retard the destabilization of the nanodroplets by Ostwald ripening (discussed in Section 2.1.7). It should be noted that both linear and branched molecules can be used provided that they have very low water solubility. Other costabilizers that have been used include dodecyl mercaptan[15] or reactive alkyl methacrylates.[24]

Monomer soluble polymers have also been used to reduce Ostwald ripening. For instance, Miller *et al.*[25,26] found that a styrene miniemulsion could be prepared by using 1 wt% of polystyrene with cetyl alcohol as the cosurfactant. Reactions proceeded at faster polymerization rates and resulted in latices with smaller particles sizes in comparison with conventional miniemulsion containing no polystyrene. By dissolving a small amount of polystyrene in the monomer phase prior to forming the miniemulsion, the polymerization kinetics became significantly faster due to a larger number of polymer particles formed in the presence of polystyrene polymer. The explanation of these results was considered to involve the entry of radicals into pre-formed polymer particles.

In an attempt to encapsulate hydrophobic material within a polymeric shell using miniemulsion polymerization techniques, Luo and Zhou[27] reported that the standard inert hydrophobe, HD, could be replaced by the use of paraffin wax, which was used as a model hydrophobic compound. The encapsulation involved the polymerization of the monomer

in a predispersed monomer-paraffin mixture. In such a system, the paraffin is soluble in the monomer (styrene) and can be used to replace the hydrophobe used in a typical miniemulsion formulation.

Another important formulation variable in miniemulsion polymerization is the use of an emulsifier or surfactant system to prevent the degradation of particles by collision (see Figure 2.2 in Section 2.1.7). For miniemulsion formulations, many different surfactants, including anionic,[18] cationic,[28] non-ionic,[29] non-reactive surfactant and reactive surfactants[30] can be used. The surfactant provides stability against physical degradation, i.e. coagulation possibly followed by coalescence. This is due to the trend toward a minimal interfacial area between the dispersed phase and the dispersion medium. In addition, by varying the amount and type of surfactant, particle size can be varied over a wide range.[5]

The surfactants used in miniemulsion polymerization should meet the same requirements as in conventional emulsion polymerization.[31] These are: (i) their structure must have polar and non-polar groups, (ii) they must be more soluble in the aqueous phase than the oil phase so as to be readily available for adsorption on the oil droplet surface, (iii) they must adsorb strongly and not be easily displaced when two droplets collide, (iv) they must be effective at low concentrations, (v) they should be relatively inexpensive, non-toxic and safe to handle, and (vi) they can be chosen to provide specific properties to the final latex.

2.1.4 Preparation methods of miniemulsions

In principle, miniemulsion preparation can be carried out by dissolving a suitable surfactant system in water and dissolving the hydrophobe in monomer (or monomer mixture), followed by premixing under stirring (see Figure 2.1). The mixture is then subjected to a highly efficient homogenization process called miniemulsification. This can be achieved by using a high shear dispersion device to disperse the premixed solution to small droplets. A variety of homogenization techniques can be used for the preparation of stable miniemulsions. Stirring used in the earlier work on miniemulsions[6] has been replaced with high shear mechanical agitation and ultrasonication. The energy transferred by simple stirring is not sufficient to prepare small, well distributed particles.[32] Therefore a much higher energy device to disperse large droplets to create smaller ones is required. After the miniemulsification process, the polymerization is started by adding a suitable initiator system.

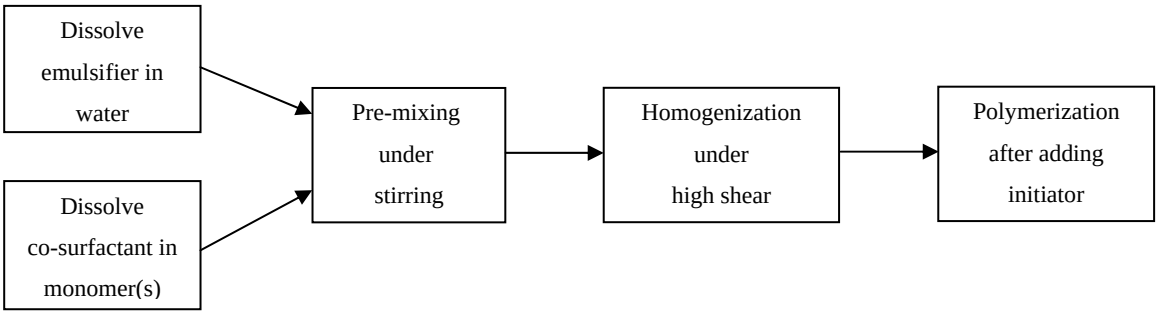

Figure 2.1: Schematic representation of miniemulsion preparation.

According to Asua[31] the following devices are the most commonly used to achieve homogenization: rotor-stator devices, sonifiers and high-pressure homogenizers. Today miniemulsification by ultrasound, first reported in 1927,[33] is used, especially for the homogenization of small latex quantities. On the other hand, rotor-stator devices, which rely on turbulence to produce the miniemulsification, are used to prepare large quantities of latex. High-pressure homogenizers such as a Microfluidizer are also used to prepare such stable miniemulsions, and are upscalable.

When sonifiers are used, the ultrasound waves cause the molecules to oscillate about their average position as the waves propagate. However, before ultrasound can be applied, pre-stirring is important in order to create droplets, which are about ten times the size of the desired miniemulsified droplets. Stirring during sonication is also important, to allow all the fluid to pass through the sonication region.[31] Problems are encountered with miniemulsions prepared by using a sonication device when stirring is not used. This is mainly due to the fact that only a small volume of the fluid around the sonifier is directly affected by the ultrasound waves. Therefore, this process makes the miniemulsion characteristics dependent on the sonication process. For instance, it has been reported that droplet size decreases with increasing sonication time.[8]

There are several possible mechanisms of droplet formation and disruption under the influence of the ultrasound waves. One proposes that during ultrasonication the droplets are further broken down by unstable oscillation of the liquid-liquid interface, as well as cavitation.[34] In the beginning, the droplets are big and the polydispersity is quite high. The monomer droplet size changes quite rapidly throughout sonication until a steady state is

reached. Due to a constant fusion and fission process, the droplet size as well as polydispersity decreases, and the miniemulsion reaches then a steady state.[5]

2.1.5 Initiators used in miniemulsions

In miniemulsions, polymerization can be initiated by using either a water-soluble or oil-soluble initiator. In the case of a water-soluble initiator, polymerization is started from the aqueous continuous phase. The polymerization is started by the initiator generating free radicals, by thermal decomposition in the aqueous phase. This is similar to conventional emulsion polymerization, where mainly water-soluble initiators are used. Polymerization involves the formation of oligomeric radicals, which will enter the monomer droplets when they reach a certain critical chain length. In this case, the initiator is added after the miniemulsification process takes place. Bechthold and Landfester[35] studied the miniemulsion polymerization of styrene using the water-soluble initiator, potassium persulfate (KPS). They found that the reaction rate was slightly increased by increasing the initiator concentration. However, increasing the initiator concentration caused a significant reduction of the average degree of polymerization.

On the other hand, an oil-soluble initiator can be mixed with the oil phase (monomer and hydrophobe) before premixing with the surfactant/water solution. Because of the small size of monomer droplets, radical recombination is then often a problem. Oil-soluble initiators are preferred when water-soluble monomers such as methyl methacrylate and vinyl chloride are used. This is due to the fact that nucleation in the water phase (also referred to as secondary or homogeneous nucleation) can take place.[36] Oil-soluble initiators are also preferred when monomers with extremely low water solubility, such as lauryl methacrylate (LMA), need to be polymerized. Here the monomer concentration in the water phase is not high enough to frequently create oligomeric radicals which can enter the droplets.

The possibility of nucleation in the water phase can also be minimized by using a redox initiation system, which contains two components (*e.g.* $(NH_4)_2S_2O_8/NaHSO_3$). In this case one component is in the aqueous phase and the other is in the oil phase.[37] Hence, the initiation is restricted to the interfacial layer of monomer droplets with the water phase.

Initiators can also be used for the stabilization of miniemulsions. Alduncin *et al.*[17] studied the ability of different oil-soluble initiators with different water solubilites, namely lauroyl peroxide (LPO), benzoyl peroxide (BPO) and 2,2'-azobis(isobutyronitrile) (AIBN), to stabilize monomer droplets against Ostwald ripening, and their efficiency in the miniemulsion polymerization of styrene. First it was found that the particle size distribution (PSD) obtained in the presence of HD was not significantly affected by the initiator type used even though they had very different solubilites and decomposition rates. However, they did find that the probability of nucleation was much larger for AIBN than for LPO and BPO. More hydrophobic initiators, such as 2,2'-azobis(2-methyl-butyronitrile) (AMBN), could also be used to initiate and stabilize some miniemulsions.[38] It was noted that the rate of polymerization significantly increased with increasing total surface area of the monomer droplets.

2.1.6 Properties of miniemulsions

One of the many advantages of the miniemulsion polymerization technique is that it extends the possibilities of the widely applied emulsion polymerization, and high solids content polymers can be successfully synthesized. Polymerizations in such miniemulsions, when carefully prepared, result in latex particles, which have about the same size as the initial droplets. The particle size is established by controlling the energy produced by the shear source and the time under shear.

In addition, particle size can be controlled by changing the surfactant type and concentration. Another important feature of miniemulsion polymerization is the ability to produce high solids content, low viscosity latices. Latices with high solids content offer numerous advantages for most industrial applications. These include: (a) lower shipping costs and (b) less water to be removed from the latex. Polydisperse latices show low viscosity due to the fact that small particles fit within the voids of the array of the big particles. Polydisperse particles are often produced by miniemulsion polymerization.[39] Ouzineb *et al.*[40] have investigated the use of miniemulsions to make high solids content, low viscosity latices using styrene and butyl acrylate as monomers. Products with solids content greater than 70 wt% and viscosities as low as 350 mPa s at a shear rate of 20 s^{-1} were obtained.

Other advantages that miniemulsion polymerization can provide over other polymerization techniques include:

- Allows the copolymerization of monomers with different water solubilities (discussed in Section 2.1.3),
- Allows the incorporation of hydrophobic materials, which often can be polymerized in emulsion polymerization with difficulty,[41]
- Polymer latices with better colloidal stability can be prepared,[5,42]
- High solids content latices with no coagulation can be obtained.[43]

2.1.7 Miniemulsion stability

In general, miniemulsions are thermodynamically unstable and separate into two phases over a period of time.[44] This is mainly because of the fact that they include very large interfaces. The growth of miniemulsion droplets is affected by two distinct mechanisms, both of which are considered as major instability processes of an emulsion system. These are droplet coalescence and molecular diffusion degradation (Ostwald ripening). To create a stable miniemulsion system, droplets must be stabilized both against Ostwald ripening and against coalescence by collisions. Stabilization against Ostwald ripening can be achieved by the addition of small amounts of a third component which must be preferentially located in the dispersed phase. Besides the molecular diffusion of the dispersed phase, destabilization of a miniemulsion can also occur by collision and coalescence processes. This can be prevented by the addition of appropriate surfactants, which provide electrostatic, steric or electrosteric stabilization to the droplets. The basic features of these two instability processes are as follows:

(1) Coalescence occurs when two droplets combine after they have collided, to form an aggregate. When the thin layer between these two neighbouring droplets is ruptured, the droplets form a new larger droplet, mixing their contents (see Figure 2.2). Thus coalescence is considered as an irreversible process unless shear is applied (*e.g.* in the initial shear process). The rate of coalescence is dependent on the droplet encounter rate (controlled by the droplet diffusion) and the properties of the droplets' surface.

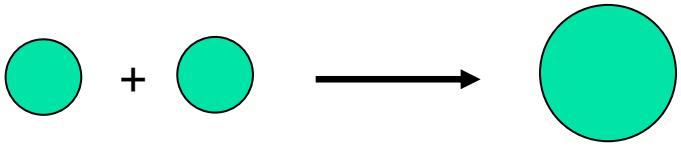

Figure 2.2: Coalescence of two droplets in miniemulsion.

(2) Ostwald ripening, as shown in Figure 2.3, is the growth of the larger monomer droplets in size at the expense of the smaller droplets. This is due to the difference in the chemical potential between droplets having different radii.[4] The growth of droplets occurs by the molecular diffusion of monomers through the continuous phase, over time. In other words, Ostwald ripening is a growth mechanism, where small particles effectively are consumed by the larger particles.

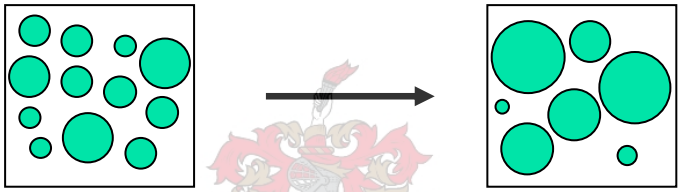

Figure 2.3: Ostwald ripening that occurs in miniemulsion.

2.1.8 Polymerization of hydrophobic monomers in miniemulsion

Miniemulsion offers a very important advantage, namely the ability to polymerize highly water-insoluble monomers in an aqueous medium.[5,42] Monomers that display some degree of water solubility, such as styrene and vinyl acetate, are regarded as good starting materials for emulsion polymerization.[45,46] On the other hand, when the monomer is very much less soluble in the water phase, miniemulsion polymerization is the most often employed alternative technique.[5]

The incorporation of hydrophobic monomers is very important due to the large number of hydrophobic monomers available for many applications. In coating applications, for instance, polymer films made from latices obtained by polymerizing hydrophobic monomers such as some acrylates and Veova monomers offer superior water resistance.[47] In this case there is an important issue to consider, namely the monomer transport limitation on the rate of polymerization. The polymerization of hydrophobic monomers is much easier in miniemulsion than in conventional emulsion polymerization because the need of mass transport through the water phase is minimized by droplet nucleation.[42]

Kitzmiller *et al.*[30] studied the rate of copolymerization for vinyl acetate and vinyl 2-ethylhexanoate in both miniemulsion and conventional emulsion polymerizations. They found that the rate of polymerization of these monomers is much slower in emulsion than in miniemulsion polymerization. This was attributed to monomer transport effects for the less water-soluble monomer. In conventional emulsion polymerization, the monomer must diffuse from the monomer droplets, across the aqueous phase, and eventually penetrate into the growing polymer particles. This can be a rate limiting issue, particularly when the monomer has very low water solubility. Since the bulk of the mass transfer resistance is from the monomer droplets into the water phase, miniemulsion polymerization may provide some advantages over conventional emulsion polymerization. In miniemulsion polymerization there is no monomer transport, since the monomer is polymerized within the nucleated droplets.

Balic[48] studied the emulsion polymerization of Veova monomers. As seen in Figure 2.4, Veova monomers are vinyl esters of versatic acid, a synthetic saturated monocarboxylic acid of highly branched structure. Due to their highly branched alkane structure these monomers have very low water solubility and a highly hydrophobic nature.

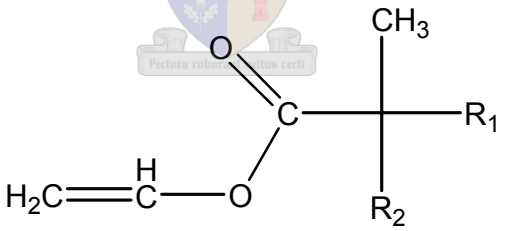

Figure 2.4: Vinyl esters of versatic acid, Veova-9, 10, 11.

Depending on the number of carbon atoms in the branched alkyl groups R_1 and R_2, three different monomers (Veova-9, 10 and 11) can be found. For Veova-9, 10 and 11, R_1 and R_2 contain 6, 7 or 8 carbon atoms respectively. Balic found that these monomers have a low polymerization rate and long inhibition periods. This was attributed to the extremely low water-solubility of the monomer in the aqueous phase. The low water-solubility of the monomer retards the formation of oligomeric radicals of sufficient length to enter the polymer particles.

2.2 Core/shell latex particles

2.2.1 Introduction

Core/shell particles are structured composite particles consisting of at least two different materials.[49] One material forms the core and the other forms the shell of the particles. These composite particles create a class of materials with unique colloidal and physical properties. The optimal combination of properties of these two different materials can often be better achieved with these structured particles than by blending the two materials. For instance, by using the core/shell concept one can prepare latices possessing two kinds of properties; one property can be achieved by the core and the other by the shell. Recently, core/shell particles with different glass transition temperatures were used to modify the mechanical properties of thermoplastics.[50,51] Core/shell particles can also be used for many other applications, such as waterborne paints and coatings, adhesives, membrane separation, biotechnology and impact modifiers.[49,52] Latices can be created with properties that cannot be achieved by the physical blending of the two materials from which the core and the shell are formed.

In the coating industry, these core/shell particles can be of a great importance due to their unique properties. For instance, by using core/shell particles which have hard and soft domains, formed from two different polymers having different T_gs, it is possible to produce binders with a high blocking resistance, caused by the hard polymer, and a low minimum film-forming temperature, caused by the low T_g polymer.[53]

2.2.2 Core/shell particle formation

Many studies have focused on understanding the formation of core/shell particles.[54,55] According to their synthesis conditions, the structure of these core/shell particles can be varied to a large extent. Both thermodynamic and kinetic factors of the polymerization reaction affect the type of structure that can be obtained.[56,57] These include core/shell structure, heterogeneous structure with occlusions of one polymer embedded in the other, inverted core/shell structures, where the core and shell materials are exchanged, or formation of raspberry-like and separated half moon structures.[58-61] Figure 2.5 shows examples of these morphologies and structures that can be obtained, where the light area is indicative of the core and the dark area is the shell.

As a result of the versatility of the core/shell morphology concept, the construction of core/shell particles leads to numerous particle morphologies, with different properties and applications. This includes the formation of core/shell particles with liquid cores and hard shells, and vice versa. Table 2.1 shows some of the applications of different core/shell particles.

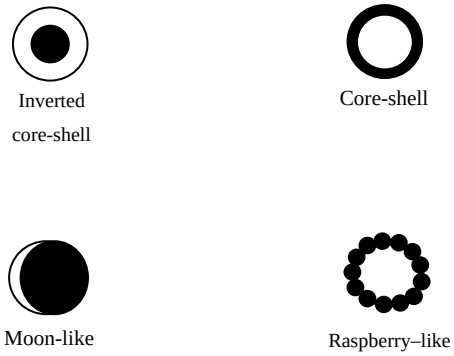

Figure 2.5: Some possible two-phase particle morphologies.

Table 2.1: Some applications of core/shell particles.[62]

Shell	Core	Application
Solid	Solid	Impact modifiers
		Drug release
Solid	Liquid	Controlled release
		Oxidation prevention
		Perfume trapping
		Carbonless copy paper
Liquid	Solid	Antifoams

Another important application of the core/shell concept is the ability to synthesize particles with hydrophobic cores encapsulated within a polymeric shell. This can be done by means of encapsulating hydrophobic materials such as hexadecane[54] or waxes[27] with a polymeric material. The resultant latices can exhibit high hydrophobicity, which can be used in many coating applications, for example, to reduce the unwanted penetration of water molecules through the coatings. This study focuses on the preparation of highly hydrophobic latices for use in coatings using the core/shell concept.

Analytical techniques such as TEM, SEM[62] and AFM have been widely used for the characterization of core/shell morphologies. Other techniques, such as solid-state NMR[63,64] and SAXS[65], have also been used. It is well known that TEM has been classically used in the characterization of these composite particles at a high level of resolution.[27,56,63] AFM[66,67] has also proven itself as a promising technique to qualify the morphology of single latex particles and to study latex dispersion films. AFM offers the advantage of working in a non-vacuum system and in an aqueous environment. These conditions are close to those being used in common industrial applications of latex films, such as barrier coatings.

2.2.3 Preparation of core/shell particles

In recent years, different techniques have been used to prepare core/shell particles. The most common process to synthesize these core/shell latex particles is two-stage seeded emulsion polymerization, which was the first general method used to prepare polymer latices having such structures.[68-71] In this case the second stage monomer is polymerized in the presence of the core seed latex. The latter can either be prepared in a separate step, in the so-called dead seeding, or *in situ* during the emulsion polymerization in a so-called live seeding. The mode of polymerization for the second stage is usually a seeded swelling batch or a semi-batch process.

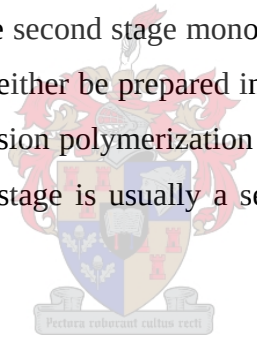

Core/shell particles can also be prepared by emulsion polymerization, using reactive surfactants that are able to copolymerize with the monomers. The resulting copolymers typically end up as a thin shell on the surface of the particles.[72-74] Other methods that have also been used to prepare core/shell particles include: suspension cross-linking,[75] coacervation,[76] solvent evaporation[77] and interfacial polymerization.[78]

The preparation of core/shell particles with hydrophobic cores, such as hexadecane or waxes, is difficult to achieve with the conventional emulsion polymerization process.[54] This is due to the high hydrophobicity and low water solubility of the core. In normal emulsion systems, no transport of the hydrophobic core component into micelles can take place, leading to phase separation. Miniemulsion polymerization, however, has been successfully used for the preparations of core/shell particles with hydrophobic cores such as hexadecane[54] or wax.[27] This was done by the initial dispersion of the hydrophobic component using a high shear device. The encapsulation was achieved by polymerization inducing phase separation

within minidroplets dispersed in an aqueous phase. Depending on the miniemulsion polymerization conditions, several possible morphologies i.e., morphologies in between the limits of complete phase separation and core/shell type particles, such as acorn or hemispherical, have been observed.[58] A schematic representation of the miniemulsion polymerization process and the formation of different morphologies, including core/shell is shown in Figure 2.6.

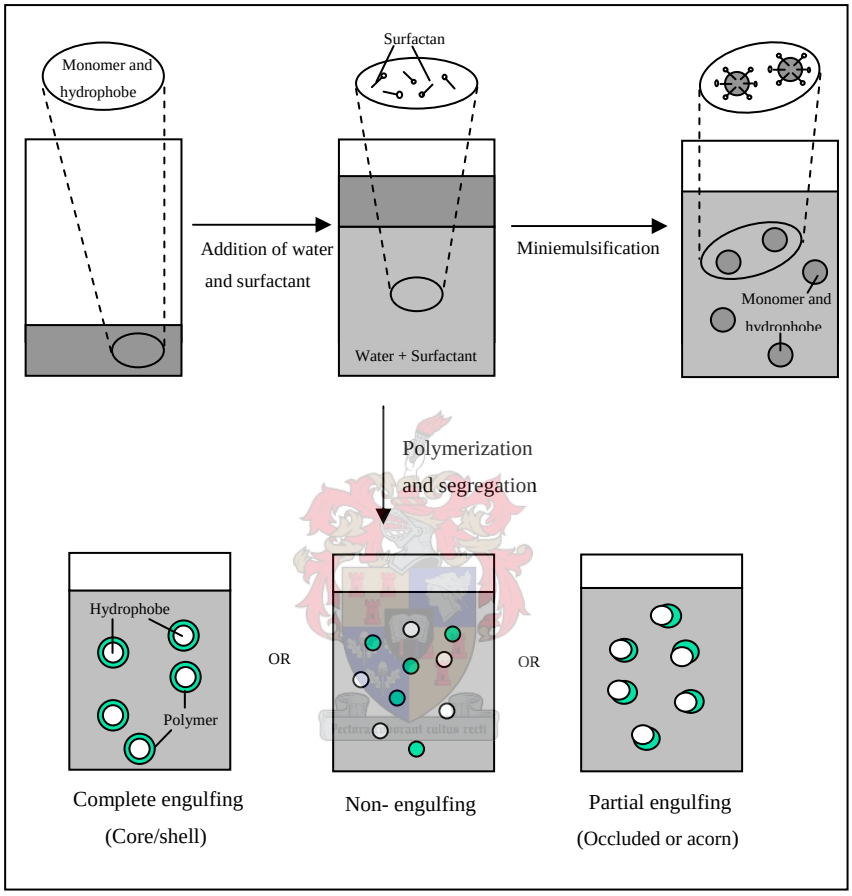

Figure 2.6: The principle of miniemulsion polymerization and the formation of different particle morphologies.[79]

In a recent study, Luo and Zhou[27] studied the nanoencapsulation of hydrophobic paraffin wax within a Sty/MAA copolymer using miniemulsion polymerization. It was found that both thermodynamic (amount and type of surfactant, amount of hydrophilic comonomer, and monomer/wax ratio) and kinetic factors (amount of crosslinking or chain transfer agent) all have a big influence on the latex morphology. The optimum levels of the surfactant as well as the hydrophilic comonomer were found to be 1.0 wt% with respect to the monomer phase. According to the thermodynamic perspective, increasing the hydrophilicity of the polymer chains should favour the encapsulation of the wax as it reduces the interfacial tension between the water and polymer and thus favours the encapsulation process.

Using 0.2 wt% of the transfer agent, particles presented a perfect core/shell morphology. In the presence of a chain transfer agent, polymer chains are shorter and have higher mobility. As a result of the increased chain mobility, the polymer chains can diffuse and overcome the kinetic barrier, leading to higher degree of phase separation, which in turn leads to more encapsulation. Changing the type of initiator from water-soluble (KPS) to oil-soluble (AIBN) had little effect on the morphology. Similarly, the solids content was found to have little effect on the morphology of the particles produced.

2.2.4 Prediction of particle morphology

Prediction of the final morphology of composite latex particles is important. The final product's properties depend largely on this morphology, that is, the arrangement of the polymers within the particles. Many publications report on the factors that influence the particle morphology in emulsion polymerization. In the preparation of poly(methyl methacrylate) (PMMA)/polyacrylonitrile (PAN) composite particles, Chen *et al.*[56] found that particles had different morphologies depending on the thermodynamic and kinetic polymerization parameters, which were predicted according to a mathematical model presented by Winzor and Sundberg[80] and Chen *et al.*[58-60]

In another publication Sundberg and Durant[81] reviewed the fundamental aspects of latex particle morphology. It was found that a great deal of basic understanding of the factors controlling the morphology had been achieved by applying equilibrium thermodynamics to phase separated particles in aqueous media. It was also found that interfacial tensions at the polymer-water interface and at the polymer–polymer interface, along with crosslinking density, were the dominant factors controlling the equilibrium morphology. However, much less progress has been made in understanding the development of non-equilibrium morphologies, where the possible number of particle structures is essentially infinite.

One theoretical approach for predicting the resulting particle morphology is to take advantage of the contributions of the interfacial and surface free energies which determine the thermodynamic driving forces for morphology development. The thermodynamic factors rely mainly on the interfacial energy between the core and shell surfaces. This means that the system attempts to minimize the overall surface free energy and the energy of molecular interaction. The thermodynamic aspects determine the equilibrium morphology based on

the minimum interfacial free energy change principle, which can be predicted by a mathematical model presented by Winzor and Sundberg[80] and Chen *et al.*[58-60] These thermodynamic factors are usually used to determine the equilibrium morphology of the final composite particles. On the other hand, kinetic factors such as the mobility of the polymer chains determine the ease with which the equilibrium morphology can be achieved. Parameters to be considered in controlling the particles morphology can be explained as follows:

2.2.4.1 Thermodynamic theory of particle formation

The key factor to be considered here is the equilibrium morphology, which determines the resulting structure provided that kinetic factors will favour the desired morphology. The most important parameter to consider is the contribution of the surface free energy. The latter can be influenced by the type of monomer used, the type and amount of surfactant used, the type and amount of initiator used for polymerization, the reaction temperature, and the difference in the hydrophobicity of the monomers used and polymers prepared.[52,60] The driving force to minimize the system's free energy often results in the more hydrophilic polymer forming on the outside of the particle, which keeps it in contact with the water phase, and thus reduces the interfacial free energy with respect to the situation where the hydrophilic polymer is found on the inside of the particle.

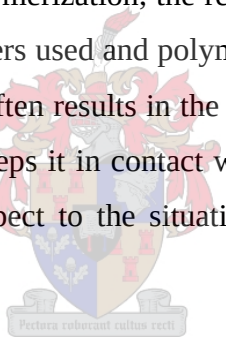

A thermodynamic theory, which was first studied by Torza and Mason in 1970,[82] is used to predict the morphology of the particles. The preferred morphology in this theory is that which has the lowest interfacial energy. Torza and Mason studied a system containing two immiscible liquids, phases 1 and 3, suspended in a third immiscible liquid, phase 2.

In their work they used the following equation to predict the particle morphology of the resultant latex:

$$S_i = \sigma_{jk} - (\sigma_{ij} + \sigma_{jk}) \qquad \textbf{(2.1)}$$

where S_i is the spreading coefficient, σ_{jk} is the interfacial tension between phase j and phase k, and σ_{ij} is the interfacial tension between phase i and phase j ($i \neq j \neq k = 1, 2, 3$).

It was found that if σ_{12} is greater than σ_{23}, then only three possible sets of values for S_i exist. These are:

$S_1<0; S_2<0; S_3>0$

$S_1<0; S_2<0; S_3<0$

$S_1<0; S_2>0; S_3<0$

These three sets of values correspond to the three possible equilibrium configurations which can be formed in this model: complete engulfment, partial engulfment and non-engulfment of the core phase. By adjusting the polymerization parameters one can prepare particles with the desired core/shell morphology provided that kinetic factors allow that. A schematic view of the different configurations with the assigned spreading coefficients is shown in Figure 2.7.

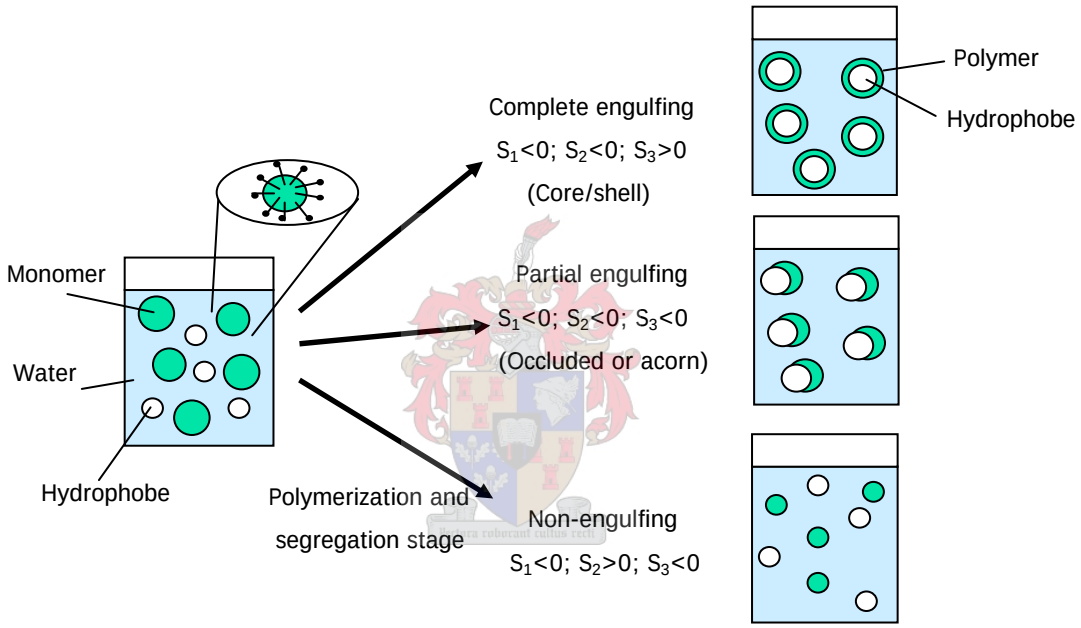

Figure 2.7: A schematic view of the possible morphologies according to the Torza and Mason thermodynamic theory.[5]

2.2.4.2 Kinetic theory of particle formation

In terms of kinetics, particle morphology is influenced by diffusion, relative rate of initiation, monomer consumption and phase rearrangements within the particles themselves. Factors to be considered are the degree of crosslinking, the viscosity at the polymerization locus, the monomer concentration, glass transition temperature, and reaction temperature. In most cases, the assumption is made that the equilibrium morphology of the final composite latex particle is determined by the thermodynamic factors while the kinetic factors will determine the ease with which the thermodynamically favoured morphology can be achieved. Mobility of the polymer chains plays an important role in determining the final morphology.

When the mobility of the polymer chains is restricted, phase separation and rearrangements of the polymer chains are slower than the polymerization rate. Hence, the predominant factors to control the particle morphology in such a case will be the kinetic factors. Non-equilibrium conditions often occur when the diffusion rate of radicals into particles, the phase separation, and the rearrangement of the polymer chains are slow compared to the rate of polymerization. Therefore, the development of particle morphology is then kinetically controlled.

Another important factor is the mobility of the entering oligomeric radicals. The non-equilibrium particle morphology of composite latex particles is very dependent on the mobility of these oligomeric radicals. Oligomeric radicals enter from the water phase and then penetrate into the polymer particles. If their diffusion rate or mobility is limited then the second stage polymer will form on the outside of the particle, making core/shell morphology more likely to occur. The work of Torza and Mason[82] can be considered as an example, where the key factor in controlling the equilibrium morphology is due to the high mobility of the liquid phases. Kinetic factors to be considered include the following:

i) Influence of anchoring effect induced by initiators

In 1985 Cho and Lee[83] studied the effect of different factors on the outcome of the particle morphology during polymerization reactions using electron microscopy. Monomers that were employed were MMA and Sty. It was found that the morphology of the studied particles could be controlled by changing the polymerization parameters. Factors that were investigated in their work included the anchoring effect of ionic terminal groups that are introduced into a sample through the use of an ionic initiator, pH, and viscosity in the polymerization locus. The authors found that the change in particle morphology was related to the type and concentration of initiator used and the polymerization temperature. Three initiators: KPS, AIBN, and 4,4´-azobis-(4-cyanovaleric acid) (ABCVA), were used in this study. The anchoring effect exerted by the ionic terminal groups introduced by ionic initiators was found to be the main factor in controlling the particle morphology. For instance, when the water-soluble initiator KPS was used, particles with core/shell morphologies were obtained. This was attributed to the anchoring effect of the terminal $-SO_4^-$ endgroup, leading to a surface-active oligomer, which anchors itself at the water/oil interface on entering the monomer droplet. Thus, the anchoring effect influenced the particle morphology.

ii) Influence of viscosity

The diffusional resistance, which is related to chain mobility, plays an important role in the rate of morphological change of the particles during the polymerization. The key factor here is the viscosity in the polymerization locus. A low viscosity in the interior of the latex particles will enhance the mobility of the polymer chains in the polymerization locus. In this case the low viscosity will increase the migration of the two immiscible phases into two different domains, which will lead to the thermodynamically favoured morphology. On the other hand, a high viscosity in the polymerization locus will decrease the degree of phase separation by creating a kinetic barrier towards polymer chain diffusion. This is most likely to occur when the T_g of at least one of the polymers is close or above the reaction temperature. Another case is when the monomer is fed slowly throughout the second stage polymerization. These conditions create an extremely high viscosity within the latex particles, which in turn makes it difficult for the two polymer phases to rearrange themselves into their thermodynamically favoured or equilibrium morphology.

According to Cho and Lee,[83] the determining factor in the generation of non-equilibrium morphologies will be the competition between phase separation and polymerization kinetics. It was found that viscosity in the polymerization locus controlled the mobility of the polymer molecules and hence the particle morphology. With a high viscosity in the polymerization locus the morphology was uneven, in which the polystyrene (PS)-rich domains were present in the PMMA-rich region. However, at low viscosity, clear phase separation between the PS-rich and PMMA-rich regions resulted, leading to a well-defined core/shell particle.

iii) Influence of polymer crosslinking

By crosslinking the polymer phase, the chain mobility is limited, which leads to the formation of composite particles that do not correspond to the minimum free energy. Then the non-equilibrium morphology is more stable because of the increased kinetic barrier to phase inversion. Sheu *et al.*[84] studied the preparation of uniform, non-spherical PS latex particles. They showed that phase separation in the resulting particles had occurred when crosslinked seed particles were used during the seeded emulsion polymerization of styrene, which led to the formation of non-spherical particles. Their study revealed that the kinetic effect led to limited phase separation occurring before polymerization. This effect increased with increasing monomer conversion.

2.3 Barrier coatings

2.3.1 Introduction

In addition to the physical properties of barrier coatings (such as porosity, smoothness and film formation), chemical characteristics are also of significance in coating applications. Coating is generally defined as the process by which a uniform layer is applied across a substrate. The most common reason for applying barrier coatings to a permeable material is to reduce the transmission rate of water and water vapour.

Wax emulsions and microemulsions are well established and extensively used in coating formulations.[85,86] They can be applied to numerous surfaces to reduce the unwanted penetration or interactions of numerous liquids (*e.g.* water and grease) and gases (*e.g.* oxygen and carbon dioxide). The term "wax" is applied to a large number of chemically different materials. Waxes are considered as organic, plastic-like substances that have the following features:

- Solid at ambient temperature, and becoming liquid when melted,
- Thermoplastic in nature,
- Combustible or flammable,
- Insoluble in water, which induces hydrophobic properties.

Waxes such as paraffin have many advantages that are useful for coating applications used as barrier materials. These are:

1. Water and water vapour resistance: These are the most important properties associated with paraffin wax.
2. Gas and odour barriers: In addition to good protection against moisture vapour, paraffin wax is a good barrier against odour and gas transmission.
3. Economy: Petroleum based waxes are very economical and their low viscosity requires relatively low machinery costs for application at high speeds.
4. Purity: Many grades of petroleum based wax are food grade, tasteless and odourless.

One problem encountered with waxes is that they are hard to emulsify and a single surfactant system is not sufficient. Fatty alcohols combined with anionic or non-ionic surfactants are most widely used for the emulsification of waxes.[87] One solution is to mix or blend a wax emulsion to a polymer emulsion such as acrylic emulsions. However, in this case there is the problem of surfactant compatibility when two different surfactant systems are used in each emulsion. In addition to compatibility problems, these latices require too much surfactant, which can be a limiting issue in terms of the barrier properties of the final films. Upon the evaporation of the water from the latex, surfactants tend to migrate to the surface of the coating, which increases the permeation of low molecular weight molecules, such as moisture vapour, through the coating.[88] Major drawbacks of using high surfactant concentrations are the water affinity of the surfactants and their tendency to migrate to the surface of the film, thus causing a decrease of the film's water resistance.[89] Excess surfactant presence during film formation can also result in improper particle packing and deformation, thereby leading to incomplete film formation and the presence of voids.[90] This causes high water uptake in the films, thus affecting the water resistance properties.

In this project wax-polymer latices with core/shell morphology were prepared to improve the barrier properties of polymeric coatings. This was done by the encapsulation of wax materials within a polymeric shell. These latices have some advantages over the other materials used in such applications. For instance, they are stable since only one surfactant is used to stabilize the latex. They also combine the properties of using wax emulsions and polymer emulsions in one stable system, since the wax is encapsulated inside the polymer structure.

In 2002,[91] core/shell latex particles containing minor amounts of wax material were used to prepare a resin composition having moisture-proof properties. This composition comprised latex particles having a core/shell structure that had a core of an aromatic vinyl compound (1-18C straight) and a branched or cyclic alkyl methacrylate copolymer (T_g of 60-95 ºC). The shell of the particles was mainly made from a styrene-butadiene copolymer having a T_g of 15-20 ºC. The latex was mixed with 1-7 parts (wt%) of paraffin wax emulsion, coated on a porous paper and dried at 105 ºC for 30 s. Permeability to moisture vapour was measured and a value of about 32 g/m^2/24 h was recorded. This is the closest available reference to the present study.

2.3.2 Barrier polymers

The use of polymers as barrier materials has become increasingly important due to the widespread use of polymeric films and rigid plastics for different applications, such as paints and coatings. The main purpose of using these polymers is to reduce the permeation of low molecular weight substances such as oxygen, water, and water vapour molecules. Barrier properties are determined by the rate of mass transport of these molecules through the polymer structure.

Polymers are not absolute barriers against water vapour, gases and organic substances. Their chemical nature is an important parameter determining their ultimate barrier properties. In addition, other physical factors may also affect the ultimate barrier properties. In general, barrier polymers can be defined as polymers that are able to restrict the passage of gases, vapours, and organic liquids through them. They are classified by the degree to which they restrict the passage of these gases and vapours (*e.g.*, oxygen and moisture vapour). The categories range from high barriers that exhibit low permeability, to low barriers that have high permeability.[92] On a molecular level, polymer chains must move aside to allow permeation. Therefore, the weaker the forces holding the polymer chains together, the more rapidly permeation will occur. These chain-to-chain interactions are determined partly by the chemical structure and nature of the polymer. On the other hand, highly branched monomers such as Veova can reduce the permeation process of a low molecular weight compound such as water in the polymers made from them. This can be attributed to the high hydrophobic nature of these monomers.[93]

The transport of low molecular weight molecules such as gases and vapours through a polymer film is affected by the solubility of these molecules in the polymer and their diffusion coefficients in the polymer.[94] The solubility is affected by the intermolecular forces between the polymer molecules and the low molecular weight molecule.[95] For example, films made from highly polar polymers such as those containing hydroxyl groups, *e.g.* poly(ethyl-co-vinyl alcohol), are excellent gas barriers but poor water and water vapour barriers.[96,97] It is mainly the hydrogen bonds formed between the polar hydroxyl groups that explain the high cohesive energy density of this film and its good gas barrier properties in the anhydrous state. However, these polar groups are also at the origin of the hydrophilic character of the polymer at high relative humidity.[97] In contrast, non-polar hydrocarbon

polymers such as polyethylene have excellent water and water vapour barrier properties but poor gas barrier properties. The latter property improves as the density of the polyethylene increases. In general, polymers must have the following properties in order to successfully be used as good barrier materials for coating applications:[98]

- Close chain-to-chain packing ability to improve polymer crystallinity,
- High chain stiffness to reduce diffusion,
- Inertness to the permeant, which means that polymers must not interact with the permeant molecules,
- Bonding or attraction between chains to reduce diffusion,
- High glass transition temperature (at least higher than the service temperature).

2.3.3 Permeability of polymeric coatings

The mechanism and transport behaviour of gases and water molecules through polymer films and membranes have attracted attention in recent years.[99] Generally speaking, the term permeability is used to describe the penetration of low molecular weight substances through a barrier. Permeability can be defined as the transmission of a permeant through a resisting material. For polymer films, permeability to gases and vapours is often important.[92] Most often the gases or vapours of interest are water vapour, oxygen, carbon dioxide, and nitrogen. Knowledge of the permeability properties of polymer materials for these low molecular weight compounds could lead to their improved utilization. For a specific permeant, the chemical composition and physical properties of the polymeric membrane determine the permeation properties, according to the following relationship:[94]

$$P = D \times S \qquad \textbf{(2.2)}$$

where P is the permeability, and D and S are the diffusion and solubility coefficients respectively.

From equation 2.2 one can see that permeability is influenced by the diffusion and solubility coefficients. A low permeability may result from a low diffusion coefficient or a low solubility coefficient, or both. These factors in turn can be greatly influenced by the chemical and physical structure of the polymer in use. In this regard, it is very important to investigate the relationship between the chemical and physical properties and the gas transport

behaviour, to explain the permeability behaviour of polymeric materials and coated polymeric films. One example is the permeation of water and water vapour through polymer films. Polymer films are often characterized in terms of their MVTR, that is, a measure of the passage of water in gaseous form through the film.

Generally, diffusion of moisture vapour is reduced significantly when the T_g of the polymer is increased and the solubility of moisture vapour is decreased as the hydrophobicity of the polymer is increased. As a result, permeability is decreased remarkably, as expected from equation 2.2. In addition, T_g influences the quality of the polymer films used as barrier coatings, which in turn can affect the barrier properties of the film. It is believed that to achieve continuous pore-free films from polymer latices, the latex particles must deform as water evaporates. The deformed particles must then coalesce after they have filled the volume formerly occupied by the water.[100] This film formation process depends on the difference between the application temperature and the MFFT, which in turn is related to the glass transition temperature of the polymer.

It is generally believed that gas permeability through a polymer membrane depends on interactions between the polymer material and gas molecules. Permeation, as shown in Figure 2.8, is a multistep process,[101] which includes:

- Adsorption
- Solution (Thermodynamic process)
- Diffusion (Kinetic process)
- Desorption

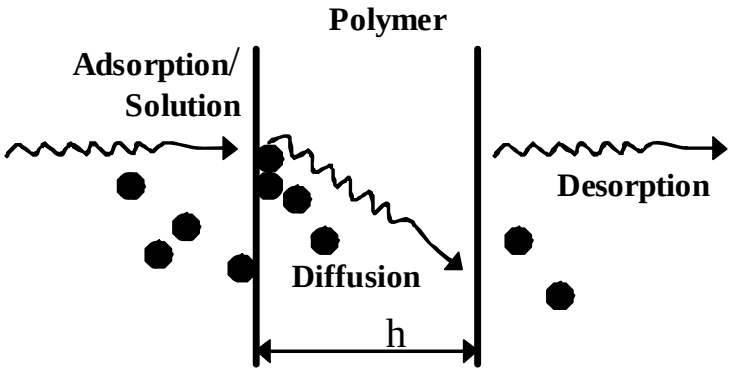

Figure 2.8: Permeation process in a polymer film of thickness h.

The crystalline content of a polymer is very important due to its influence on the polymer permeability. Amorphous polymers, which are incapable of efficient packing, lead to highly permeable membranes, while crystalline polymers such as linear polymers have better chain packing, which leads to low permeant permeability.[94] In a crystalline polymer, the diffusion is decreased, and hence permeability is also decreased. Tsuji *et al.*[102] observed that the water vapour transmission rate (WVTR) of poly(L-lactic acid) (PLLA) films decreased rapidly from 230 to 130 g/m^2/24 h when increasing the crystallinity from 0 to 20%. On the other hand, polymers with bulky groups in the backbone lead to poor packing ability, which leads to higher permeability. Mogri and Paul[99] focused on the barrier properties of polymeric materials with reference to amorphous, semi-crystalline and crystalline states. In their study, the gas permeability of poly(alkyl acrylate)s was measured as a function of temperature in both the amorphous and crystalline states. It was found that permeability in the amorphous state was affected by the chemical structure of the polymer. Results showed that permeability in the amorphous state increases as the side-chain length becomes longer, but showed mixed trends in the crystalline state. It was believed that differences in crystalline structure, crystalline morphology, and a constrained amorphous state contributed to the mixed trends.

Semi-crystalline polymers and blends have more complex behaviour than most other polymers. Permeability at the phase boundaries of polymer blends could differ from those in the bulks of the components. In a semi-crystalline polymer, diffusion of the penetrant typically occurs by passing around the crystals. The degree of crystallinity, crystallite size, shape, and orientation (overall morphology), all influence gas transport properties. If the penetrant cannot enter the crystal then the diffusion is said to be tortuous, since the path is not a random walk but rather the penetrant is often reflected at the crystal surface. Although gas sorption and permeation apparently proceed mainly in amorphous regions, some contribution is also provided by the more loosely packed crystalline regions.[103] The reason is related to the well-known behaviour of semi-crystalline materials, first described by Michaels and Bixler,[104] who showed that an increase in the content of the crystalline fraction in polyethylene leads to a decrease in permeability, diffusion, and solubility coefficients. It is believed that crystallites tend to impede penetrant mobility in the surrounding amorphous phase. Crystalline phases act as impermeable obstacles; therefore, their presence in a material makes diffusion paths across a membrane longer and more tortuous.

Cross-linking of polymer chains also affects the permeation properties of the polymer. It restricts their mobility, and thus decreases their permeability, due mainly to the decrease in the diffusion coefficient.[98] On the other hand, the presence of bulky substituents, which hinder bond rotation, enhance gas permeability. While the nature of the substituent influences permselectivity, permeability is related to interaction between the polymer and the permeant. Water, for example, is a unique penetrant; its polar nature enables it to form hydrogen bonds with itself and to interact strongly with polar groups of the polymer. In a water/polymer system, water permeability is influenced by not only the nature of water molecules, but also the hydrophobicity of polymer. Thus hydrophobic non-polar monomers lead to polymers with lower water permeability.

2.3.4 Effect of temperature and humidity on permeability

Permeability can be affected by several physical properties, such as humidity and temperature[105]. Many polymers, particularly those having polar groups, can absorb moisture from the atmosphere or from a liquid in contact with the polymer. Also, if such a polymer is in contact with a humid environment it absorbs water. This has the effect of swelling or plasticizing the polymer. Plasticization occurs when the polymer/water interactions are strong.[106] Plasticization or swelling increases polymer chain mobility and, in doing so, it increases the rate of penetrant transport in the material and reduces the barrier properties of the polymer. The ability of different polymers to absorb water from a humid environment depends on the type of polymer. For instance, water does not affect the permeabilities of some non-polar polymers, including polyolefins, vinylidene chloride copolymers and acrylonitrile copolymers.[94] In other polar polymers, including ethylene-vinyl alcohol copolymers and most polyamides, the permeability increases with increasing relative humidity. Permeability often also varies with temperature according to the Arrhenius equation:[105]

$$P = P_o \exp(-E_p / RT) \qquad \textbf{(2.3)}$$

where P_o is a constant, E_p is the activation energy for permeation, R is the gas constant, and T is the absolute temperature.

The temperature dependence of permeability is related to a diffusion coefficient and a solubility coefficient. This can be expressed by the following two equations:

$$D = D_o \exp(-E_d / RT) \quad \textbf{(2.4)}$$

$$S = S_o \exp(-\Delta H_{sol} / RT) \quad \textbf{(2.5)}$$

where D_o and S_o are constants, E_d is the activation energy for diffusion, and ΔH_{sol} is the heat of solution for the permeant in the polymer.

The temperature at which the barrier polymer is used can therefore also be of a great importance. For instance, if the polymer has a T_g higher than the application temperature, the polymer will be in its glassy state, and the segments will have little mobility. Thus, a diffusing molecule will have a much more tortuous path through the polymer, leading to a less permeable material. If the polymer has a T_g lower than the application temperature, the polymer will be in its amorphous state, leading to a more permeable material. Therefore, the recommended temperature of use will be below the T_g of the polymer, and the polymer will consequently have improved barrier properties.[103]

Pectora roborant cultus recti

2.4 References

(1) Landfester, K.; Bechthold, N.; Forster, S.; Antonietti, M. *Macromolecular Rapid Communications* **1999**, *20*, 81-84.

(2) Miller, C.; Sudol, E.; Silebi, C.; El-Aasser, M. *Journal of Polymer Science: Part A: Polymer Chemistry* **1995**, *33*, 1391-1408.

(3) Sudol, E.; El-Aasser, M. *Miniemulsion Polymerization*, In *Emulsion Polymerization and Emulsion Polymers*, Lovell, P.; El-Aasser, M., Eds.; John Wiley & Sons Ltd.: New York, 1997; pp 699-722.

(4) Soma, J.; Papadopoulos, K. *Journal of Colloid and Interface Science* **1996**, *181*, 225-231.

(5) Antonietti, M.; Landfester, K. *Progress in Polymer Science* **2002**, *27*, 689-757.

(6) Ugelstad, J.; El-Aasser, M.; Vanderhoff, J. *Journal of Polymer Science: Polymer Letters Edition* **1973**, *11*, 503-513.

(7) Hansen, F.; Ugelstad, J. *Journal of Polymer Science: Polymer Chemistry Edition* **1979**, *17*, 3069-3082.

(8) Rodriguez, V.; El-Aasser, M.; Asua, J.; Silebi, C. *Journal of Polymer Science: Part A: Polymer Chemistry* **1989**, *27*, 3659-3671.

(9) Kim, N.; Sudol, E.; Dimonie, V.; El-Aasser, M. *Macromolecules* **2004**, *37*, 2427-2433.

(10) Aizpurua, I.; Barandiaran, M. *Polymer* **1999**, *40*, 4105-4115.

(11) El-Aasser, M.; Sudol, E. *Features of Emulsion Polymerization*, In *Emulsion Polymerization and Emulsion Polymers*, Lovell, P.; El-Aasser, M., Eds.; John Wiley & Sons Ltd.: New York, 1997; pp 37-58.

(12) Schork, F.; Poehlein, G.; Wang, S.; Reimers, J.; Rodrigues, J.; Samer, C. *Colloids and Surfaces A: Physicochemical and Engineering Aspects* **1999**, *153*, 39-45.

(13) Wang, S.; Schork, F. *Journal of Applied Polymer Science* **1994**, *54*, 2157-2164.

(14) Reimers, J.; Schork, F. *Journal of Applied Polymer Science* **1996**, *59*, 1833-1841.

(15) Mouran, D.; Reimers, J.; Schork, F. *Journal of Applied Polymer Science* **1996**, *34*, 1073-1083.

(16) Tang, P.; Sudol, E.; Adams, M.; El-Aasser, M.; Asua, J. *Journal of Applied Polymer Science* **1991**, *42*, 2019-2028.

(17) Alduncin, J.; Forcada, J.; Asua, J. *Macromolecules* **1994**, *27* (8), 2256-2261.

(18) Choi, Y.; El-Asser, M.; Sudol, E.; Vanderhoff, J. *Journal of Polymer Science: Part A: Polymer Chemistry* **1985**, *23*, 2973-2987.

(19) Unzue, M.; Asua, J. *Journal of Applied Polymer Science* **1993**, *49*, 81-90.

(20) Masa, J.; Arbin, L.; Asua, J. *Journal of Applied Polymer Science* **1993**, *48*, 205-213.

(21) Landfester, K.; Bechthold, N.; Tiarks, F.; Antonietti, M. *Macromolecules* **1999**, *32*, 5222-5228.

(22) Delgado, J.; El-Aasser, M.; Vanderhoff, J. *Journal of Polymer Science: Part A: Polymer Chemistry* **1986**, *24*, 861-874.

(23) Lim, M.; Chen, H. *Journal of Polymer Science: Part A: Polymer Chemistry* **2000**, *38*, 1818-1827.

(24) Chern, C.; Chen, T. *Colloid and Polymer Science* **1997**, *275*, 546 - 554

(25) Miller, C.; Sudol, E.; Silebi, C.; El-Aasser, M. *Macromolecules* **1995**, *28* (8), 2754-2764.

(26) Miller, C.; Blythe, P.; Sudol, E.; Silebi, C.; El-Aasser, M. *Journal of Polymer Science: Part A: Polymer Chemistry* **1994**, *32*, 2365-2376.

(27) Luo, Y.; Zhou, X. *Journal of Polymer Science: Part A: Polymer Chemistry* **2004**, *42*, 2145-2154.

(28) Landfester, K.; Betchthold, N.; Tiarks, F.; Antonietti, M. *Macromolecules* **1999**, *32*, 2679-2683.

(29) Chern, C.; Liou, Y. *Polymer* **1999**, *40*, 3763-3772.

(30) Kitzmiller, E.; Miller, C.; Sudol, E.; El-Aasser, M. *Macromolecular Symposia* **1995**, *92*, 157-168.

(31) Asua, J. *Progress in Polymer Science* **2002**, *27*, 1283-1346.

(32) Abismail, B.; Canselier, J.; Wilhelm, A.; Delmas, H.; Gourdon, C. *Ultrasonics Sonochemistry* **1999**, *6*, 75-83.

(33) Wood, R.; Loomis, A. *Philosophical Magazine* **1927**, *4*, 417-436.

(34) Tang, P.; Sudol, E.; Silebi, C.; El-Aasser, M. *Journal of Applied Polymer Science* **1991**, *43*, 1059-1066.

(35) Bechthold, N.; Landfester, K. *Macromolecules* **2000**, *33*, 4682-4689.

(36) Saethre, B.; Mork, P.; Ugelstad, J. *Journal of Polymer Science: Part A: Polymer Chemistry* **1995**, *33*, 2951-2959.

(37) Wang, C.; Yu, N.; Chen, C.; Kuo, J. *Journal of Applied Polymer Science* **1996**, *60*, 493-501.

(38) Blythe, P.; Klein, A.; Phillips, J.; Sudol, E.; El-Aasser, M. *Journal of Polymer Science: Part A: Polymer Chemistry* **1999**, *37*, 4449-4457.

(39) Erdem, B.; Sudol, E.; Dimonie, V.; El-Aasser, M. *Journal of Polymer Science: Part A: Polymer Chemistry* **2000**, *38*, 4431-4440.

(40) Ouzineb, K.; Graillat, C.; McKenna, T. *Journal of Applied Polymer Science* **2005**, *97*, 745-752.

(41) Wu, X.; Schork, F. *Industrial & Engineering Chemistry Research* **2000**, *39*, 2855-2865.

(42) Schork, F.; Luo, Y.; Smulders, W.; Russum, J.; Butte, A.; Fontenot, K. *Advances in Polymer Science* **2005**, *175*, 129-255.

(43) Tauer, K.; Mueller, H.; Schellenberg, C.; Rosengarten, L. *Colloids and Surfaces A: Physicochemical and Engineering Aspects* **1999**, *153*, 143-151.

(44) Katsumoto, Y.; Ushiki, H.; Mendiboure, B.; Graciaa, A.; Lachaise, J. *Colloid and Polymer Science* **2000**, *278*, 905-909.

(45) Wang, X.; Sudol, E.; El-Aasser, M. *Macromolecules* **2001**, *34*, 7715-7723.

(46) Wang, X.; Sudol, E.; El-Aasser, M. *Langmuir* **2001**, *17*, 6865-6870.

(47) Bassett, D. *Journal of Coatings Technology* **2001**, *73*, 42-55.

(48) Balic, R. PhD thesis, University of Sydney: Sydney, Australia, 2000.

(49) Dimonie, V.; Daniels, E.; Shaffer, O.; El-Aasser, M. *Control of Particle Morphology*, In *Emulsion Polymerization and Emulsion Polymers*, Lovell, P.; El-Aasser, M., Eds.; John Wiley & Sons Ltd.: New York, 1997; pp 293-326.

(50) Nelliappan, V.; El-Aasser, M.; Klein, A.; Daniels, E.; Roberts, J.; Pearson, R. *Journal of Applied Polymer Science* **1997**, *65*, 581-593.

(51) Lu, M.; Keskkula, H.; Paul, D. *Polymer* **1996**, *37*, 125-135.

(52) Stubbs, J.; Sundberg, D. *Journal of Coatings Technology* **2003**, *75*, 59-67.

(53) Schuler, B.; Baumstark, R.; Kirsch, S.; Pfau, A.; Sandor, M.; Zosel, A. *Progress in Organic Coatings* **2000**, *40*, 139-150.

(54) van Zyl, A.; Sanderson, R.; de Wet-Roos, D. ; Klumperman, B. *Macromolecules* **2003**, *36* (23), 8621-8629.

(55) Meng, F.; Hiemstra, C.; Engbers, G.; Feijen, J. *Macromolecules* **2003**, *36*, 3004-3006.

(56) Chen, W.; Zhu, M.; Song, S.; Sun, B.; Chen, Y.; Adler, H. *Macromolecular Materials and Engineering* **2005**, *290*, 669-674.

(57) Kirsch, S.; Doerk, A.; Bartsch, E.; Sillescu, H.; Landfester, K.; Spiess, H.; Maechtle, W. *Macromolecules* **1999**, *32*, 4508-4518.

(58) Chen, Y.; Dimonie, V.; El-Aasser, M. *Journal of Applied Polymer Science* **1991**, *42*, 1049-1063.

(59) Chen, Y.; Dimonie, V.; El-Aasser, M. *Macromolecules* **1991**, *24* (13), 3779-3787.

(60) Chen, Y.; Dimonie, V.; Shaffer, O.; El-Aasser, M. *Polymer International* **1993**, *30*, 185-194.

(61) Chen, Y.; Dimonie, V.; El-Aasser, M. *Journal of Applied Polymer Science* **1992**, *45*, 487-499.

(62) Loxley, A.; Vincent, B. *Journal of Colloid and Interface Science* **1998**, *208*, 49-62.

(63) Kirsch, S.; Landfester, K.; Shaffer, O.; El-Aasser, M. *Acta Polymerica* **1999**, *50*, 347-362.

(64) Landfester, K.; Boeffel, C.; Lambla, M.; Spiess, H. *Macromolecules* **1996**, *29*, 5972-5980.

(65) Dobashi, T.; Yeh, J.; Ying, Q.; Ichikawa, K.; Chu, B. *Langmuir* **1995**, *11*, 4278-4282.

(66) Schellenberg, C.; Akari, S.; Regenbrecht, M.; Tauer, K.; Petrat, F.; Antonietti, M. *Langmuir* **1999**, *15*, 1283-1290.

(67) Sommer, F.; Duc, T.; Pirri, R.; Meunier, G.; Quet, C. *Langmuir* **1995**, *11*, 440-448.

(68) Winnik, M.; Zhao, C.; Shaffer, O.; Shivers, R. *Langmuir* **1993**, *9*, 2053-2066.

(69) Stutman, D.; Klein, A.; El-Aasser, M.; Vanderhoff, J. *Industrial & Engineering Chemistry Product Research and Development* **1985**, *24*, 404-412.

(70) Hughes, L.; Brown, G. *Journal of Applied Polymer Science* **1961**, *5*, 580-588.

(71) Grancio, M.; Williams, D. *Journal of Polymer Science: Part A-1* **1970**, *8*, 2617-2629.

(72) Busci, A.; Forcada, J.; Gibanel, S.; Heroguez, V.; Fontanille, M.; Gnanou, Y. *Macromolecules* **1998**, *31* (7), 2087-2097.

(73) Roy, S.; Favresse, P.; Laschewsky, A.; de-la-Cal, J.; Asua, J. *Macromolecules* **1999**, *32* (8), 5967-5969.

(74) Guyot, A.; Tauer, K. *Advances in Polymer Science* **1994**, *111*, 43-65.

(75) Arshady, R. *Polymer Engineering and Science* **1989**, *29*, 1746-1758.

(76) Arshady, R. *Polymer Engineering and Science* **1990**, *30*, 905-914.

(77) Arshady, R. *Polymer Engineering and Science* **1990**, *30*, 915-924.

(78) Frere, Y.; Danicher, L.; Gramain, P. *European Polymer Journal* **1998**, *34*, 193-199.

(79) Tiarks, F.; Landfester, K.; Antonietti, M. *Langmuir* **2001**, *17*, 908-918.

(80) Winzor, C.; Sundberg, D. *Polymer* **1992**, *33*, 3797-3810.

(81) Sundberg, D.; Durant, Y. *Polymer Reaction Engineering* **2003**, *11* (3), 379-432.

(82) Torza, S.; Mason, S. *Journal of Colloid and Interface Science* **1970**, *33*, 67-83.

(83) Cho, I.; Lee, K. *Journal of Applied Polymer Science* **1985**, *30*, 1903-1926.

(84) Sheu, H.; El-Aasser, M.; Vanderhoff, J. *Journal of Polymer Science: Part A: Polymer Chemistry* **1990**, *28*, 629-651.

(85) Hagenmaier, R.; Baker, R. *Journal of Agricultural and Food Chemistry* **1994**, *42*, 899-902.

(86) Hagenmaier, R.; Shaw, P. *Journal of Agricultural and Food Chemistry* **1991**, *39*, 1705-1708.

(87) Eccleston, G. *Colloids and Surfaces A: Physicochemical and Engineering Aspects* **1997**, *123-124*, 169-182.

(88) Holmberg, K.; Jonsson, B.; Kronberg, B.; Lindman, B. *Surfactants and Polymers in Aqueous Solution*. Second ed.; John Wiley & Sons Ltd.: England, 2003; pp 227-259.

(89) Mulvihill, J.; Toussaint, A.; Wilde, M. *Progress in Organic Coatings* **1997**, *30*, 127-139.

(90) Keddie, J. *Materials Science and Engineering* **1997**, *21*, 101-170.

(91) Mitsuru, D.; Hideo, T. Japanese Patent 2002339289, **2002**.

(92) Combellick, W. *Barrier Polymers*, In *Encyclopedia of Polymer Science and Engineering*, Mark, H.; Bikales, N.; Overberger, C.; Menges, G., Eds.; John Wiley & Sons, Inc.: New York, 1985; pp 176-192.

(93) Vandezande, G.; Smith, O.; Bassett, D. *Vinyl Acetate Polymerization*, In *Emulsion Polymerization and Emulsion Polymers*, Lovell, P.; El-Aasser, M., Eds.; John Wiley & Sons Ltd.: New York, 1997; pp 593-587.

(94) Delassus, P. *Barrier Polymers*, In *The Wiley Encyclopedia of Packaging Technology*, Brody, A.; Marsh, K., Eds.; John Wiley & Sons, Inc.: New York, 1997; pp 71-77.

(95) Mills, N. *Plastics Microstructure Properties and Applications*. Edward Arnold Ltd.: 1986; pp 225-226.

(96) Zhang, Z.; Britt, I.; Tung, M. *Journal of Applied Polymer Science* **2001**, *82*, 1866-1872.

(97) Zhang, Z.; Britt, I.; Tung, M. *Journal of Polymer Science: Part B: Polymer Physics* **1999**, *37*, 691-699.

(98) Sangaj, N.; Malshe, V. *Progress in Organic Coatings* **2004**, *50*, 28-39.

(99) Mogri, Z.; Paul, D. *Polymer* **2001**, *42*, 7765-7780.

(100) Toussaint, A.; De Wilde, M.; Molenaar, F.; Mulvihill, J. *Progress in Organic Coatings* **1997**, *30*, 179-184.

(101) Hernandez, R. *Polymer Properties*, In *The Wiley Encyclopedia of Packaging Technology*, Brody, A.; Marsh, K., Eds.; John Wiley & Sons, Inc.: New York, 1997; pp 758-765.

(102) Tsuji, H.; Okino, R.; Daimon, H.; Fujie, K. *Journal of Applied Polymer Science* **2006**, *99*, 2245-2254.

(103) Alentiev, A.; Drioli, E.; Gokzhaev, M.; Golemme, G.; Ilinich, O.; Lapkin, A.; Volkov, V.; Yampolskii, Y. *Journal of Membrane Science* **1998**, *138*, 99-107.

(104) Michaels, A.; Bixler, H. *Journal of Polymer Science* **1961**, *50*, 393-413.

(105) DeLassus, P. *Barrier Polymers*, In *Encyclopedia of Chemical Technology*, Howe-Grant, M., Ed.; John Wiley & Sons, Inc.: New York, 1992; pp 931-962.

(106) Stacye, R.; Mary, E. *Polymer* **2004**, *45*, 2641-2649.

CHAPTER 3

EXPERIMENTAL

3.1. Introduction

In this chapter the experimental methods used to synthesize and characterize the core/shell latices are described. Miniemulsion polymerization was successfully used for the preparation of latex particles with core/shell morphology. This was done by the encapsulation of different waxes and an oil with hydrophobic monomers, using an *in situ* miniemulsion polymerization reaction. Monomers that were used include MMA, BA and Veova-10.

In addition to the common hydrophobe, HD, typically used in miniemulsion,[1,2] two different types of wax were used as the core of the particles. Waxes that were used include paraffin wax (PW 58/60, mp: 58-60 ºC) and microcrystalline wax (Microwax 40/60, mp range: 40-70 ºC). Typical differential scanning calorimetry (DSC) scans showing the crystallization and melting peaks of the two waxes are shown in Appendix 1. The purpose was to see the effect of the hydrophobicity and crystalline content of these two waxes on the hydrophobicity and barrier properties of the final polymer films in terms of water and water vapour penetration. The wax in all formulations, except those in which HD was used, was used as a hydrophobe and a replacement for the standard inert cosurfactant, HD.[3] The properties of the two waxes used, according to the manufacturer, are shown in Table 3.1.

Paraffin and microcrystalline waxes are both derived from petroleum. However, they differ in that paraffin wax consists principally of normal alkanes, while microcrystalline wax contains substantial proportions of branched and cyclic saturated hydrocarbons, in addition to normal alkanes (see Figure 3.1).[4,5]

Paraffin waxes contain predominantly straight-chain hydrocarbons, with an average chain length of 20 to 30 carbon atoms. They are characterized by a clearly defined crystal structure and have the tendency to be hard and brittle.

Table 3.1: Paraffin and microcrystalline wax properties according to the manufacturer (Pac. Chem. Cc.).

Wax	Type	Melting point (ºC)	Degradation temperature (ºC)	Contact angle with water (º)
PW 58/60	Semi-refined paraffin	58-60	308	106
Microwax 40/60	Microcrystalline	40-70	411	98

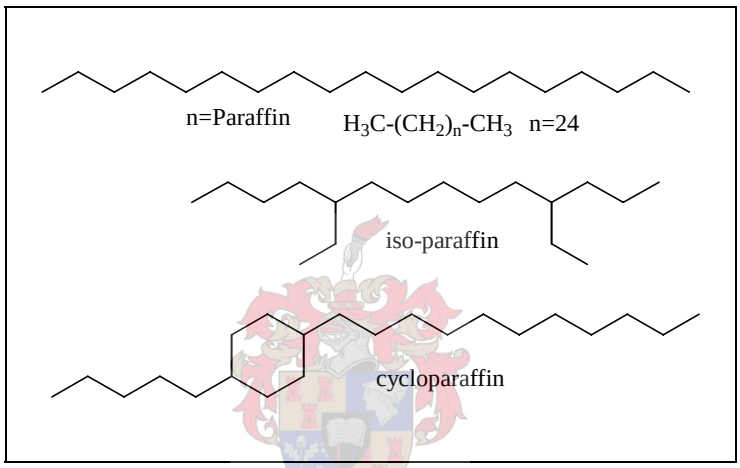

Figure 3.1: Different hydrocarbons found in paraffin and microcrystalline waxes.

Microcrystalline waxes on the other hand differ from paraffin waxes in that they have poorly defined crystalline structure and very minute crystals or micro crystals, they are of darker colour, and generally have higher viscosities and melting points. Microcrystalline waxes tend to vary much more widely than paraffin waxes with regard to physical characteristics. They can range from being soft and tacky to being hard and brittle, depending on the compositional balance.

The effects of the following on the hydrophobicity and barrier properties, in terms of water and moisture vapour of the resultant polymer films, were investigated: the amount of surfactant used, the wax/polymer ratio, the amount of Veova-10 monomer (the most hydrophobic monomer), the molecular weight of the resulting copolymers, and the degree of crosslinking of the copolymer shell.

The copolymers were obtained by polymerizing Veova-10 (30 wt%) with MMA (38 wt%) and BA (32 wt%) in batch miniemulsion polymerization. This composition gives copolymers with theoretical T_g values of about 8.5 ºC (a real T_g of about 8 ºC measured by DMA is shown in Appendix 3). KPS (0.15 wt% relative to monomer) was used as an initiator, and the polymerization was carried out at 85 ºC over 3 hours. In all experiments (except for the surfactant variation series, in Section 3.3.1), 1 wt% sodium dodecylbenzene sulfonate (SDBS) relative to monomer was used as a surfactant to stabilize the latices.

Particle morphology was determined by using two different methods, including TEM and AFM. TEM was used to directly visualize the particle morphology, while AFM was used as an imaging tool to monitor the film formation processes of the synthesized latices and to determine their particle morphologies. In addition to topographic and phase information obtained by AFM, it was also possible to display the particles in a three-dimensional view, with a nanometer resolution, which gave more information on the films prepared.

The hydrophobicity of the polymer films made from the synthesized latices was determined from static contact angle measurements. Conductivity measurements were used to infer information about the migration of surfactant molecules to the films' surfaces. Water uptake was also used to obtain an indication about the water affinity of the final films produced. Barrier properties of the final polymer films were measured by using the MVTR test as indicated in Appendix 2. In the following sections the formulations, preparation and characterization of the core/shell latices that were prepared are described.

3.2. Materials

The monomers vinyl neodecanoate (Veova-10, Aldrich, 99%), butyl acrylate (BA, Aldrich, 99%), and methyl methacrylate (MMA, Aldrich, 99%) were all washed with 0.3M potassium hydroxide (KOH, Associated Chemical Enterprises, 85%) solution, followed by distillation under reduced pressure in order to remove the inhibitor. The monomers were further washed with deionized water, dried using $MgSO_4$, and stored at -5 °C prior to use. Sodium dodecylbenzene sulfonate (SDBS, Rhodacal DS/4-E25, Rhodia HPCII), potassium persulfate (KPS, Aldrich, 99.99%), sodium bicarbonate ($NaHCO_3$, R&S Scientific 99.5%), Microwax 40/60 (Pac. Chem. Cc.), Paraffin wax 58/60 (Pac. Chem. Cc.), hydrochloric acid (HCl, Aldrich, 37% in water), methanol (Aldrich 98%), tetrahydrofuran (THF, Chromasolv,

Aldrich, 99.9%), deuterated chloroform ($CDCl_3$, Aldrich, 99.8%), and hexadecane (Aldrich, 99%) were all used as received, without any further purification. Distilled deionized (DDI) water, obtained from a Milli-Q purification system, was used for the preparation of all miniemulsions.

3.3. Latex synthesis

Veova-10 (4.0 g), BA (4.2 g), MMA (4.99 g), and HD or wax were premixed with a sodium bicarbonate (used as buffer) and SDBS/water solution. The mixture was first stirred for 10 minutes (pre-emulsification) and then sonicated using a Sonics & Materials Inc. Vibracell VCX 750 ultrasonicator for 15 minutes, at 90% amplitude, a pulse rate of 2.5 s, and a cut-off temperature of 60 ºC when paraffin wax was used and 70 ^{o}C when microcrystalline wax was used. This was done in order to avoid wax phase separation due to crystallization during sonication (T_m of paraffin wax ~ 58-60 ^{o}C, T_m of microcrystalline wax ~ 40-70 ^{o}C). After miniemulsification, the solution was immediately transferred to a 100-ml three neck flask and suspended in an oil bath heated to 60 ^{o}C when paraffin wax was used and 70 ^{o}C when microcrystalline wax was used. The miniemulsion was degassed for 30 minutes, the temperature was raised to 85 ^{o}C and the initiator KPS (0.0133 g) was added. The reaction was carried out for 3 h under a nitrogen atmosphere after which it was cooled to room temperature. A typical formulation recipe for the latex synthesis is tabulated below (see Table 3.2).

Table 3.2: Miniemulsion formulation recipe for the synthesis of core-shell wax/polymer latices.

Reagents	**Weight (g)**
Veova-10	4.0
BA	4.2
MMA	4.99
SDBS	0.13 (1.0 wt%/oil phase)
HD or Wax	1.4 (10 wt%/oil phase)
$NaHCO_3$	0.026
KPS	0.0133 (0.1 wt%/oil phase)
DDI water	28.5

The theoretical T_g value of the glass transition temperature of the copolymer was calculated by using the Fox equation:[6]

$$\frac{1}{T_{g(copolymer)}} = \frac{w_1}{T_{g_1}} + \ldots + \frac{w_i}{T_{gi}} \qquad \textbf{(3.1)}$$

In this equation, T_g is the glass transition temperature of the resultant copolymer, T_{gi} is the glass transition of the constituent monomer's homopolymer and w_i is the weight fraction of that particular monomer in the copolymer composition. The T_gs values of the monomers used were 115 ºC for MMA, -54 ºC for BA and -3 ºC for Veova-10.[7,8]

In order to investigate the effects of the following on the hydrophobicity and barrier properties of the polymer films prepared, a series of reactions were carried out: (i) the amount of surfactant was varied, (ii) the wax/polymer ratio was varied, (iii) the amount of Veova-10 monomer (the most hydrophobic monomer) was varied, (iv) the molecular weight of the resulting copolymer was varied and (v) the degree of crosslinking of the copolymer shell was varied. The reactions that were carried out are described in Sections 3.3.1-3.3.5.

3.3.1 Variation of the amount of surfactant used

Different quantities of SDBS were used as surfactant, including 0.5, 1.0, 1.5, 2.0, 2.5 and 3.0 wt% relative to the total amount of monomer used (13.19 g). In all of these experiments, 10% paraffin wax was used as the core, and MMA/BA/Veova-10 copolymers as the shell of the particles. Table 3.3 shows the quantities of SDBS used, and the relative percentages to the total amount of monomers used, to investigate the effect of surfactant concentration on the hydrophobicity and barrier properties of the final core/shell latex films to water and water vapour.

Table 3.3: Quantities of SDBS used to investigate the effect of surfactant concentration on the hydrophobicity and barrier properties of the final polymer films.

Experiment Code	Quantity of SDBS (g)	Percentage SDBS (wt%)
Hus 1	1.60	3.0
Hus 2	1.32	2.5
Hus 3	1.08	2.0
Hus 4	0.80	1.5
Hus 5	0.52	1.0
Hus 6	0.28	0.5

3.3.2 Variation of the amount and type of wax used

A series of experiments in which the ratio of wax/polymer was 10, 20, 30, 40 and 50 wt% was carried out to investigate the effect of the amount of wax on the barrier and hydrophobicity properties of the final polymer films with respect to water and water vapour molecules. Two different waxes, namely paraffin wax (mp: 58-60 ºC) and microcrystalline wax (mp: 40-70 ºC), were used in order to investigate the effect of the type of wax on the barrier properties and the hydrophobicity of the final polymer films. Tables 3.4 and 3.5 show the quantities and percentages of paraffin and microcrystalline wax (relative to the total amount of monomers) used to investigate the effect of type and wax content on the hydrophobicity and barrier properties of the resulting films to water and water vapour respectively.

Table 3.4: Quantities of the paraffin wax used to investigate the effect of type and wax content on the hydrophobicity and barrier properties of the final polymer films.

Experiment Code	Quantities of wax (g)	Percentage wax (wt%)
Hus 7	1.32	10
Hus 8	2.64	20
Hus 9	3.96	30
Hus 10	5.28	40
Hus 11	6.60	50

Table 3.5: Quantities of the microcrystalline wax used to investigate the effect of type and wax content on the hydrophobicity and barrier properties of the final polymer films.

Experiment Code	Quantities of wax (g)	Percentage wax (wt%)
Hus 12	1.32	10
Hus 13	2.64	20
Hus 14	3.96	30
Hus 15	5.28	40
Hus 16	6.60	50

3.3.3 Variation of the molecular weight of the copolymer shell

In an attempt to determine the effect of the molecular weight of the copolymer shell on the hydrophobicity and permeation properties of the resultant polymer films to water and

moisture vapour molecules, copolymers with different molecular weights were prepared. In order to obtain copolymers with different molecular weights, different quantities of the transfer agent (1-dodecanethiol) were used in the polymerization. Table 3.6 shows the amounts and the relative percentages of the transfer agent used in all experiments.

Table 3.6: Quantities and percentages of the transfer agent (1-dodecanethiol) used to investigate the effect of the molecular weight of the copolymer shell on the hydrophobicity and barrier properties of the final polymer films.

Experiment Code	Amount of transfer agent (1-dodecanethiol) (g)	Percentage 1-dodecanethiol (wt%)
Hus 17	0.0066	0.015
Hus 18	0.014	0.100
Hus 19	0.020	0.150
Hus 20	0.027	0.200
Hus 21	0.033	0.250

3.3.4 Variation of the amount of Veova-10 monomer

The amount of Veova-10 monomer (the most hydrophobic monomer used) was varied, to include 10, 20, 30, 40, 50 and 60 wt% relative to the total amount of monomer. A 1:1 ratio of the other two monomers (MMA and BA) was used in all experiments. This was done in an attempt to determine the effect of Veova-10 monomer on the hydrophobicity and permeation properties of the resultant films in terms of water and moisture vapour. Table 3.7 shows the amounts and percentages of Veova-10 monomer used in all experiments.

Table 3.7: Quantities and percentages of Veova-10 monomer used to investigate the effect of the most hydrophobic monomer on the hydrophobicity and barrier properties of the resultant polymer films.

Experiment Code	Amount of Veova-10 monomer (g)	Percentage Veova-10 monomer (wt%)
Hus 22	1.319	10
Hus 23	2.638	20
Hus 24	3.957	30
Hus 25	5.276	40
Hus 26	6.595	50
Hus 27	7.914	60

3.3.5 Variation of the crosslinking in the copolymer shell

The amount of crosslinking agent (ethylene glycol dimethacrylate, EGDMA) was varied; including 2, 4, 6, 8, 10 and 12 wt% relative to the total amount of monomers (see Table 3.8). This was done in an attempt to see the effect of crosslinking in the copolymer on the hydrophobicity and permeation properties of the resultant polymer films to water and water vapour molecules.

Table 3.8: Quantities and percentages of EGDMA used to investigate the effect of the degree of crosslinking in the copolymer shell on the hydrophobicity and barrier properties of the resultant polymer films.

Experiment Code	Amount of EGDMA (g)	Percentage of EGDMA (wt%)
Hus 28	0.265	2
Hus 29	0.530	4
Hus 30	0.795	6
Hus 31	1.060	8
Hus 32	1.320	10
Hus 33	1.583	12

3.4 Analytical techniques and measurements

Various analytical techniques were used for the characterization of the resultant polymer latices. The analytical methods that were employed in this study and the purpose of using them are listed below.

- Size-exclusion chromatography (SEC) was used to determine the molecular weight of the copolymers involved.
- Transmission electron microscopy (TEM) was used to determine latex particle sizes and their particle morphologies.
- Atomic force microscopy (AFM) was employed for the confirmation of core/shell particles formation and to study their film formation behaviour.
- Dynamic light scattering (DLS) was used to determine the particle size of the synthesized latices.

- Contact angle values were used to infer the hydrophobicity of the final polymer films' surface.
- Conductivity measurements were used to obtain information about surfactant migration in the final films.
- Water uptake measurements were used to determine the water affinity of the resultant polymer films.
- MVTR tests were used to measure the permeation properties of the final polymer films in terms of moisture vapour.

3.5. Latex characterization

Characterization of the polymer latices that were prepared was performed using various methods. Particle morphology was determined by TEM and AFM analyses. Other latex information was obtained by using techniques such as SEC and DLS. Water affinity was determined by using water uptake measurements. Surfactant migration information was obtained from conductivity measurements. Hydrophobicity of the final films was determined using contact angle measurements. MVTR tests were used to determine the barrier properties of the resultant polymer membranes in terms of moisture vapour. The following determinations were carried out:

Pectora roborant cultus recti

3.5.1 Particle size: The particle size of the latices was determined by dynamic light scattering at 25 °C using a Malvern Instruments Zetasizer 1000 HAS with a fixed scattering angle of 90°, assuming a monomodal distribution. Latex samples were prepared by diluting a drop of the respective latex in distilled deionized water (~4 ml). The instrument was first calibrated with a nano-standard solution with a particle size of 220 nm, before a latex sample was run.

3.5.2 Solids content: The solids content of the latices was determined by drying ~ 0.3 g of the latex at 180 °C in a Moisture Analyzer (HR73) for 15 minutes. Solids content was measured as follows:

$$\text{Solids content (\%)} = \frac{X_1 - X_2}{X_1} \times 100 \qquad \textbf{(3.2)}$$

where X_1 and X_2 are the latex weight before and after drying respectively.

3.5.3 Molar mass distributions: Molar mass distributions were measured via size exclusion chromatography (SEC). The latices were precipitated with concentrated hydrochloric acid, the precipitate was washed several times with methanol, then with deionized water, and finally dried under reduced pressure. The dried latex samples were dissolved in HPLC-grade THF (5 mg/ml) for 24 h and filtered through a 0.45-μm nylon filter. The SEC system used for the analyses comprised a Waters 610 Fluid Unit, Waters 410 Differential Refractometer at 30 °C, Waters 717_{plus} Autosampler and Waters 600E System Controller (run by Millenium^{32} V3.05 software). THF (HPLC-grade) sparged with IR-grade helium was used as an eluent at a flow rate of 1 ml/min. Two PLgel 5 μm Mixed-C columns and a PLgel 5 μm Guard pre-column were used. The column oven was kept at 35 °C and the injection volume was 100 μl. The system was calibrated with narrow poly(methyl methacrylate) standards (5 mg/ 1 ml THF), ranging from 2 500 to 898 000 g mol^{-1}.

3.5.4 Transmission electron microscopy (TEM): Transmission electron microscopy images were obtained from a JEOL 200 CX instrument at the University of Cape Town. To better define the particles edges, the diluted latex samples (0.05%) were stained with the negative staining uranyl acetate (UAc). A drop of each diluted sample was mixed with a drop of UAc solution (2%), and then mounted on 200-mesh copper grids. The copper grids were left to dry at room temperature before the analysis was performed. No further staining was applied to the dried latex particles. Contrast between the core and the shell domains was the result of the different path length and material densities of the constituting materials. This resulted in increased scattering of the incident e^--beam from the core material, resulting in a darker region on the TEM images.

In the case of preferential staining, the latex was additionally stained with the staining agent ruthenium tetroxide (RuO_4) to enhance the contrast of the copolymer shell, in addition to the negative staining agent UAc to define particle edges. A drop of the diluted latex (0.05%) was mixed with a drop of a mixture of UAc solution (2%) and RuO_4 solution (1%). A drop of the resultant mixture was then mounted on 200-mesh copper grids. The copper grids were left to dry at room temperature before the analysis was performed.

3.5.5 Hydrophobicity: The hydrophobicity of the polymer films was determined from static contact angle measurements. Contact angle measurements were made using a

stereomicroscope (Nikon SMZ-2T, Japan), connected to a camera. A 1 μL drop of deionized water was placed on the flat surface of a polymer film. The films were prepared by drying ~3 ml of the latex in an aluminum pan for 24 h at a temperature of about 100 ºC. A photograph of each drop was then taken with computer software (Scion Image). The contact angle of the water droplet with the surface of the film was then measured and reported as an angle theta (θ) (see Figure 3.2). The average contact angle values for each sample were based on the average contact angles from the pictures of 10 drops of water, using the formula:

$$Tan(\theta / 2) = h/r \qquad \textbf{(3.3)}$$

where h is the height of the drop and r its radius at the interface with the polymer film surface (see Figure 3.2).

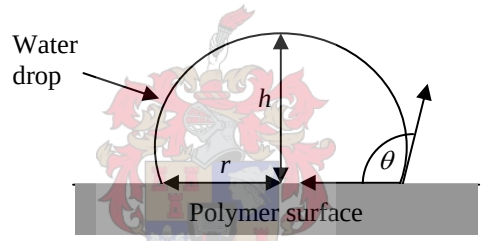

Figure 3.2: Contact angle (θ) of a water drop on a polymer surface.

3.5.6 Atomic force microscopy (AFM): Atomic force microscopy images were obtained from a Veeco MultiMode AFM instrument in non-contact mode. Latices with copolymer shells, which have T_g values of about 25 ºC were used. The MMA/BA/Veova-10 ratio in the copolymer shell was varied in order to have the desired T_g value. The latex films were typically cast below their T_g by putting a drop of the latex onto a silicon wafer. The latex was then spread onto the silicon wafer using a microscope slide and dried at room temperature to remove the water. A sequence of AFM images was then acquired using AFM in the tapping mode to monitor the film formation process, from which the shell domains of the core/shell particles can be seen. After the films were entirely dry, the temperature was increased to above the T_g of the copolymer shell to show the wax core domains. As soon as the copolymer shell reaches its T_g particles start to coalesce, leading to the wax core becoming visible as it becomes exposed to the surface. AFM images of the resultant film

were also recorded at a higher temperature of about 50-60 ºC at which the wax cores will start to melt, forming a flat film.

In contrast to the standard contact mode, AFM in tapping mode scans the surface morphology of the core/shell particles with no damage, leading to images with a remarkable quality and resolution. Both topography and phase images of the latex films at different temperatures and times were recorded. The phase image shows material contrasts, where harder parts appear in lighter colours.[9] The topography image shows the individual particles from which the size of the core/shell particles could be determined. The core diameter was also measured as soon as the cores became visible at the surface. From the topography image the surface roughness could also be determined. This indicates how corrugated (larger value of surface roughness) or smooth (lower value of surface roughness) the film surface is. In addition to the topographic and phase images, 3D images (where the core/shell particles are seen in three dimensions) with nanometer resolution were also recorded.

3.5.7 Monomer conversion: For all experiments, monomer conversion was determined gravimetrically. Samples were taken from the reaction vessel over time in order to determine the monomer conversion (see equation 3.4). Monomer conversion was plotted vs. time for each series of experiments.

$$\text{Monomer conversion (\%)} = \frac{X_1 - X_2}{X_1} \times 100 \qquad \textbf{(3.4)}$$

where X_1 and X_2 are the latex weight before and after drying respectively.

3.5.8 Moisture vapour transmission rate (MVTR): Films made from the synthesized core/shell latices were coated on a porous support (standard paperboard) and their MVTR values were determined using a Heraeus Votsch humidity cabinet, type VTRK 300. The measurements were performed at 30 ºC and 90% relative humidity (RH). The coatings were applied to the paperboard by means of a K-bar (giving a 12 µm wet film) and coating machine. The coating was then dried at a temperature of about 100-110 ºC for 1-2 minutes. The coated paperboard was then characterized primarily by determining the MVTR (as indicated in Appendix 2).

3.5.9 Conductivity and water uptake measurements: Films with similar surface areas (10 cm^2) were placed in deionized water. Films were prepared by drying ~3 ml of the latex in a glass slide at 100 ºC for 24 h. Conductivity and water uptake (w.u.) of the films were measured. Deionized water, with an electrical conductivity lower than 1.5 µS/cm, was used for all measurements.

Conductivity was measured for each series of films after a period of time (about two weeks) with a Cond 730 inoLab WTW Series conductimeter.

Water uptake is defined as the weight increase relative to the initial mass of the film over a period of time (about 25 days):

$$w.u. = \frac{m_2 - m_1}{m_1} \quad \textbf{(3.5)}$$

where m_1 and m_2 are the film weight before and after immersing into water respectively.

The specific surface ($S_{spec.}$) of the films is defined as follows:

$$S_{spec.} = \frac{S}{m} \quad \textbf{(3.6)}$$

where S is the total surface of the film in meters^2, and m its mass in g.

Normalized water uptake ($w.u._{norm}$) was plotted versus time, taking into consideration the average mass ($m_{ave.}$) of each series of films and average specific surface:

$$w.u._{norm} = w.u. \times \frac{S_{spec.\ ave.}}{S_{spec.}} = w.u. \times \frac{m}{m_{ave.}} \quad \textbf{(3.7)}$$

3.6 References

(1) Sudol, E.; El-Aasser, M. *Miniemulsion Polymerization*, In *Emulsion Polymerization and Emulsion Polymers*, Lovell, P.; El-Aasser, M., Eds.; John Wiley & Sons Ltd.: New York, 1997; pp 699-722.

(2) Landfester, K.; Bechthold, N.; Forster, S.; Antonietti, M. *Macromolecular Rapid Communications* **1999**, *20*, 81-84.

(3) Luo, Y.; Zhou, X. *Journal of Polymer Science: Part A: Polymer Chemistry* **2004**, *42*, 2145-2154.

(4) Dorset, D. *Energy & Fuels* **2000**, *14*, 685-691.

(5) Stauffer, T.; Venditti, R.; Gilbert, R.; Kadla, J. *Journal of Applied Polymer Science* **2002**, *83*, 2699-2704.

(6) Fox, D.; Allen, R. *Compatibility*, In *Encyclopedia of Polymer Science and Engineering*, Bikales, M.; Menges, O., Eds.; John Wiley & Sons, Inc.: New York, 1985; pp 758-775.

(7) Lesko, P.; Sperry, P. *Acrylic and Styrene-Acrylic Polymers*, In *Emulsion Polymerization and Emulsion Polymers*, Lovell, P.; El-Aasser, M., Eds.; John Wiley & Sons Ltd.: New York, 1997; pp 619-655.

(8) Vandezande, G.; Smith, O.; Bassett, D. *Vinyl Acetate Polymerization*, In *Emulsion Polymerization and Emulsion Polymers*, Lovell, P.; El-Aasser, M., Eds.; John Wiley & Sons Ltd.: New York, 1997; pp 593-587.

(9) Digital Instruments Veeco Metrology Group. *MutiMode™ SPM Instruction Manual Version 4.31ce*. 1996.

CHAPTER 4

RESULTS AND DISCUSSION: MORPHOLOGY DETERMINATION

4.1 Introduction

Hydrophobic core/shell latex particles, with both liquid and hard cores, were synthesized by an *in situ* miniemulsion process. Different materials, including an oil (hexadecane), linear wax (paraffin) and branched wax (microcrystalline) were used as the cores of the particles. The hexadecane oil has a melting point (mp) of 18 ºC while paraffin and microcrystalline waxes have melting peak ranges between 58-60 ºC and 40-70 ºC respectively. The shell of the particles was mainly made from a copolymer containing three relatively hydrophobic monomers, namely: methyl methacrylate, butyl acrylate and Veova-10. Particles with the desired morphology were successfully made using the miniemulsion technique as a one-step nanoencapsulation technique. The results of particle morphology determination are presented below.

Pectora roborant cultus recti

4.2 Particle morphology determination

Particle morphology was mainly determined by two different techniques: TEM and AFM. TEM was used to directly visualize the morphology of the investigated core/shell particles at the nanometer level, while AFM was used to determine the particle morphology by scanning the films' surface produced from the synthesized core/shell latices during the film formation process. The results obtained using these two techniques are described in Sections 4.2.1 and 4.2.2.

4.2.1 Results of transmission electron microscopy (TEM) analysis

In an attempt to determine the particle morphology using the low T_g latices (theoretical T_g of about 8.5 ºC), film formation behaviour was observed to occur during the TEM analysis.

This prevented the determination of the individual particle morphology using these low T_g latices due to the fact that the core/shell structure could not be maintained during the analysis. Figure 4.1 shows TEM images of the particles that were prepared, showing the film formation behaviour observed. Table 4.1 shows the characteristics of the low T_g latices used for the TEM analysis.

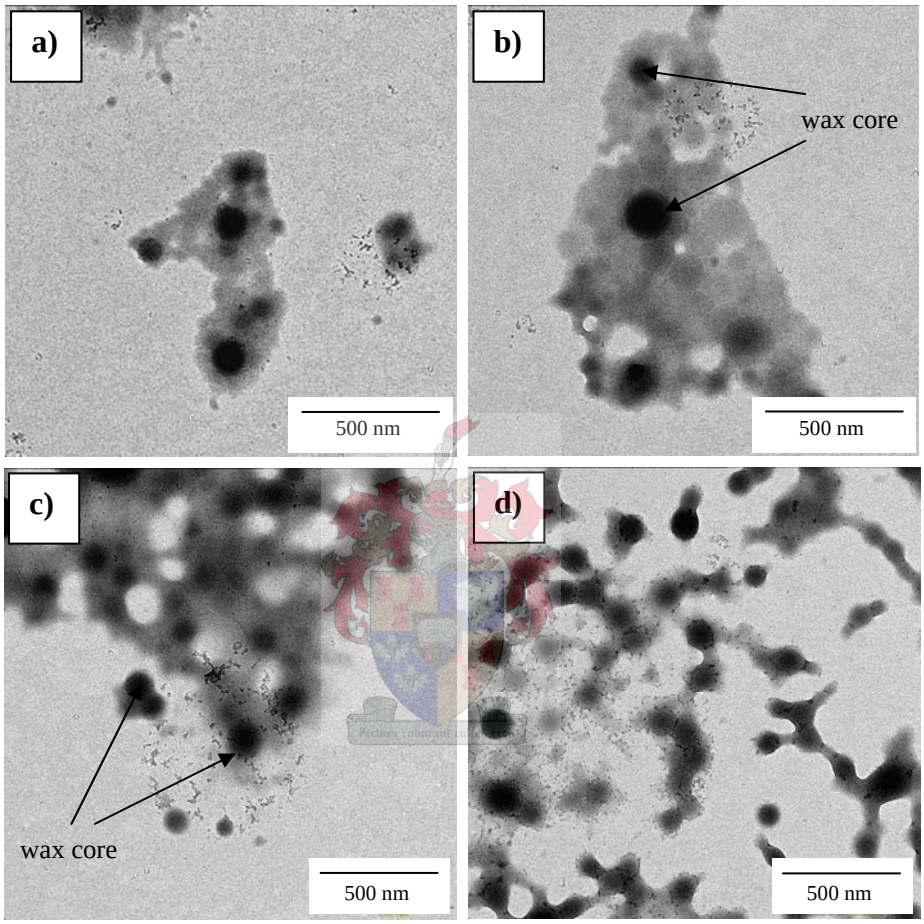

Figure 4.1: TEM images of particles prepared using two different waxes, showing film formation occurring during TEM analysis: a) and b) different areas of the same sample that contains 50 wt% microcrystalline wax, and c) and d) different areas of the sample, which contains 30 wt% paraffin wax.

Table 4.1: The characteristics of the low T_g latices used for the TEM analysis.

Amount of wax (wt%)	Theoretical T_g of the polymer (°C)	Solids content (%)	Average particle size measured by DLS (nm)
50% microcrystalline wax	8.5	16.18	185
30% paraffin wax	8.5	21.11	152

The observed film formation most probably occurred during the sample preparation due to the low T_g of the MMA/BA/Veova-10 copolymer shell or as a result of the melting of the copolymer shell under the effect of the electron beam of the TEM instrument.[1] Images 4.1 (a) and (b) show particles prepared using 50 wt% microcrystalline wax, while images 4.1 (c) and (d) show the particles that contain 30 wt% paraffin wax. The dark areas represent the wax core of the particles surrounded by lighter areas, which represent the copolymer film layer. This is quite normal considering the low T_g value of the copolymer shell (lower than room temperature), and no crosslinking on the copolymer shell was performed. The particles will therefore melt and deform as a result of the effect of the electron beam of TEM or during the sample preparation due to their low T_g values.

The TEM images did nonetheless show that the latices were relatively monodisperse even at low surfactant concentrations. Figure 4.2 shows TEM images of particles prepared using different surfactant concentrations (SDBS) and different amounts of microcrystalline wax as the core of the particles. The characteristics of these latices are described in Table 4.2 below.

Table 4.2: The characteristics of the latices made with different amounts of surfactant and wax showing the monodispersity of the latices produced.

Amount of wax (wt%)	Amount of surfactant used (wt%)	Solids content (%)	Average particle size measured by DLS (nm)
10% paraffin wax	1.0	35.79	195
10% paraffin wax	2.5	28.07	97
10% microcrystalline wax	1.0	28.23	154
30% microcrystalline wax	1.0	25.54	173

As seen in images 4.2 (a) and (b) the particle size decreased noticeably as the amount of surfactant increased. On the other hand the particle size increased significantly as the amount of wax (which was used as the hydrophobe) in the core increased, from 10 wt% to 30 wt% relative to monomer (see images 4.2 (c) and (d)).

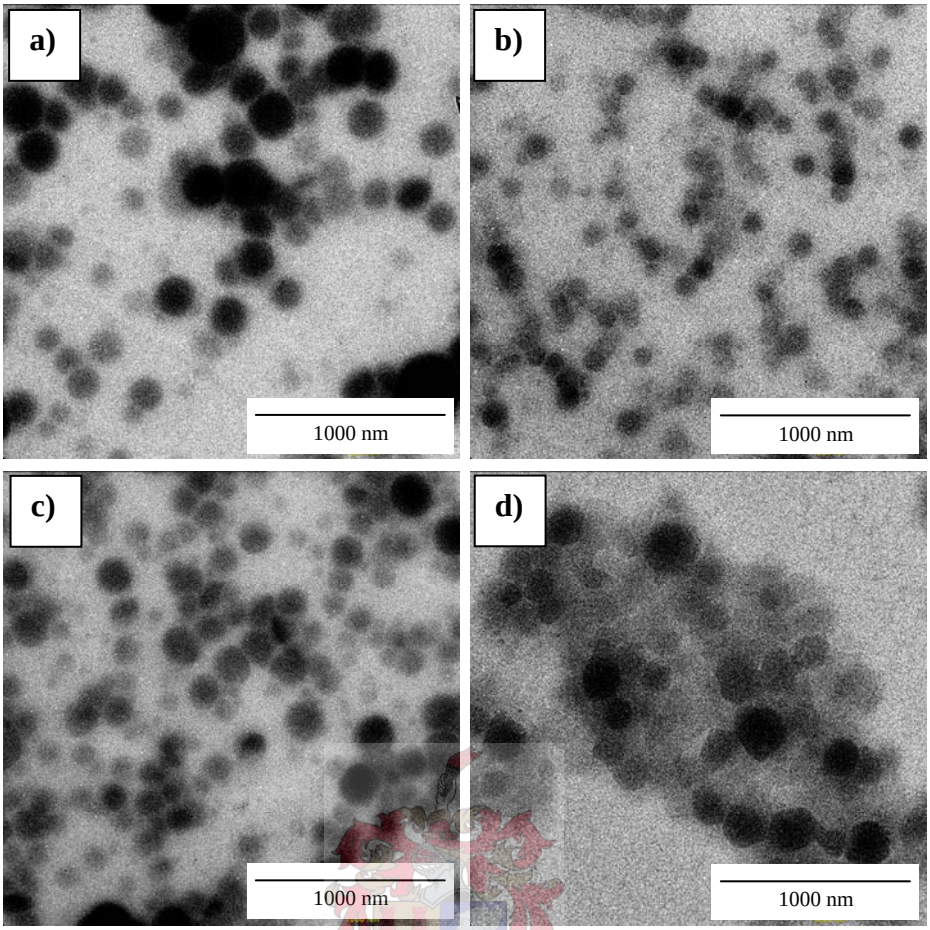

Figure 4.2: TEM images of particles made with different amounts of surfactant and wax showing the monodispersity of the latices produced using: a) 10 wt% paraffin wax, 1 wt% SDBS, b) 10 wt% paraffin wax, 2.5 wt% SDBS, c) 10 wt% microcrystalline wax, 1 wt% SDBS and d) 30 wt% microcrystalline wax, 1 wt% SDBS.

These results were similar to the miniemulsion polymerization reported by Tiarks *et al.*[1] They studied the preparation of hollow polymeric nanocapsules (core/shell particles) prepared by miniemulsion polymerization of different monomers in the presence of different quantities of the surfactant (SDBS) and the hydrophobe (hexadecane) relative to the monomers used. Monomers that were used in that study included Sty and MMA. The authors found that the presence of a large amount of surfactant or hydrophobe can significantly change the particle size of a miniemulsion. An increase in the particle size was observed when a low amount of surfactant was used. In addition, by decreasing the monomer to HD ratio, a significant increase in the particle size was observed. These results were obtained for both systems used, namely MMA/HD and Sty/HD. For the system MMA/HD, changes in the ratios between MMA:HD of 24:1 to 1:5 led to an increase in the diameter of particles from 73 nm to 160 nm.

Also for the Sty/HD system, a particle diameter of 101 nm was observed for the latex made with 2.5 wt% HD relative to styrene, increasing to 184 nm when the HD increased to the Sty:HD ratio of 1.5:4.5.

In the present study, and in order to determine the morphology of the synthesized core/shell particles, particles with a copolymer shell that has a high T_g value had to be prepared. The MMA/BA/Veova-10 ratio in the copolymer shell was varied (15 wt% BA, 65 wt% MMA and 20 wt% Veova-10 were used) in order to obtain the desired T_g value of about 50 ºC. This was mainly done to maintain the core/shell structure and to prevent the deformation of the copolymer shell during the TEM measurements. The results in Sections 4.2.1.1 and 4.2.1.2 show that core/shell particles were successfully synthesized when latices with a high T_g copolymer shell were used. The characteristics of the latices that have higher T_g values of about 50 ºC, as used for the TEM analysis, are summarized in Table 4.3.

Table 4.3: The characteristics of the core/shell latices prepared with HD and wax as the core material and higher T_g copolymer shell used for the TEM analysis.

Amount of HD or wax relative to monomer (wt%)	Theoretical T_g of the polymer (ºC)	Solids content (%)	Average particle size as measured by DLS (nm)
50% HD	50	23.72	167
30% paraffin wax	50	29.57	193
30% microcrystalline wax	50	26.32	180

4.2.1.1 Hexadecane (HD) as a core

Hexadecane is the most commonly used hydrophobe to counteract the influence of Ostwald ripening in a miniemulsion system.[2,3] The addition of a small amount of the hydrophobe reduces the Ostwald ripening by effectively creating an osmotic pressure in every droplet, which suppresses monomer diffusion from smaller to bigger droplets (discussed in Chapter 2). However, the use of a high amount of the hydrophobe relative to the total amount of monomer(s) could lead to the preparation of particles with hydrophobic liquid cores encapsulated within a polymeric shell.[1]

In a recent study, van Zyl *et al.*[4] prepared polymeric nanocapsules with liquid cores using an *in situ* miniemulsion polymerization. Hexadecane in high quantities (1:1 ratio to the

monomer), was used as the liquid-core of the nanocapsules and it acted as the hydrophobe required in a miniemulsion system. Their results showed that using this ratio of HD relative to monomer did not influence the expected particle size (50-500 nm) and stability in a miniemulsion system.

In the present study, a monomer to hexadecane ratio of about 1:2 was used for the preparation of particles with liquid hydrophobic cores. To determine the particle morphology, a uranyl acetate (UAc) negative stain was used to better define the particle edges,[5,6] which otherwise would have had very little contrast against the support film. Figure 4.3 shows TEM images of the synthesized core/shell particles prepared using 50 wt% of HD relative to the total amount of monomers. Images clearly indicate that core/shell particles were successfully synthesized using HD as the core of the particles.

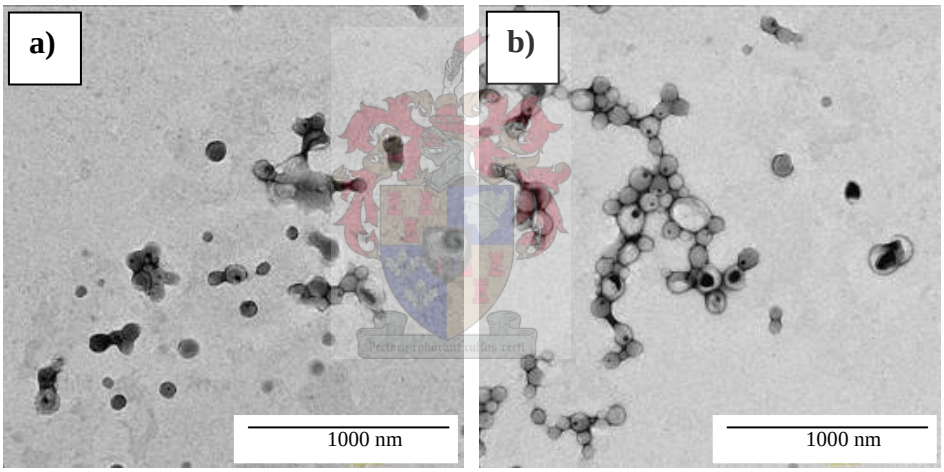

Figure 4.3: TEM images of core/shell particles: a) and b) showing different areas of the same sample prepared using 50 wt% hexadecane as the core of the particles.

The lighter areas are representative of the copolymer shell, while the darker areas represent the core oil, which presumably disappeared due to the high vacuum of the TEM,[7] leading to the UAc ending up inside the hollow particles, which appeared as dark spots in the TEM images. The UAc stain can more effectively scatter a greater proportion of electrons and thus produced darker domains in the TEM images. Figure 4.4 shows high-magnification images of the synthesized particles along with a scale bar, indicating that particles with diameters of less than 200 nm were obtained. This corresponded well with the average particle size data measured by DLS (see Table 4.3).

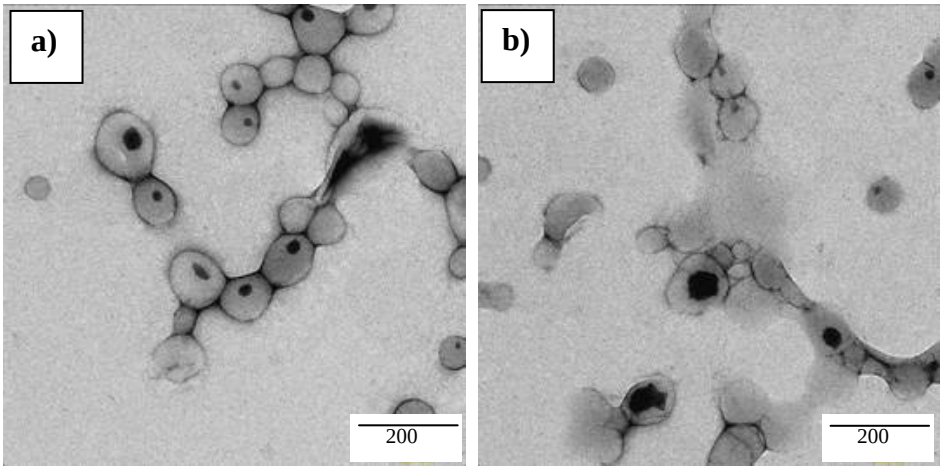

Figure 4.4: Higher magnification of core/shell particles: a) and b) showing different areas of the same sample synthesized using 50 wt% hexadecane as the core of the particles.

Figure 4.5 shows a close-up of individual particles along with a scale bar indicating the average particle size. The images suggest that the particles are partially destroyed due to the removal of HD under the high vacuum used in the TEM. As a result of that the particles became hollow and, with the presence of uranyl acetate inside the hollow cavity, the core domains appeared as dark spots with a contrast similar to that of the particle edges, which were delineated by the UAc negative stain.

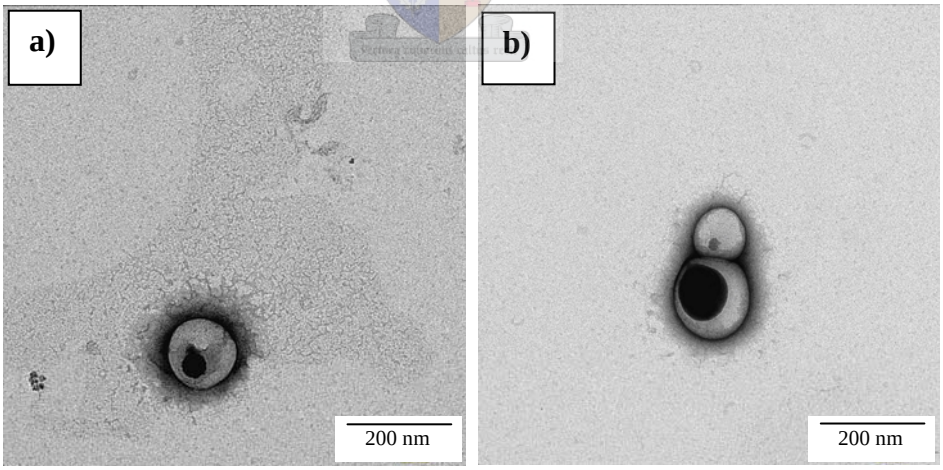

Figure 4.5: High magnification TEM images: a) and b) showing a close-up of individual core/shell particles synthesized using 50 wt% hexadecane.

The particle size of the core/shell latices synthesized using higher amounts of hexadecane compared well with conventional miniemulsion data. Most of these conventional miniemulsion polymerizations[8,9] were carried out with the addition of the hydrophobe (hexadecane) to reduce Oswald ripening, but in much smaller quantities compared to the

monomer. In the present study, however, the weight ratio of the hydrophobe (hexadecane) to monomer is almost 1:2. This did not influence the expected particle size (50-500 nm) associated with miniemulsion polymerization.[3]

4.2.1.2 Paraffin and microcrystalline wax as a core

TEM analysis was run for the latices containing 30 wt% wax as the core of the particles, which have a copolymer shell with a T_g value of about 50 ºC. Figure 4.6 shows TEM images of wax-polymer core/shell particles prepared using the two different waxes (paraffin and microcrystalline wax) as the core of the particles. Images 4.6 (a) and (b) show different areas of the same sample containing particles prepared using 30 wt% paraffin wax as the core, while images 4.6 (c) and (d) show lower and higher magnification images of particles prepared using 30 wt% microcrystalline wax as the core respectively.

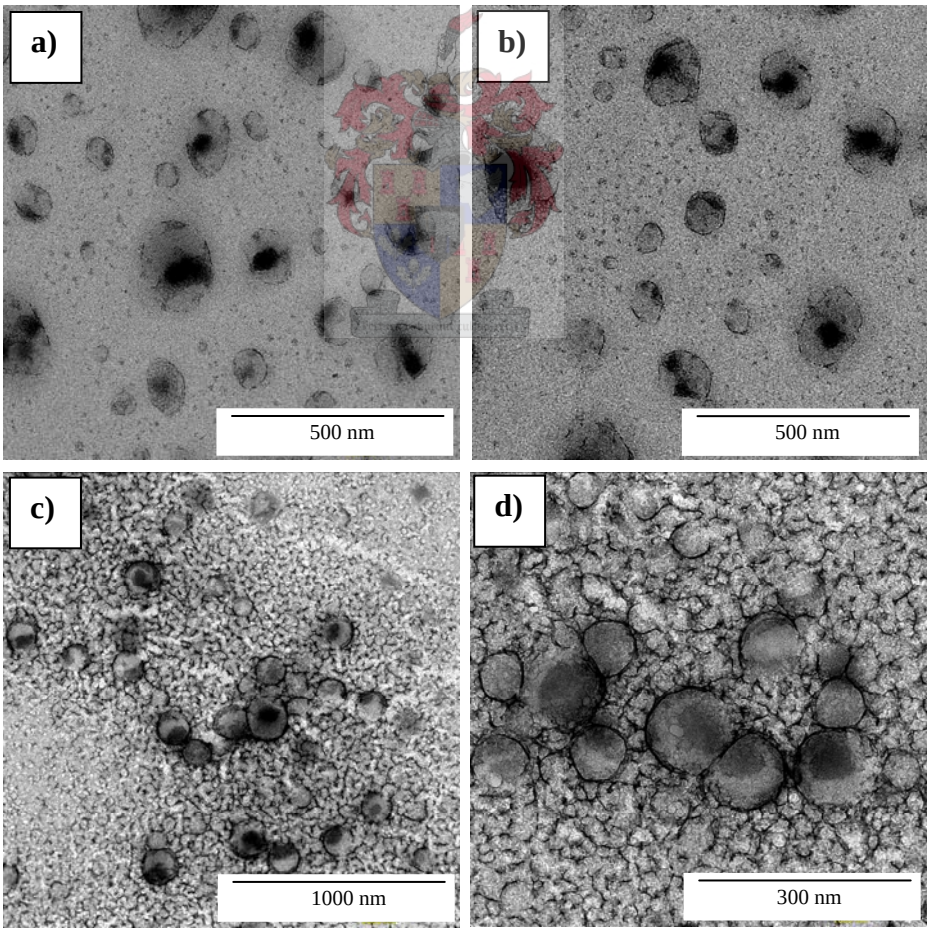

Figure 4.6: TEM images of wax-polymer core/shell particles containing different types and amounts of wax in the core: a) and b) show different areas of particles that contain 30 wt% of paraffin wax as a core, while c) and d) show low and higher magnification of the particles that contain 30 wt% microcrystalline wax respectively.

As seen in images 4.6 (a) and (b), some particles had deformed morphological structures, which could be due to the high vacuum conditions used in TEM. This is quite normal, considering the fact that no crosslinking agents were added to the copolymer shell. The particles may therefore easily deform if no further strengthening (crosslinking) is performed and lead to visually deformed particles. In addition, polymer particles can undergo radiation beam damage when exposed to the high energy electron beam of TEM,[10,11] which led to the observed damaged particles.

The poor contrast observed in images 4.6 (a) and (b), is due to the fact that the amount of UAc used for the negative staining was not enough to adequately define the particle edges. The agglomeration of particles visible in images 4.6 (c) and (d) can also be due to the phenomenon associated with the drying process, occurring because of the ability of Veova-10 (T_g = -3 ºC) to form films near room temperature. This could also be due to the high concentration of the sample, which led to the observed overlapping particles. However in both cases the overall core/shell morphology is clearly visible due to the different electron densities of the wax core and the copolymer shell. This indicates that a core/shell morphology was obtained using the two types of wax investigated.

It is well known that TEM results depend strongly on the ability to induce a contrast between different structures, through different electron densities in the particles. This can usually be accomplished by using different staining techniques which rely on different chemical reactivities of the different polymer phases with the staining agent.[10-12] In a recent study Kirsch *et al.*[13] reported that RuO_4 was used for the preferential staining of polymer domains to enhance the contrast of certain phase regions in core/shell particles that contain poly(butylacrylate) (PBA). In the present study, the core is made from wax material, which will not be stained by the RuO_4, while the outer shell is made from a copolymer containing a substantial amount of PBA (15 wt%) which will be stained by RuO_4.

Therefore, to confirm the formation of wax-polymer core/shell particles, one latex was additionally stained by the preferential staining with RuO_4 to enhance the contrast of the copolymer shell after it was stained by the negative staining agent UAc to define particle edges. Figure 4.7 shows lower and higher magnification TEM images of the particles prepared using 50% paraffin wax as the core and MMA/BA/Veova-10 copolymer in the shell stained additionally with RuO_4.

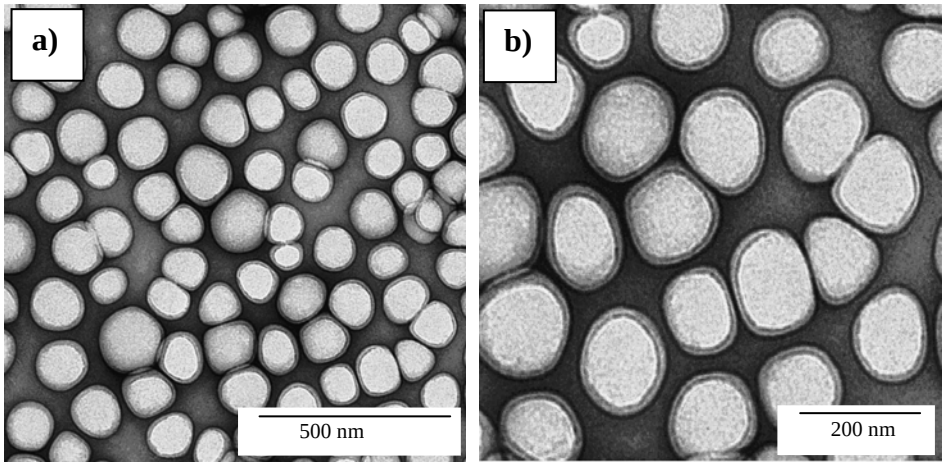

Figure 4.7: TEM images for particles prepared using 50 wt% paraffin wax preferentially stained by RuO_4 for the PBA domains: a) lower magnification and b) higher magnification.

Particles with core/shell morphology, where the stained copolymer shell appears in darker gray, while the inner wax core, which is not stained by the RuO_4, appears in lighter gray in the TEM images, are clearly visible. This indicates that a core/shell structure was successfully obtained using the paraffin wax as the core. The preparation of wax-polymer core/shell particles using the two types of waxes as a core of the particles was confirmed by AFM analysis (see Section 4.2.2).

Although the predominant particle morphology is core/shell, Figure 4.8 shows the existence of a population of solid spherical particles of polymer. These particles are most likely caused by secondary nucleation (discussed in Chapter 2), which will result in the formation of polymer particles that contain only shell material.

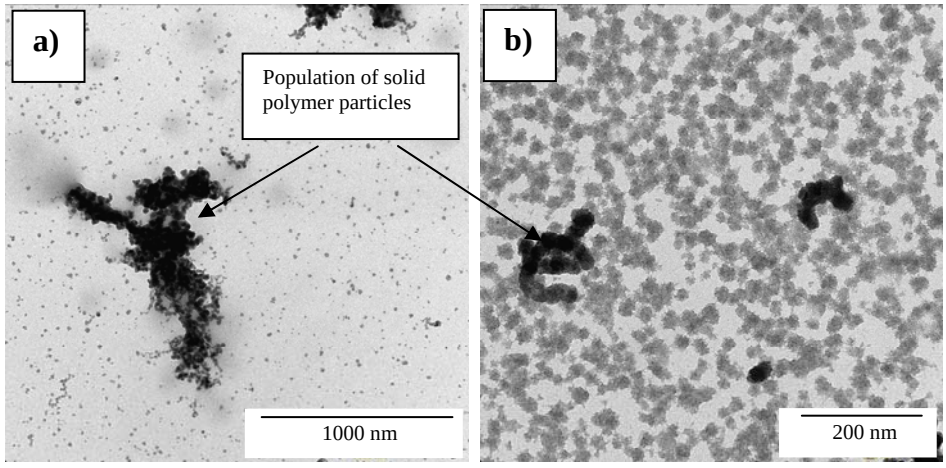

Figure 4.8: TEM images of latex particles containing 20 wt% paraffin wax showing the existence of solid polymer particles that were caused by secondary nucleation of polymer materials in the aqueous phase at: a) low magnification and b) higher magnification.

This was similar to results obtained by van Zyl *et al.*[14] who studied the synthesis of liquid-filled polymeric nanocapsules by the use of a living polymerization technique. In an attempt to prepare particles with HD cores, the authors observed the existence of a population of solid spherical particles. They attributed that to the secondary nucleation of polymer particles which resulted in the formation of particles that do not contain core material.

4.2.2 Results of atomic force microscopy (AFM) analysis

In coating applications the film formation or coalescence behaviour of latex particles greatly affects the final properties of the resulting coatings. In addition, particle size and morphology can significantly influence the film formation behaviour of these polymer latices. AFM is a technique ideally suited for studying the surface of a dried or drying film. Recently, a number of papers have been published that describes the use of AFM in the study of film formation of polymer latices.[15,16]

In a more recent study, AFM has been used for determining the microstructure of thermosetting matrices toughened by the incorporation of core/shell particles.[17] It has been demonstrated that AFM can be used to determine the detailed microstructure of polymeric materials featuring core/shell structure. In addition to the topographical images, another AFM capability such as phase imaging was used. AFM also allows studying the images in a three-dimensional perspective, providing morphological information with nanometer resolution.

Meincken and Sanderson[18] studied the effect of the polymer structure and particle size on the film formation process of core/shell latex polymers by AFM. It was shown that AFM is a powerful technique for the determination of particle size and morphology of such composite latices by scanning the film surfaces during the film formation process. In another study Kirsch *et al.*[19] used AFM to study the particle morphology and the surface structure of the dispersion films prepared using a hard core of 66% PMMA/34% PBA copolymer and a soft shell of pure PBA. Using AFM in the tapping mode, the analysis of the morphology of single particles, clearly identified particles with core/shell structure.

In the present study, AFM was used to monitor the drying and film formation process of the synthesized core/shell latices to determine their particle morphology. Latices with

copolymer shells having theoretical glass transition temperatures of about 25 ºC were used. The MMA/BA/Veova-10 ratio in the copolymer shell was varied in order to obtain the desired T_g value. AFM images were recorded over a certain temperature range (below and above the glass transition temperature of the shell particles and the melting point of the wax cores) and as a function of time during the film formation process. The characteristics of the synthesized core/shell latices used for the AFM analysis are described in Table 4.4 below.

Latex films were typically cast below their glass transition temperature to show coalescence of particles. After the film was dried, a sequence of AFM images was then acquired to monitor the ordering of the particles and the subsequent deformation from which the shell material could be seen. Different types of images were recorded, including: topography, phase and 3D images. All images were recorded in the tapping mode. The phase image shows material contrasts, where harder parts would appear in lighter colours.[20] The non-destructive tapping mode combined with phase imaging allows materials of different mechanical behaviour to be distinguished on a nanometer-scale.[21,22] This was used to distinguish between the hard wax core phase and the soft copolymer shell phase.

Table 4.4: The characteristics of core/shell latices prepared with HD and wax as core material used for the AFM analysis.

Amount of HD or wax used (wt%)	T_g of the polymer (ºC)	Solids content (%)	Average particle size measured by DLS (nm)
30% HD	25	29.84	135
30% paraffin wax	25	33.33	135
30% microcrystalline wax	25	31.60	123

The topography image shows the individual particles from which the size of the particles could be determined using computer software (Topometrix) by measuring the valley-to-valley distance. From the topography images the surface roughness could also be determined, which indicates how corrugated (larger value of surface roughness) or smooth (lower value of surface roughness) the film surface is. In addition to the topographic and phase images, 3D images, where the core/shell particles are seen in three dimensions with nanometer resolution, were also recorded.

After the film was entirely dry, the temperature was increased to above the T_g of the copolymer shell and below the melting point of the wax in order to show the wax core particles, which retained their spherical shape and appear at the surface. The core diameter was then measured as soon as the cores became visible at the surface. After that the temperature was increased to above the melting point of the wax used as the core, which resulted in a flat film due the melting and flattening of the wax cores forming a flat film.

The surface roughness of the sample was measured for all topographic images. This gave an indication about the film formation kinetics, where the less pronounced the individual particles are, the lower the surface roughness is.

4.2.2.1 Hexadecane (HD) as a core

As seen in Sections 4.2.2.2 and 4.2.2.3, AFM was successfully used to determine the particle morphology of the latices made with the two different types of wax as the core. Results indicate that particles made from the two different waxes had the core/shell morphology. However, AFM could not be used to determine the particle morphology of the HD-containing latex. This was due to the fact that HD (mp = 18 ºC) is in the liquid state at the temperature range of analysis. Figure 4.9 shows AFM images of the latex prepared containing 30 wt% HD as the core. The phase image clearly shows the disruption caused by the liquid hexadecane, which most probably was not encapsulated with the copolymer shell.

The lighter area is representative of the copolymer shell (harder than the HD oil phase), while the dark areas represent the HD phase in the AFM images. The HD was spread over the latex film, leading to an interrupted AFM image. The particles are however still clearly visible in the topography and the 3D images in Figure 4.9.

4.2.2.2 Paraffin wax as a core

AFM analysis was run for the latex containing 30% weight fraction paraffin wax with respect to monomer and 1 wt% surfactant during the film formation process. Figure 4.10 shows the topography, the phase and the 3D images after 5 minutes of heat application at 20 ^{o}C.

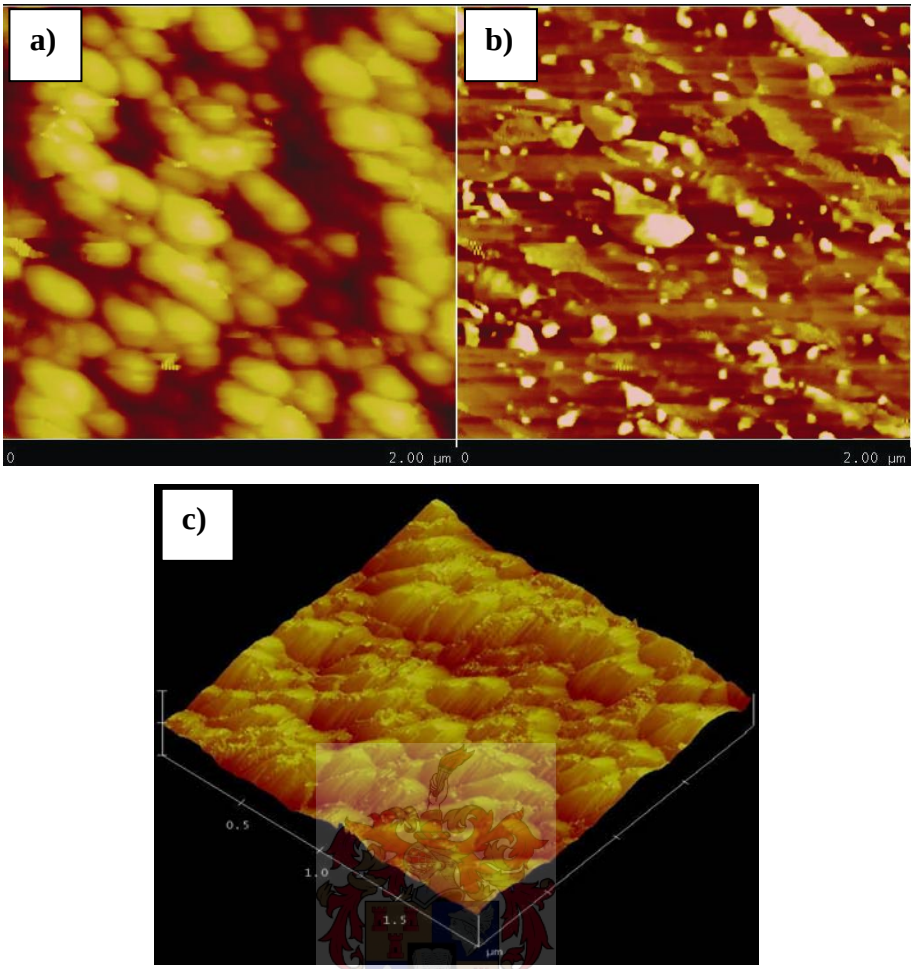

Figure 4.9: AFM images of HD-containing particles showing the disruption caused by the HD during the AFM analysis: a) the topography, b) the phase and c) the 3D images.

The topography image (a) in Figure 4.10 shows individual particles with diameters ranging from 130-180 nm, which is in a good agreement with the average particle size measured by DLS (see Table 4.4). The phase image shows no contrast, which means that all core particles are covered entirely with the copolymer shell. It also means that no phase separation or acorn structure is present, suggesting that all wax particles were encapsulated within the polymeric layer in a core/shell structure.

After 60 minutes of heat application to the sample at 25 ºC (see phase image in Figure 4.11), the shell polymer started to deform, flow, and interdiffuse at its T_g, forming a matrix around the harder wax cores, which retained their spherical shape and appeared at the surface. This is to be expected, since the wax cores had not yet reached their melting point.

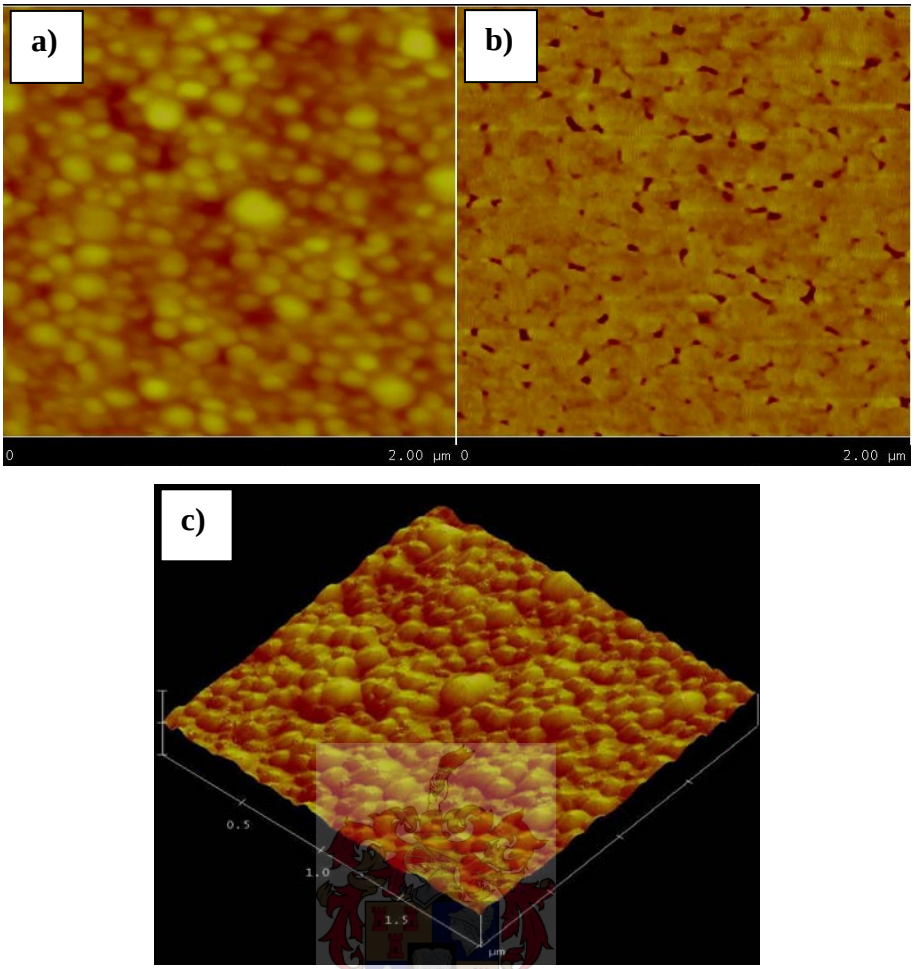

Figure 4.10: AFM images of wax-polymer core/shell particles after 5 minutes of heat application at room temperature (20 ºC): a) the topography, b) the phase and c) the 3D images of latex containing 30% solids and 30 wt% paraffin wax.

In addition, the phase image shows a clear contrast, meaning that the wax cores could clearly be distinguished from the surrounding shell matrix. Some of the core particles are, however, still partly covered with the copolymer shell, which most probably was not softened and melted completely. From the topography image (see also the 3D image), the size of the core particle was measured, giving particles with smaller diameters of 30-50 nm.

Further heating of the sample (at about 60 ºC) resulted in a flat film, which means that the wax core particles were melted entirely, forming a flat film. The topography, the phase and the 3D images of the sample after 120 minutes of heat application at 60 ºC are shown in Figure 4.12. From image 4.12 (b) one can see that some material contrast distributed along the film surface was observed, meaning that, after melting, the wax cores were homogenously mixed with the polymer matrix, forming a flat film.

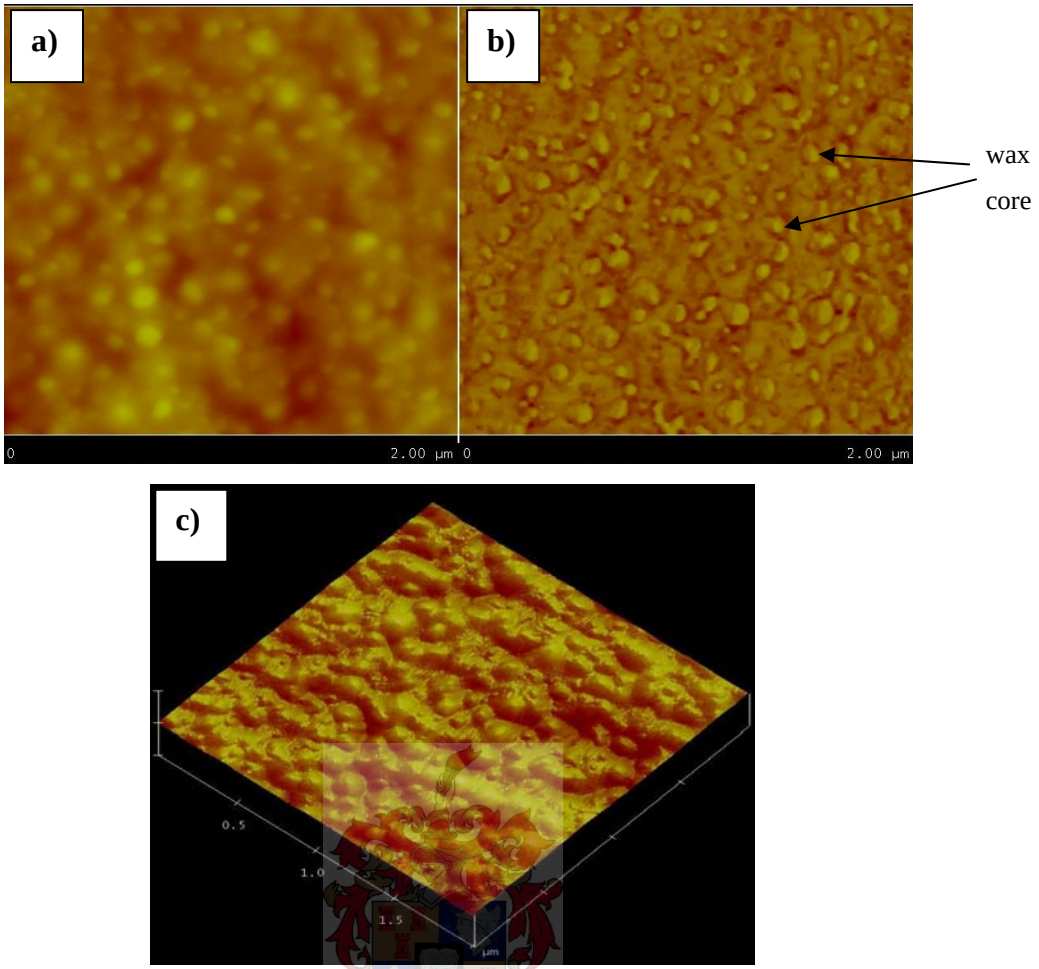

Figure 4.11: AFM images of wax-polymer core/shell particles containing 30% paraffin wax in the core after 60 minutes of heat application at 25 ºC: a) the topography, b) the phase and c) the 3D images.

The surface roughness was measured for all topographic images, where the less pronounced the individual particles are the lower the surface roughness is. Table 4.5 shows the surface roughness evolution as a function of time and temperature of the latex film containing 30 wt% paraffin wax as a core. As seen in Table 4.5, the surface roughness decreased noticeably as a function of temperature and time. At temperatures below the T_g of the polymer shell (below 25 ºC) the surface roughness is high and as the temperature and time increased the surface roughness decreased. This means that the core particles, which have smaller sizes than the whole core/shell particles, appeared after the copolymer shell started flowing, leading to smoother and flatter films with less surface roughness. When the temperature is raised, reaching the melting point of the wax cores, the surface roughness decreased even further, which means that the wax core particles melted entirely when they reached their melting point.

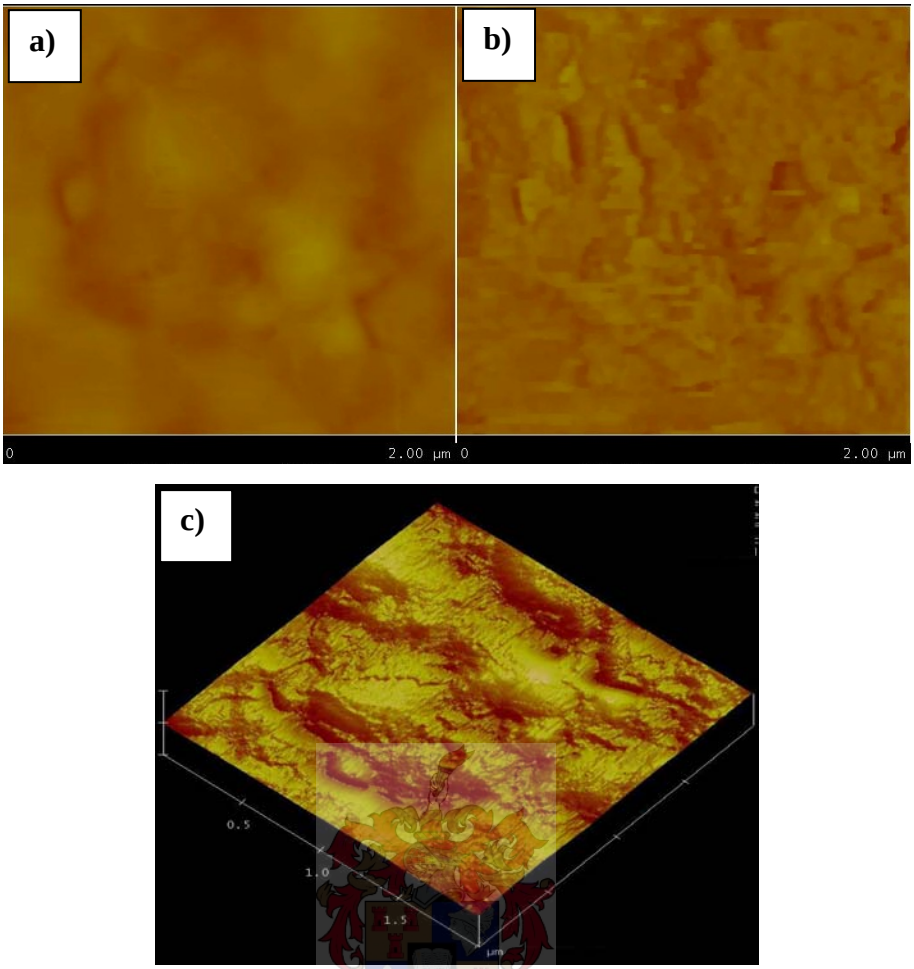

Figure 4.12: AFM images of wax-polymer core/shell particles containing 30% paraffin wax at 60 ºC: a) the topography, b) the phase and c) the 3D images.

Table 4.5: Surface roughness evolution of latex film containing 30 wt% paraffin wax as a core vs. time and temperature.

Time of heat application (min)	Temperature (ºC)	Surface roughness (nm)
2	20	10.5
5	20	9.2
30	25	8.5
60	25	6.7
90	25	5.3
120	25	4.8
120	60	3.1

Figure 4.13 shows the surface roughness of the film vs. time at increased temperature from 20 to 60 ºC. The surface roughness decreased with time, which means that particles continuously melted as a function of time and temperature, leading to a final flat film with

a lower value of surface roughness of about 3.1 nm. This was similar to data reported in the literature by Glinel *et al.*[23] In that study, AFM was used to inspect the morphology of paraffin wax-coated polyelectrolyte films. Images showed that wax particles are well and randomly distributed over the surface, with a surface roughness of 27 nm. After annealing at 60 ºC, images showed that the film appeared continuous and homogeneous, with a decreased surface roughness of 6.5 nm as a result of wax melting.

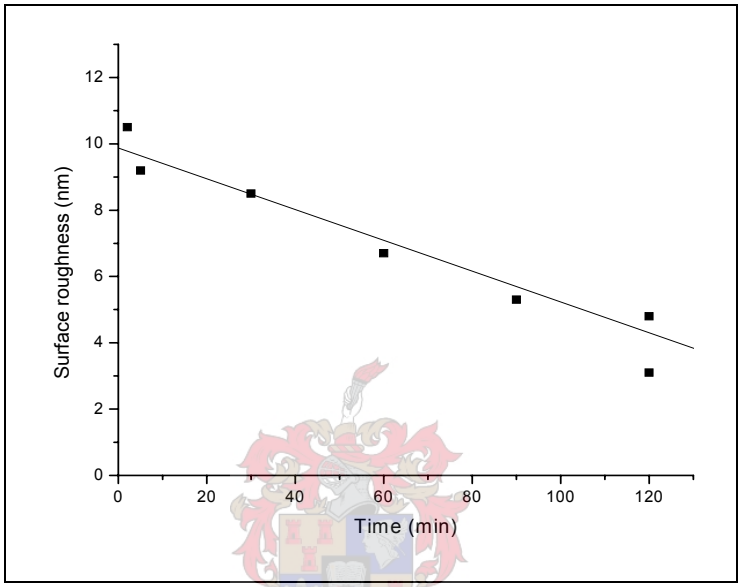

Figure 4.13: Surface roughness (by AFM) evolution vs. time for the 30% paraffin wax-containing latex at increased temperature, from 20 to 60 ºC.

4.2.2.3 Microcrystalline wax as a core

AFM analysis was run for the latex containing 30% weight fraction microcrystalline wax with respect to monomer and 1 wt% surfactant during the film formation process. Figure 4.14 shows the AFM images of core/shell particles containing 30% microcrystalline wax after 5 minutes of heat application at 24 ºC.

The topography image shows individual particles with a diameter ranging from 80-140 nm, which was also in good agreement with the average particle size measured by DLS (see Table 4.4). The phase image shows no contrast, which means that all core particles are entirely covered with the copolymer shell. This also means that no phase separation or acorn structures are present, suggesting that all the particles had the core/shell structure.

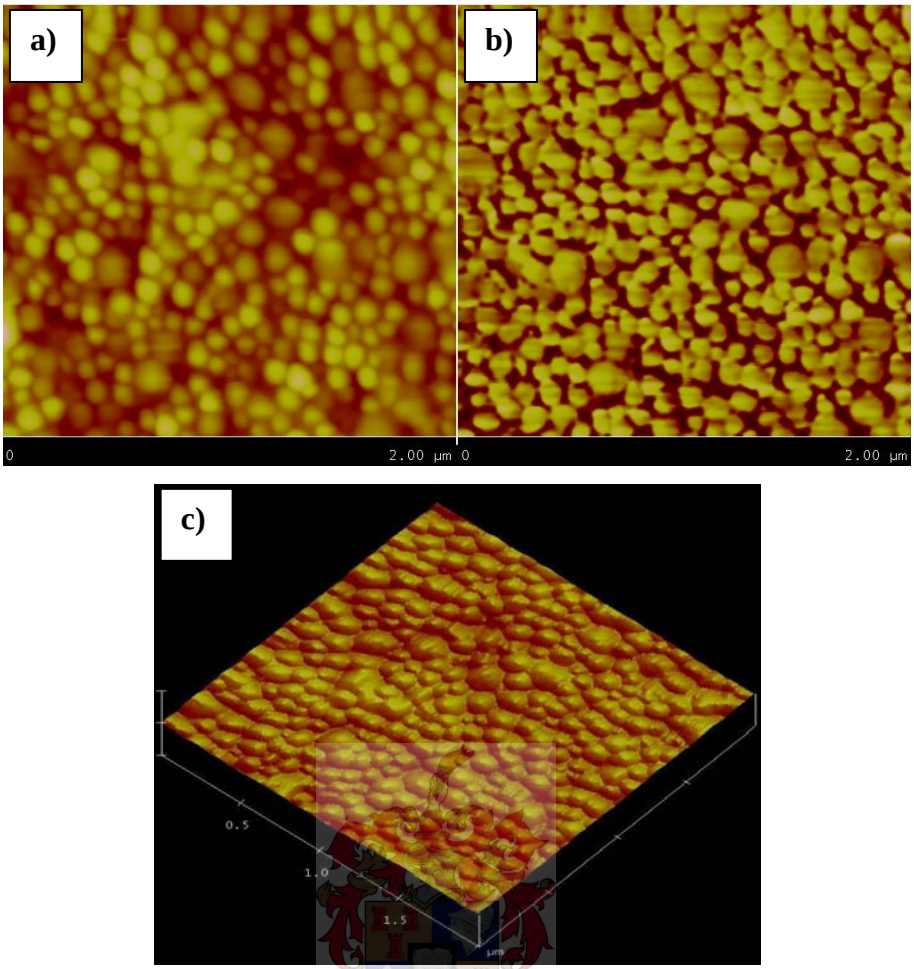

Figure 4.14: AFM images of wax-polymer core/shell particles containing 30% microcrystalline wax after 5 minutes at room temperature (24 °C): a) the topography, b) the phase and c) 3D images.

When the sample was heated at 24 ºC for 60 minutes, the shell copolymer started flowing (see the phase and topography images in Figure 4.15). The phase image shows a clear contrast, distinguishing between the wax in the core and the copolymer in the shell. Some of the core particles are, however still partly covered with shell polymer, which was not completely softened. The large spherical structure observed in images 4.15 (a), (b) and (c) could be due to the fact that some of the wax core particles started to melt and coagulate together as the time and temperature increased. This is quite normal considering the fact that microcrystalline wax has a wide range of melting temperatures starting from about 25 ºC (see Appendix 1).

Further heating of the sample to about 60 ºC for 65 minutes (see Figure 4.16) resulted in a flat film with mixed material contrast, which means that all wax core particles were melted and homogenously distributed on the film surface (see phase image in Figure 4.16).

As can be seen in the topography and the 3D image in Figure 4.16, no individual particles are recognizable, meaning that the core particles have melted entirely, leading to a flat film surface.

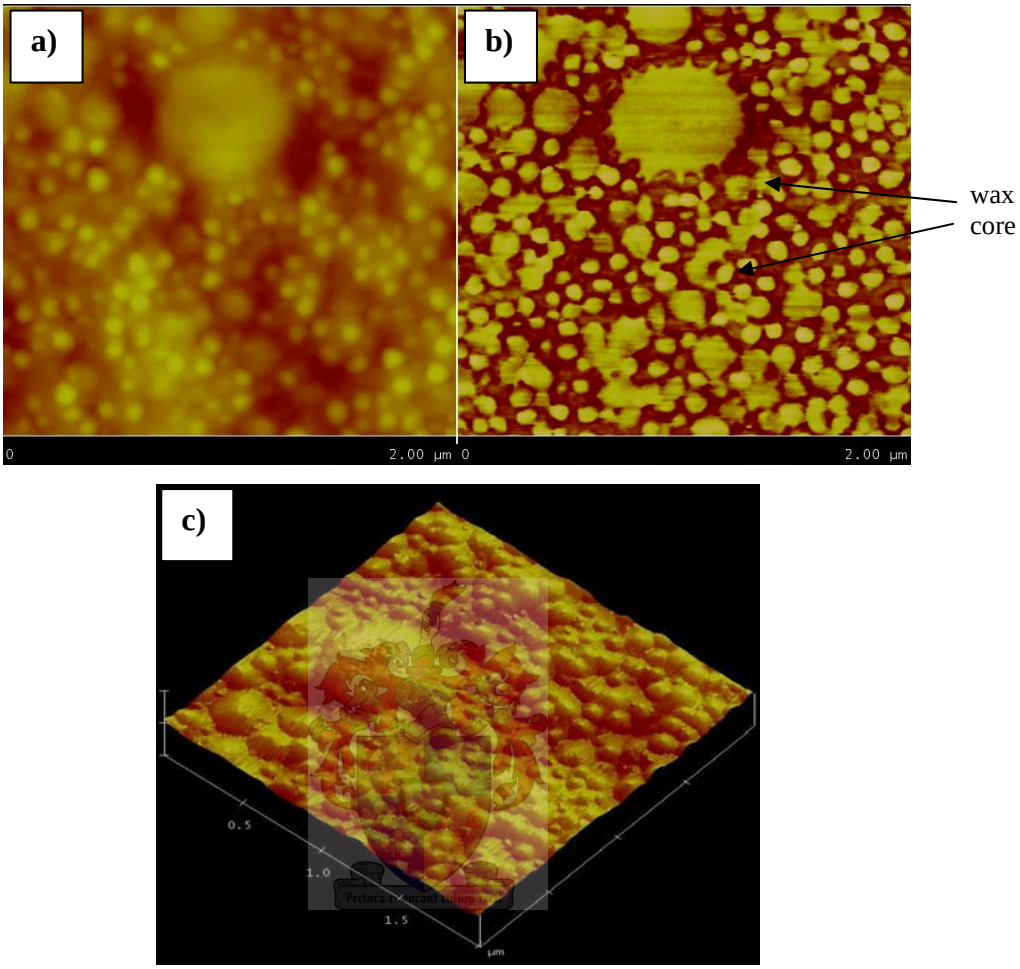

Figure 4.15: AFM images of the wax-polymer core/shell particles containing 30% microcrystalline wax after 60 minutes at 24 ºC: a) the topography, b) the phase and c) the 3D images.

The surface roughness was measured for all topographic images, where the less pronounced the individual particles are, the lower the surface roughness is. Table 4.6 shows the surface roughness evolution as a function of time and temperature. It was noted that the surface roughness decreased with time and temperature. This suggests that the copolymer shell continually deformed as the time and temperature were increased, until the shell reached its T_g. At a temperature of about 60 ºC, the surface roughness decreased sharply, which indicates that the wax core had melted, leading to the lower value of surface roughness of about 4.7 nm (see Figures 4.16 and 4.17).

Table 4.6: Surface roughness evolution of sample containing microcrystalline wax as a core vs. time and temperature.

Time of heat application (min)	Temperature (ºC)	Surface roughness (nm)
5	24	8.4
15	24	7.3
30	24	7.2
60	24	7.0
65	60	4.7

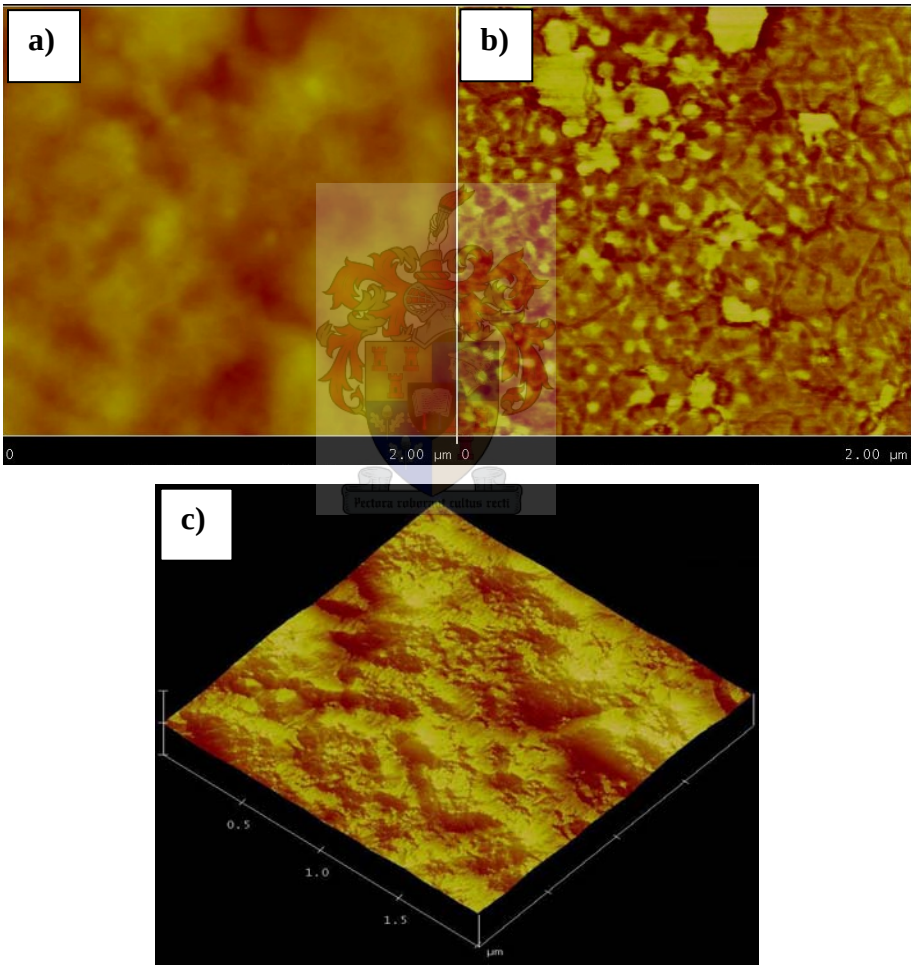

Figure 4.16: AFM images of wax-polymer core/shell particles containing 30% microcrystalline wax at an increased temperature of about 60 ºC: a) the topography, b) the phase and c) the 3D images.

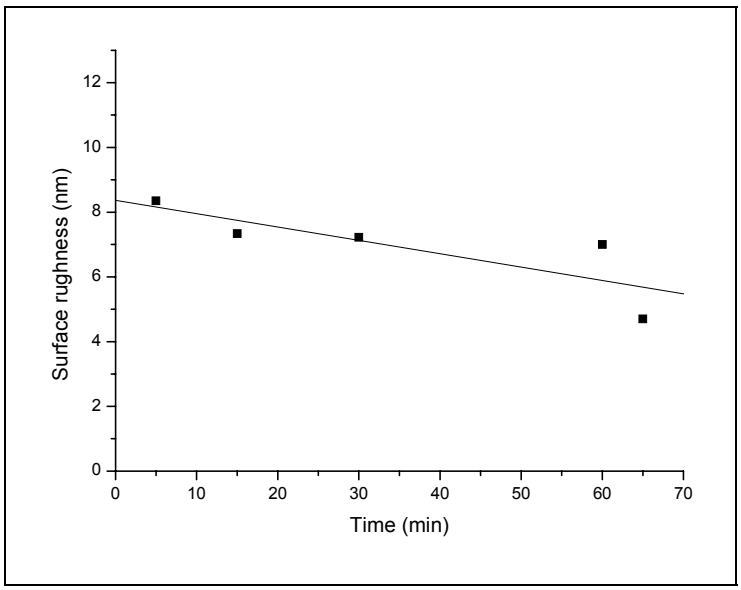

Figure 4.17: Surface roughness (by AFM) evolution vs. time for the 30% microcrystalline wax-containing latex at increased temperature between 24 and 60 ºC.

4.3 References

(1) Tiarks, F.; Landfester, K.; Antonietti, M. *Langmuir* **2001**, *17*, 908-918.

(2) Landfester, K.; Bechthold, N.; Forster, S.; Antonietti, M. *Macromolecular Rapid Communications* **1999**, *20*, 81-84.

(3) Sudol, E.; El-Aasser, M. *Miniemulsion Polymerization*, In *Emulsion Polymerization and Emulsion Polymers*, Lovell, P.; El-Aasser, M., Eds.; John Wiley & Sons Ltd.: New York, 1997; pp 699-722.

(4) van Zyl, A. ; de Wet-Roos, D.; Sanderson, R.; Klumperman, B. *European Polymer Journal* **2004**, *40* (12), 2717-2725.

(5) Ferguson, C.; Russell, G.; Gilbert, R. *Polymer* **2002**, *43*, 6371-6382.

(6) Ferguson, C.; Russell, G.; Gilbert, R. *Polymer* **2003**, *44*, 2607-2619.

(7) van Zyl, A.; Sanderson, R.; de Wet-Roos, D. ; Klumperman, B. *Macromolecules* **2003**, *36* (23), 8621-8629.

(8) Landfester, K. *Macromolecular Symposia* **2000**, *150*, 171-178.

(9) Landfester, K.; Bechthold, N.; Tiark, F.; Antonietti, M. *Macromolecules* **1999**, *32*, 5222-5228.

(10) Chen, Y.; Dimonie, V.; El-Aasser, M. *Macromolecules* **1991**, *24* (13), 3779-3787.

(11) Dimonie, V.; Daniels, E.; Shaffer, O.; El-Aasser, M. *Control of Particle Morphology*, In *Emulsion Polymerization and Emulsion Polymers*, Lovell, P.; El-Aasser, M., Eds.; John Wiley and Sons Ltd.: New York: 1997; pp 293-326.

(12) Kirsch, S.; Doerk, A.; Bartsch, E.; Sillescu, H.; Landfester, K.; Spiess, H.; Maechtle, W. *Macromolecules* **1999**, *32*, 4508-4518.

(13) Kirsch, S.; Landfester, K.; Shaffer, O.; El-Aasser, M. *Acta Polymerica* **1999**, *50*, 347-362.

(14) van Zyl, A.; Bosch, R.; McLeary, J.; Sanderson, R.; Klumperman, B. *Polymer* **2005**, *46*, 3607-3615.

(15) Wang, Y.; Juhue, D.; Winnik, M.; Leung, O.; Goh, M. *Langmuir* **1992**, *8(3)*, 760-762.

(16) Goh, M; Juhue, D.; Leung, O.; Wang, Y.; Winnik, M. *Langmuir* **1993**, *9*, 1319-1322.

(17) Marieta, C.; Remiro, P.; Garmendia, G.; Harismendy, I.; Mondragon, I. *European Polymer Journal* **2003**, *39*, 1965-1973.

(18) Meincken, M.; Sanderson, R. *Polymer* **2002**, *43*, 4947-4955.

(19) Kirsch, S.; Stubbs, J.; Leuninger, J.; Pfau, A.; Sundberg, D. *Journal of Applied Polymer Science* **2004**, *91*, 2610-2623.

(20) Digital Instruments Veeco Metrology Group. *MutiMode™ SPM Instruction Manual Version 4.31ce*. 1996.

(21) Schuler, B.; Baumstark, R.; Kirsch, S.; Pfau, A.; Sandor, M.; Zosel, A. *Progress in Organic Coatings* **2000**, *40*, 139-150.

(22) Sommer, F.; Duc, T.; Pirri, R.; Meunier, G.; Quet, C. *Langmuir* **1995**, *11*, 440-448.

(23) Glinel, K.; Prevot, M.; Krustev, R.; Sukhorukov, G.; Jonas, A.; Hohwald, H. *Langmuir* **2004**, *20*, 4898-4902.

CHAPTER 5

RESULTS AND DISCUSSION: HYDROPHOBICITY AND BARRIER PROPERTIES

5.1 Determination of hydrophobicity and barrier properties

The effects of the following factors on the hydrophobicity and barrier properties of the resultant latex films to water and water vapour were investigated: (i) the amount of surfactant used in the miniemulsion formulation, (ii) the wax/polymer ratio for both waxes, (iii) the amount of Veova-10 monomer, (iv) the molecular weight of the resulting copolymer shell and (v) the degree of crosslinking of the copolymer shell. The results are presented in Sections 5.1.1-5.1.5.

5.1.1 Influence of the amount of surfactant

The effect of surfactant concentration on the hydrophobicity and barrier properties of the final core/shell latex films was investigated. Latices with different SDBS surfactant concentration were prepared. To ensure proper wax encapsulation within the polymeric shell, a small amount of paraffin wax (10 wt% relative to monomer) was used as the core in all formulations.[1] Figure 5.1 shows the monomer conversion of the miniemulsion polymerization of Veova-10 (30 wt%) with MMA (38 wt%) and BA (32 wt%) in the presence of different quantities of SDBS. KPS (0.0133g) was used as the initiator and the polymerization was carried out at 85 ºC. All latices prepared were stable and polymerization reactions proceeded with high final monomer conversions (96-100%).

However, an increase in the rate of polymerization with increasing surfactant concentration was observed. This was attributed to the larger number of monomer droplets present in the miniemulsion[2,3] when a higher amount of surfactant was used.

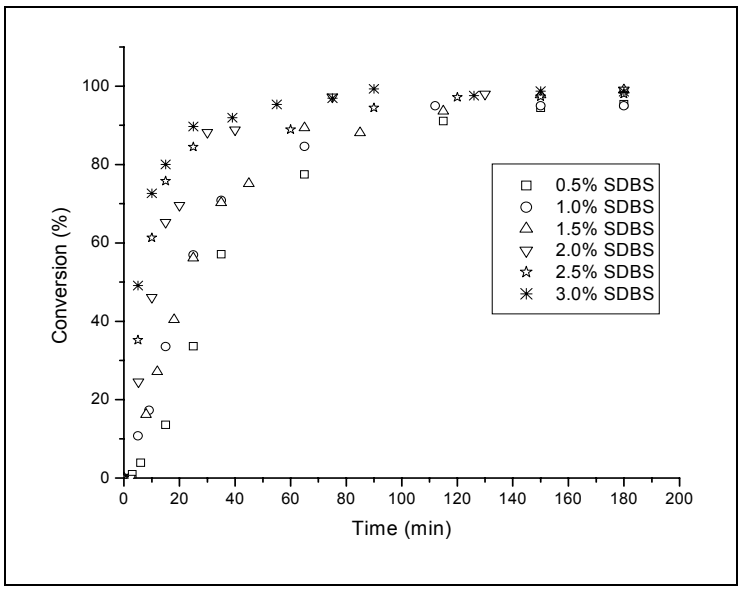

Figure 5.1: Gravimetric conversion curve of the miniemulsion polymerization of Veova-10 (30 wt%) with MMA (38 wt%) and BA (32 wt%) in the presence of 10 wt% paraffin wax using 0.5, 1.0, 1.5, 2.0, 2.5 and 3.0 wt% of SDBS as a surfactant and KPS as the initiator at 85 ºC.

Since monomer droplets are the locus of nucleation in miniemulsion systems,[4] a higher number of monomer droplets resulted in a higher number of particles being formed. Thus shorter reaction times were needed for the latices containing higher surfactant amounts (i.e., 2.5 and 3.0 wt% relative to monomer).[5]

The effect of particle size on the rate of polymerization was in good correspondence with data reported in the literature.[6] Authors, such as Bechthold and Landfester,[3] also found that particle size had a strong effect on the polymerization kinetics of styrene miniemulsion. Their results indicated that the maximum reaction speed shows a strong particle size dependence and is proportional to the particle number: i.e., the smaller the particles, the faster is the reaction.

The explanation of this could be related to the fact that these small submicron monomer droplets, which have large total droplet interfacial surface area, are capable of capturing most of the oligomeric free radicals produced in the aqueous phase, and the droplets become the locus of nucleation. Thus more radicals or oligomeric radicals in the aqueous solution can enter the monomer droplets or the growing polymer particles, leading to a higher polymerization rate.

The effect of particle number on the polymerization rate can also be illustrated by the classical rate equation for emulsion polymerization,[7-10] given as:

$$R_p = \frac{k_P [M]_P \bar{n} N_P}{N_A} \quad \textbf{(5.1)}$$

$$N_P = k' [\mathrm{S}]^{n_s} [I]^{n_i} \quad \textbf{(5.2)}$$

where R_p is the rate of polymerization, k_p is the propagation rate coefficient, $[M]_p$ is the monomer concentration in the particles, $\bar{n}$ is the average number of free radicals per particle, N_p is the number of particles, N_A is Avogadro's number, [S] and [I] are the concentrations of surfactant and initiator, respectively, k' is a constant and n_s and n_i are equal to 0.6 and 0.4 respectively.

In the context of the above discussion, equation 5.1 shows that the number of particles (N_p) contributes to the overall polymerization rate considerably. From equation 5.2 one can also see that a higher surfactant concentration will lead to a greater number of particles present in the polymerization reaction. Therefore a higher polymerization rate is expected when a higher number of particles (stabilized with higher surfactant concentration) is present in the miniemulsion reaction.

The effect of surfactant concentration used in the miniemulsion formulation on the particle size is presented in Table 5.1. This table shows the average particle size of the latices prepared using different quantities of SDBS as the surfactant, and the static contact angle of the films prepared from those latices. The particle size shows a strong dependence on the surfactant concentration, indicating that surfactant concentration played a very important role in determining the size of the latex particles. Particle size decreased from 158 nm for the latex containing 0.5 wt% surfactant to 94 nm for the latex containing 3.0 wt% surfactant. This was attributed to the fact that when increasing surfactant concentration, the latex particle size decreased, since more surfactant molecules are available to stabilize a larger number of smaller monomer droplets. These smaller droplets are produced by the droplet break-up during the sonication step. Droplet break-up is caused by cavitation, which is regarded as a crucial mechanism in ultrasound miniemulsification.[11]

These results agreed well with data reported in the published literature regarding miniemulsion polymerization, by Asua.[12] The effect of surfactant concentration on droplet size in miniemulsions was also described elsewhere.[13-15]

Table 5.1: Average particle size of latices prepared using 0.5, 1.0, 1.5, 2.0, 2.5 and 3.0 wt% of SDBS and the static contact angles (average of 10 measurements) of the films produced from those latices.

Surfactant (wt%)	Average particle size (nm)	Static contact angle (^{o})
3.0	94	100
2.5	95	102
2.0	96	103
1.5	128	105
1.0	152	109
0.5	158	110

Asua[12] showed that surfactant concentration decreases droplet size by influencing droplet coalescence through lowering the contact force between monomer droplets, due to the electrostatic and steric interactions. This leads to a smaller critical droplet size below which coalescence takes place and above which it does not, and hence smaller monomer droplets can be stabilized. Although it was shown that the decrease in the initial droplet size with increasing surfactant concentration is due to a reduction of the coalescence, it was found that the droplet size could not be reduced below a critical size for break-up. It was also argued that the decrease of the droplet size was very pronounced at low surfactant concentrations and reaches a minimum size that cannot be significantly reduced by further increasing the surfactant concentration.

In the present study, it was also found that latices prepared with higher amounts of surfactant were more translucent than latices prepared with lower amounts of surfactant. This was attributed to the decreased particle size when higher amounts of surfactant were used. This was similar to results reported by Antonietti and Landfester,[16] who studied the miniemulsion polymerization of Sty using SDS as the surfactant. They found that the particle size decreased from 180 nm (when 0.3 wt% SDS relative to styrene was used) to 32 nm (when 50 wt% SDS relative to styrene was used). Their results also showed that as the amount of surfactant increased, the latex became more translucent as a result of the decreased particle size. The same results were also observed by van Zyl *et al.*,[17] who studied the role of

surfactant in controlling particle size and stability in the miniemulsion polymerization of polymeric core/shell nanocapsules. Their study revealed that at high surfactant concentration relative to monomer, the miniemulsion was almost translucent, as a result of the presence of small particles with a diameter less than 50 nm. Core/shell nanocapsules with a particle diameter as small as 36 nm could be synthesized by increasing the surfactant concentration from 0.1 to 2% (wt% to aqueous phase).

The effect of different surfactant systems on the water sensitivity of latex films based on poly (butyl acrylate-co-methyl methacrylate) was recently investigated by Butler *et al.*[18] Three different types of surfactant systems (ionic, polymeric, and electrostatic stabilizers) were used. Their results revealed that water sensitivity was found to be strongly dependent on the surfactant system used in the polymer preparation. Many factors, such as the surfactant mobility and compatibility with the latex polymer, latex stability, and surfactant/polymer polarity, appear to affect the water uptake of a film.

In the present study, the effect of surfactant concentration on the hydrophobicity, water uptake and the permeation of moisture vapour through the resultant films was studied. The effect of surfactant concentration on the hydrophobicity of the final films was studied through static contact angle measurements. It was found that the hydrophobicity of the resultant films' surfaces increased significantly with decreasing surfactant concentration. As shown in Table 5.1, static contact angles (θ) varied between $\theta = 100^{o}$ for the film cast from the latex containing 3 wt% surfactant and $\theta = 110^{o}$ for the film made from the latex containing 0.5 wt% surfactant. This clearly indicates that surfactant concentration played a very important role in determining the hydrophobicity of the final polymer films. This was attributed to the fact that surfactant molecules migrate towards the film surfaces during film formation, which results in film with low water contact angle.[19] When less surfactant was used, less surfactant migration could happen, which resulted in a relatively hydrophobic film, whereby a water droplet will remain on its surface with a contact angle higher than 90^{o}.[20]

Similarly, an increase in the water uptake of the films with increasing surfactant concentration was observed. Figure 5.2 shows the water uptake of different films cast from latices that contained different SDBS concentrations. Water uptake of about 42% weight ratio with respect to the film weight was measured for the film made from the latex prepared with 3 wt% SDBS at 23 days, decreasing to about 15% weight ratio for the film made

from the latex that contains 0.5 wt% SDBS. In addition, an abrupt change in the water uptake rates between about 4-5 days was observed for all films.

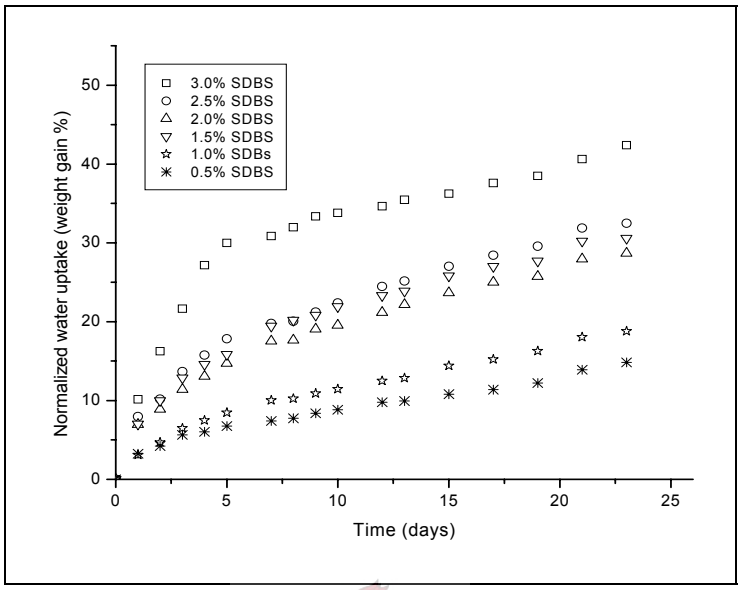

Figure 5.2: Influence of the amount of surfactant - Evolution of the water uptake vs. time.

Similar results were recently reported by Aramendia *et al.*[21] who observed an increase in the water uptake of acrylic films, which resulted from the existence of hydrophilic surfactant domains inside the film. The explanation of this is related to the fact that during film drying, surfactant molecules tend to migrate towards both the film-air interface and the film-substrate interface and concentrate in aggregates,[22] increasing the water affinity and sensitivity of the film.[23] Thus, higher surfactant concentration resulted in films with higher water uptake. The decrease in the hydrophobicity of the films' surface (i.e., low static contact angle values) with increasing surfactant concentration (see Table 5.1) can also explain the fact that higher water uptake was observed when high surfactant amounts were used. This means that the increase of the hydrophobicity of the films' surface (higher static contact angle) with decreasing surfactant concentration in the latices could also be the reason for a decrease in the water uptake of the films.[24]

The migration of surfactants has been observed in several latex systems in which surfactant was exuded to film/air and film/substrate interfaces with passing time. Tzitzinou *et al.*[25] observed a high surfactant concentration present at the air/surface interface of latices based on a copolymer of methyl methacrylate, butyl methacrylate (BMA) and methacrylic acid (MAA).

Zhao *et al.*[26] also reported the exudation of surfactants in poly(butyl methacrylate) latex to film/air and film/substrate interfaces. Exudation of surfactants has also been reported in other polymers such as poly(2-ethyl hexyl methacrylate)[27,28] and in poly(ethyl acrylate-co-methacrylic acid)[29] latices.

In this study, surfactant migration was investigated using conductivity measurements (see Section 3.5). The results showed that surfactant migration increased notably as the concentration of surfactant increased in the latex film. Figure 5.3 shows the evolution of the conductivity of the water in which different films prepared from different latices made with different SDBS concentrations were immersed.

Water conductivity (in which the film was immersed) increased significantly as the amount of surfactant in the film was increased, indicating that more surfactant migration towards the film surfaces was taking place. On immersion into water, the surfactant was washed off, leading to an increase of the conductivity of water in which the film was immersed.

Surfactant concentration was also expected to affect the permeation of water vapour molecules in the final polymer films. It has been reported that when latices are used as film-forming polymers, the surfactant can migrate toward the interfaces, creating a separate phase and entrapped in pockets, which increases penetration of water and in general the water sensitivity of the film.[30,31]

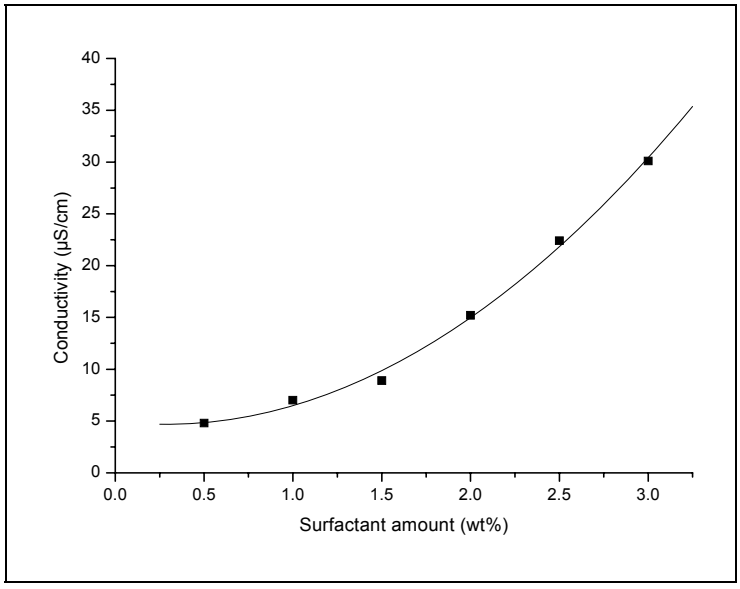

Figure 5.3: Influence of the amount of surfactant - Conductivity vs. surfactant amount used.

In addition, water can diffuse through the polymer or penetrate through defects, pores, or channels present inside the film.[21] While surfactants prevent aggregation of latex particles upon synthesis and storage, their presence in the polymer film (upon the evaporation of the water from the latex) becomes disadvantageous in terms of the barrier properties of the final film. Major drawbacks are the water affinity of the surfactants and their ability to migrate to the surface of the film, leaving behind grooves and pores in the film structure. Therefore a higher surfactant concentration present during the film drying may result in a higher water vapour permeability in the film by creating new paths to water penetration.

Figure 5.4 shows the MVTR values vs. surfactant amount used. MVTR increased considerably with increasing surfactant concentration in the film. MVTR measured about 181 g/m^2/24 h for the film cast from the latex made with 3 wt% surfactant, decreasing to about 130 g/m^2/24 h for the film cast from the latex that contained only 0.5 wt% surfactant. This could be explained by the fact that during film drying surfactants may undergo phase separation, forming lumps, tenths of microns wide, distributed throughout the film, which can extend far down into the film.[32] On exposure to water the surfactant will be partially dissolved in the water and washed out of the film, with the result that deep cavities appear where the lumps had been. Excess surfactant presence during film formation can also result in incomplete film formation and the presence of voids.[30] As a result of these voids, more water vapour molecules can penetrate faster through the film, leading to higher MVTR values, and thus affecting the water resistance properties of the film.

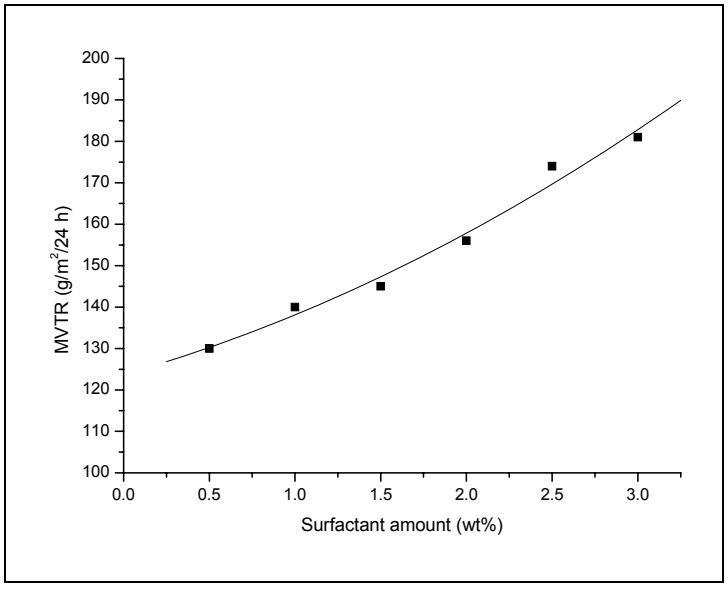

Figure 5.4: Influence of the amount of surfactant - MVTR vs. surfactant amount used.

5.1.2 Influence of the type and amount of wax used

The effect of the type of wax on the hydrophobicity and barrier properties of the final films was studied using two different waxes. For each type of wax, the effect of the wax/polymer ratio on the hydrophobicity and barrier properties was also investigated. Two different types of wax with different hydrophobicity and crystalline content, namely paraffin and microcrystalline waxes, were used (see Section 3.1).

Variation in the ratio of the wax to polymer was expected to have a two-fold effect: (1) encapsulation becomes less favourable with increasing wax/polymer ratio[1] and (2) the hydrophobicity of the resulting polymer films was expected to increase with increasing wax content due to the hydrophobic nature of the wax. In addition, water permeation in the final films was expected to be reduced due to a decrease of both the solubility and diffusion coefficients of water molecules.[33] The highly hydrophobic structure of the wax will result in a major reduction in the solubility coefficient, while the presence of crystalline content introduced by the wax will lead to a large decrease in the diffusion coefficient. Thus water permeation through the film is expected to decrease significantly when using both types of wax.

For comparison, one latex was prepared using hexadecane (3 wt% relative to monomer) instead of wax in order to compare the difference in the hydrophobicity and barrier properties of wax-containing latices and the latex prepared without wax. Hexadecane (bp. 287 ºC) is a very hydrophobic liquid, and is commonly used as a costabilizer or cosurfactant in the miniemulsion formulation.[14]

To decrease the effect of surfactant on the hydrophobicity and barrier properties of the final films, a low amount of SDBS (1 wt% relative to the emulsified phase – wax and monomer) was used as the surfactant. Figures 5.5 and 5.6 show the monomer conversion of the miniemulsion polymerization in the presence of different quantities of paraffin and microcrystalline wax, respectively. All polymerization reactions proceeded with high monomer conversions of ~90-97% and gave stable latices with a low amount of coagulum (< 1% relative to the latex weight). Generally, the rate of polymerization increased with increasing wax content (i.e., shorter reaction time was observed for latices prepared with 40 and 50 wt% of wax relative to monomer). Particle size increased noticeably with

increasing the wax/polymer ratio both for latices containing paraffin and microcrystalline wax (see Table 5.2).

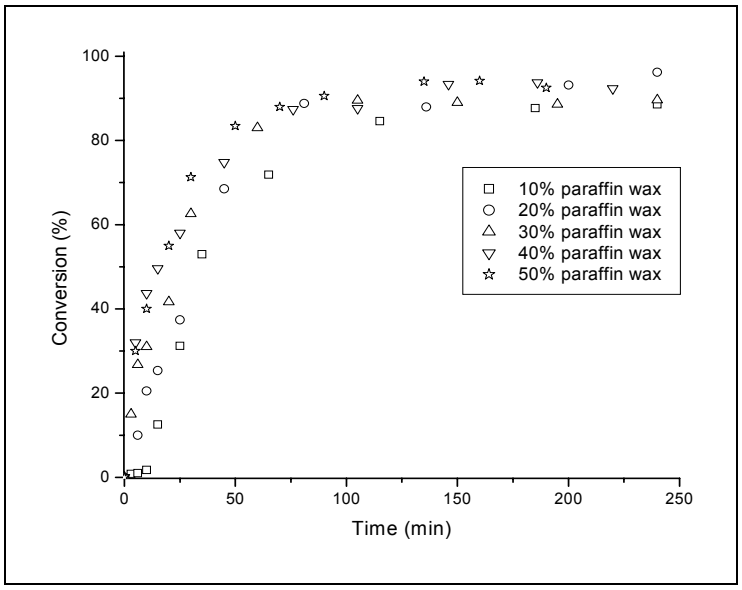

Figure 5.5: Gravimetric conversion curve of the miniemulsion polymerization of Veova-10/MMA/BA in the presence of 10, 20, 30, 40 and 50 wt% paraffin wax using 1.0% of SDBS as a surfactant.

Increasing amounts of wax led to the formation of latices with larger particle sizes. This was in good correspondence with results reported in the literature.[34] It was also noted that latices prepared with lower amounts of waxes are more translucent than latices prepared with higher amounts of wax. This was attributed to the smaller particle size[16,17] produced when low amounts of wax (used as a hydrophobe) were used.

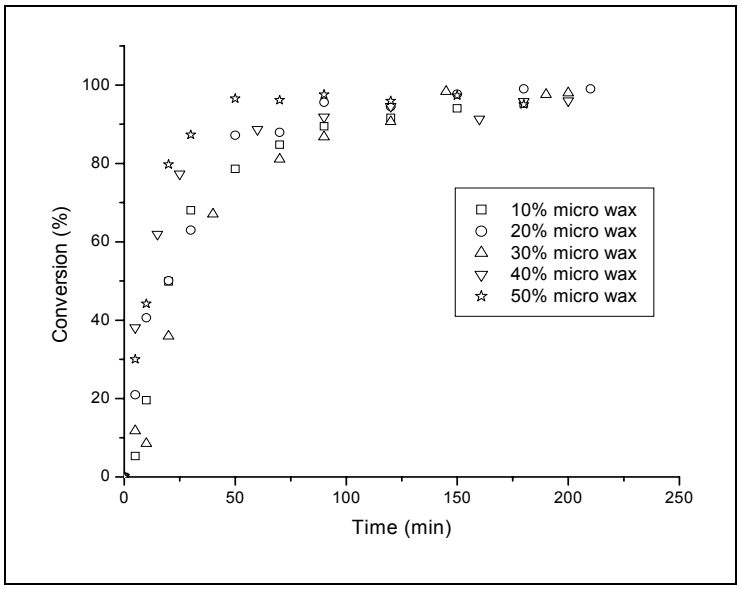

Figure 5.6: Gravimetric conversion curve of the miniemulsion polymerization of Veova-10/MMA/BA in the presence of 10, 20, 30, 40 and 50 wt% of microcrystalline wax using 1.0% of SDBS as a surfactant.

Table 5.2: Average particle size of latices prepared using 10, 20, 30, 40 and 50% of paraffin and microcrystalline wax.

Amount of wax (wt%)	Average particle size of latices made with paraffin wax (nm)	Average particles size of latices made with microcrystalline wax (nm)
10	158	123
20	173	154
30	192	173
40	195	196
50	216	214

The average molecular weights and the polydispersity of the latices made with paraffin wax are listed in Table 5.3. It was noted that the weight average molecular weight ($\overline{M}_w$) and the number average molecular weight ($\overline{M}_n$) increased slightly with increasing wax content. This might be correlated to the fact that the initiation efficiency inside a particle (where exit of one of the pair of radicals is required for a useful initiation event) may be affected by the increased amount of wax in the core. As the amount of wax increases in the core, the shell radius may be decreased noticeably.[34] This will lead to an increased probability of exit of one of a pair of radicals (smaller distance for exiting species to diffuse) from monomer droplets. Therefore, a higher exit rate may result in an effective initiation rate, and shorter chains, due to higher termination rates.

Figure 5.7 shows the SEC results for the latices prepared using 10, 20, 30 and 50% paraffin wax. Another sample in which HD was used instead of paraffin wax is also shown. In each spectrum, the right peak corresponds to Veova-10/MMA/BA copolymer and the left peak is the paraffin wax. The wax peak height corresponded to the amount of wax present in the latex.

Contact angle measurements showed that hydrophobicity of the films' surface was improved significantly by using both paraffin and microcrystalline wax instead of HD in the miniemulsion formulation. Static contact angles (θ) increased from $\theta = 70^{o}$ for the film made from the latex containing 3 wt% HD to $\theta = 105^{o}$ and 104^{o} for the latices containing 10 wt% paraffin and 20 wt% microcrystalline wax, respectively (see Figure 5.8).

Table 5.3: $\overline{M}_n$, $\overline{M}_w$ and polydispersity of the copolymers prepared using different quantities of paraffin wax.

Amount of wax (wt%)	$\overline{M}_n$ (g/mol)	$\overline{M}_w$ (g/mol)	$\overline{M}_w / \overline{M}_n$
10	67500	677000	10.0
20	67700	685000	10.1
30	82000	764000	9.33
50	61400	770000	12.5
0.0 (3 wt% HD)	91000	865000	9.5

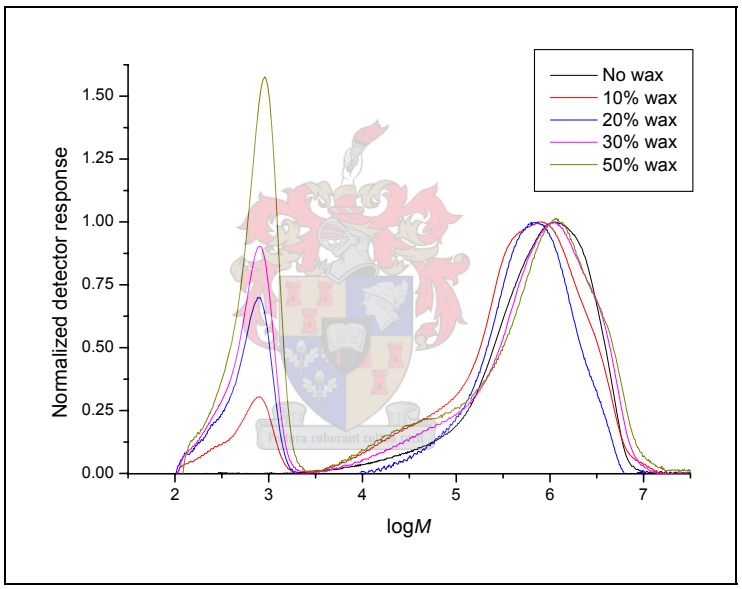

Figure 5.7: SEC chromatograms of copolymers prepared using various amounts of paraffin wax.

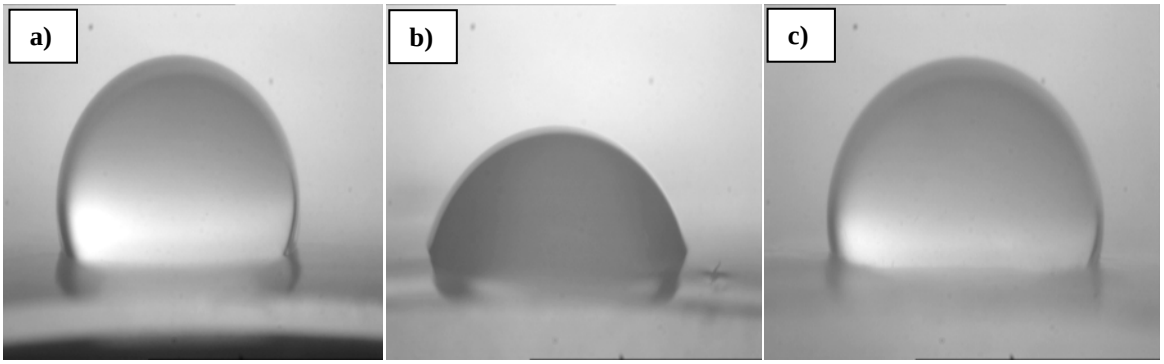

Figure 5.8: Static contact angle of hexadecane (HD) and wax containing latices: a) 10 wt% paraffin wax (contact angle: 105º), b) 3 wt% HD (contact angle: 70º) and c) 20 wt% microcrystalline wax (contact angle: 104º).

Table 5.4: Static contact angles (average of 10 measurements) of the latices prepared using 10, 20, 30, 40 and 50 wt% paraffin and microcrystalline wax.

Amount of wax (wt%)	Contact angle of films that contain different quantities of paraffin wax (º)	Contact angle of films that contain different quantities of microcrystalline wax (º)
10	105	80
20	106	104
30	105	105
40	106	104
50	105	105

However, the hydrophobicity of the films' surface remained largely unaffected by the increased amount of both paraffin and microcrystalline wax (except for 10 wt% microcrystalline wax where the static contact angle of 80º was recorded). Table 5.4 shows the static contact angles of the films prepared using different quantities of paraffin and microcrystalline wax, where static contact angles (θ) between 104° and 106º were recorded for most polymer films. In the case of paraffin wax this was similar to the static contact angle of the pure wax (106º). However, in the case of microcrystalline wax the hydrophobicity of the films' surface was even higher than that of the pure wax (98º). The combination of the hydrophobic nature of the Veova-10 monomer and the presence of microcrystalline wax could explain the relatively higher static contact angle of the films (see Section 5.1.4). The fact that an increasing wax amount had no effect on the static contact angle of the films indicates that a substantial fraction of both waxes (from ~10% for paraffin wax and ~20% for microcrystalline wax) migrated to the films' surfaces. This indicated that surface characteristics were dominated mostly by the wax, leading to similar hydrophobic surfaces with similar contact angle values. This agrees well with AFM results (see Section 4.2.2).

Water uptake measurements also showed that the water uptake of the films decreased noticeably when either paraffin or microcrystalline wax was used instead of HD in the miniemulsion formulation (see Figures 5.9 and 5.10). This is to be expected since wax materials have very hydrophobic structures, that can greatly decrease the water uptake of a permeable material such as paper.[35] Water uptake measured about 30% film weight increase at 23 days for the film containing no wax, decreasing to about 17% and 18% for the films made with 50 wt% paraffin and microcrystalline wax respectively.

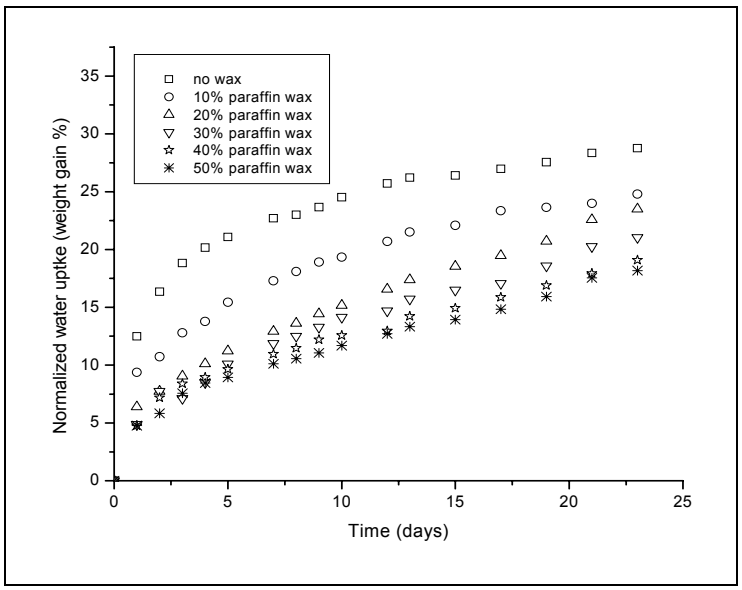

Figure 5.9: Water uptake vs. time of paraffin wax-containing films.

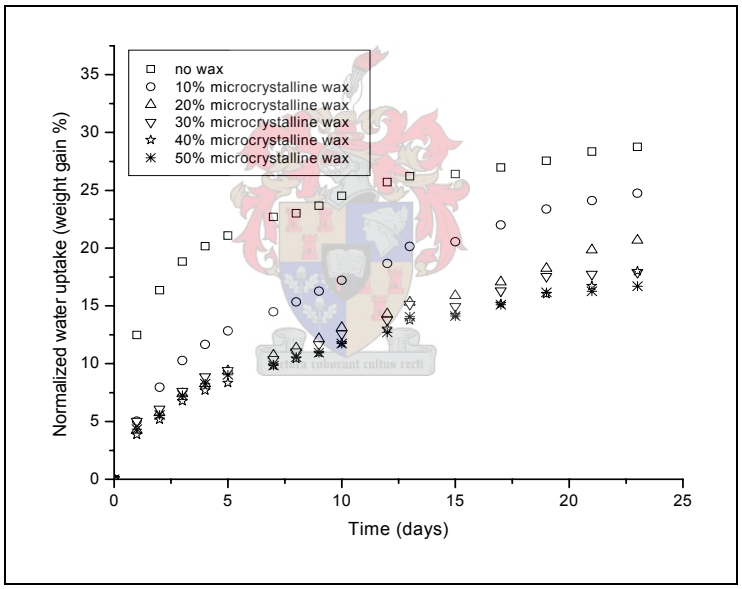

Figure 5.10: Water uptake vs. time of microcrystalline wax-containing films.

In addition, changing the amount of paraffin and microcrystalline wax in the miniemulsion formulation reduced the water uptake of the final films significantly. As seen in Figures 5.9 and Figure 5.10, water uptake measured about 25% weight increase for both films made with 10 wt% paraffin or microcrystalline wax, decreasing to about 18% and 17% weight increase for the films made with 50 wt% paraffin or microcrystalline wax respectively. This was attributed to the high hydrophobicity and crystallinity of paraffin and microcrystalline wax (the static contact angle of paraffin wax is 106º and that of microcrystalline wax is 98º). The presence of a substantial amount of wax (increasing from 10 to 50 wt% relative to

monomer) in the film resulted in a smaller fraction of sites for water absorption, leading to a lower final water uptake.

Figure 5.11 shows the effect of the amount of paraffin and microcrystalline wax on the conductivity of the water in which the films were immersed (DDI water with a conductivity of ~1.4 μS/cm was used). This was used to infer information about surfactant migration towards the film surfaces during the film formation. High surfactant migration will result in a film with high water conductivity (in which the film was immersed). It was found that changing the amount of paraffin and microcrystalline wax in the miniemulsion formulation had two different effects on the conductivity of the water in which the films were immersed.

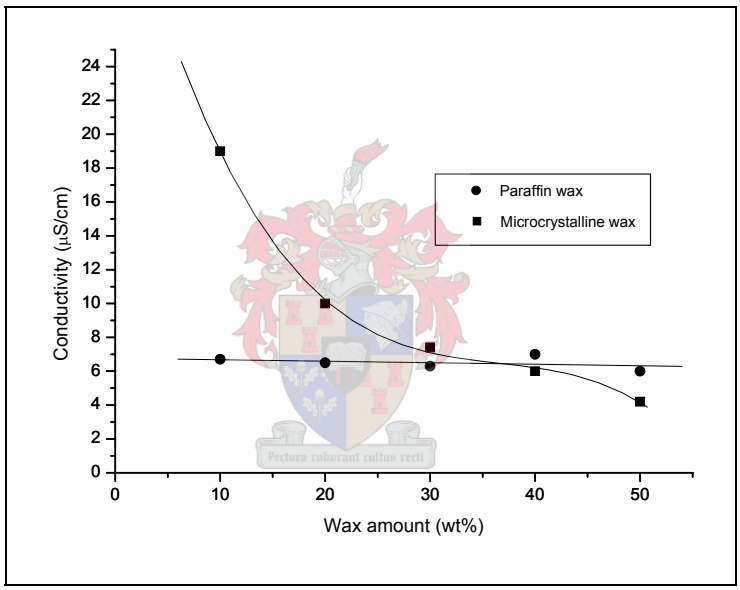

Figure 5.11: Influence of the amount and type of wax - Conductivity vs. wax amount used.

Generally, below 50 wt% paraffin wax, the conductivity (and hence surfactant migration) is less than that of the microcrystalline wax. This was attributed to the high crystalline content in paraffin wax, which contains mainly straight chain n-alkanes.[36] This prevented surfactant molecules from migrating to the films' surface due to the high packing ability, as a result of the high crystallinity of the paraffin wax. On the other hand, water conductivity was independent of the change in the amount of paraffin wax used in the miniemulsion formulation (see Figure 5.11). This can be explained by the fact that for all compositions the film surface properties are dominated by the paraffin wax (see AFM results in Section 4.2.2 and contact angle results in Section 5.1.2), implying that little surfactant is found at the surface and hence similar conductivity values were obtained. Such a migration can be

expected because it leads to an overall reduction in the surface energy of the latex films. This agreed well with data reported in the literature. Using contact angle and electron spectroscopy for chemical analysis (ESCA) measurements, Schuman *et al.*[37] showed that paraffin wax molecules migrated to the surface of films made with styrene-butadiene latices.

In contrast to what was found for paraffin wax, water conductivity decreased significantly with increasing the amount of microcrystalline wax in the film. At a wax content below 40 wt% microcrystalline wax, the conductivity is high, and as the amount of microcrystalline wax increased the conductivity decreased significantly. At 50 wt% microcrystalline wax the conductivity decreased drastically, to below than that of the 50 wt% paraffin wax. This could be attributed to the fact that when microcrystalline wax was used in higher quantities, association (due to its small crystals) with the surfactant would inhibit its migration towards the interface.

Changes in the amount of paraffin and microcrystalline wax were also expected to have a large impact on the water permeation in the final films. Wax has frequently been used to reduce the unwanted penetration of water molecules through permeable material.[38,39] It has also been reported that paraffin wax can be used to efficiently limit the water diffusion in polyelectrolyte multilayers made from poly(allylamine hydrochloride) (PAH) and poly(styrene sulfonate) (PSS).[40] The method consisted of adsorbing wax particles atop the film using electrostatic assembly, followed by the subsequent melting of the particles at a raised temperature. It was found that the wax particles can form a barrier, decreasing water sorption in the films. However, voids or gaps in the adsorbed wax layers still allow some penetration of water molecules into the underlying polyelectrolyte film. It was suggested that in order to achieve complete prevention of water diffusion, fusion of the wax particles into a homogeneous smooth layer is required. Schuman *et al.*[37] also found that the MVTR of a paperboard coated with styrene-butadiene latices was substantially reduced by the addition of a small amount of paraffin wax (5 wt%) to the coating.

In present study, MVTR measurements showed that as the amount of paraffin or microcrystalline wax increased, the permeation of water vapour molecules decreased noticeably as a result of the reduction of the water penetration in the film. However, Figure 5.12 shows that paraffin wax had a bigger impact than the microcrystalline wax on the MVTR values due to the higher hydrophobicity and crystallinity of paraffin wax

(contact angle of paraffin wax: 106º compared to microcrystalline wax: 98º). MVTR measured about 284 g/m^2/24 h for the film that contained 10 wt% paraffin wax, decreasing to 160 g/m^2/24 h for the film that contained 50 wt% paraffin wax. The film containing 10 wt% microcrystalline wax had a MVTR value of about 820 g/m^2/24 h, decreasing to about 620 g/m^2/24 h for the film that contained 50 wt% microcrystalline wax (see Figure 5.12).

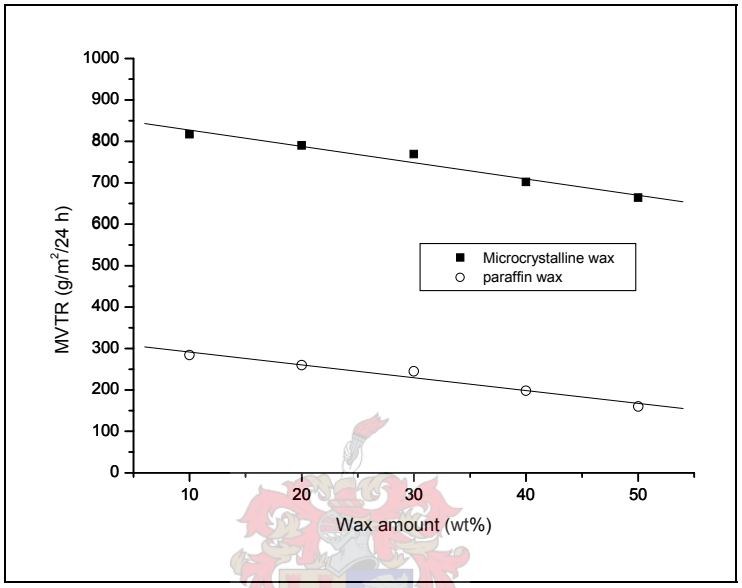

Figure 5.12: Influence of the type and amounts of wax - MVTR vs. wax amount used.

The high hydrophobicity of paraffin wax resulted in lower water solubility in the final film. In addition, the high ability of paraffin wax to crystallize led to lower water diffusion in the film. As a result of the combined effect of the solubility and diffusion coefficients, the MVTR is decreased (as expected from equation 2.2 in Section 2.3.3), thus increasing the final barrier properties of the film.[33]

5.1.3 Influence of the molecular weight of the copolymer shell

The effect of the molecular weight of the polymeric shell on the hydrophobicity and permeation properties of water and water vapour molecules of the resultant films was investigated. Latices containing 10 wt% paraffin wax in the core with different molecular weight copolymer shells were prepared. The copolymer shell was prepared by polymerizing Veova-10 (30 wt%) with MMA (38 wt%) and BA (32 wt%), which gives a copolymer with a T_g of about 8.5 ºC. KPS (0.0133 g) was used as the initiator and the polymerization was carried out at 85 ºC. All latices prepared were stable and polymerization reactions proceeded

with high final monomer conversions (96-100%). Molecular weight was controlled by adding different amounts of transfer agent (1-dodecanethiol) relative to monomer in the miniemulsion formulation. Table 5.5 shows the weight average molecular weight, number average molecular weight and polydispersity of the polymers produced. The SEC chromatograms of copolymers prepared using different quantities of the transfer agent are shown in Figure 5.13.

Table 5.5: Weight average molecular weight, number average molecular weight and polydispersity of the polymers produced by adding different amounts of the transfer agent, 1-dodecanethiol.

Amount of 1-dodecanethiol (wt%)	Paraffin wax (wt%)	$\overline{M}_w$ (g/mol)	$\overline{M}_n$ (g/mol)	Polydispersity ($\overline{M}_w / \overline{M}_n$)
0.05	10	746000	190000	3.96
0.10	10	457000	110000	4.16
0.15	10	260000	106000	2.44
0.20	10	165000	58000	2.90
0.25	10	130000	57000	2.24

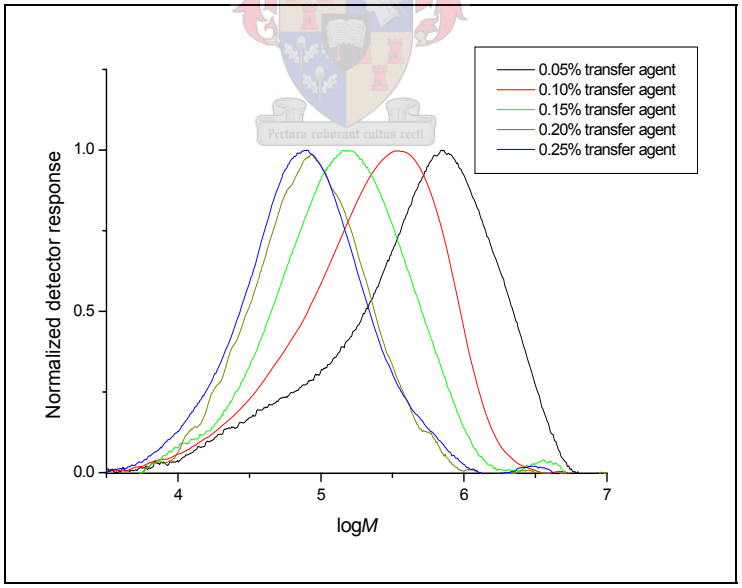

Figure 5.13: SEC chromatograms of copolymers prepared using different quantities of transfer agent (1-dodecanethiol).

Figure 5.14 shows the monomer conversion vs. time of the latices prepared, which was determined gravimetrically. It was found that all polymerization reactions proceeded with high monomer conversion (between 94 to 99%) and a low amount of coagulation (less

than 0.5% relative to latex weight). It was also noted that adding different amounts of transfer agent had no significant effect on the rate of polymerization. Similar polymerization rates were observed for all the polymerization reactions (see Figure 5.14). In addition, particle size was largely unaffected by the presence of transfer agent (see Table 5.6), which explains the fact that similar polymerization rates were observed for all polymerization reactions.

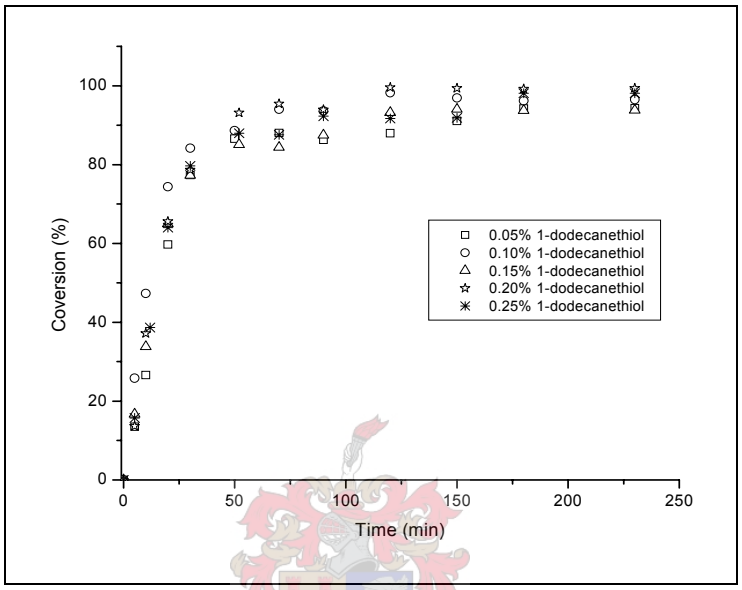

Figure 5.14: Gravimetric conversion curve of the miniemulsion polymerization of Veova-10/MMA/BA in the presence of 0.05, 0.1, 0.15, 0.2 and 0.25% of the transfer agent.

A small difference in terms of the water uptake of the resultant films with changing the molecular weight of the copolymer was noticed. Figure 5.15 shows the effect of molecular weight on the water uptake of the final films produced. Water uptake at 23 days was about 35% weight increase for the film made with relatively low molecular weight copolymer ($\overline{M}_n$ =57000 and $\overline{M}_w$ =130000), decreasing to about 24% weight increase for the film that was made with higher molecular weight copolymer ($\overline{M}_n$ =190000 and $\overline{M}_w$ =746000). The higher molecular weight polymer chains resulted in films with more chain entanglements, leading to lower water uptake values. This could be also due to the fact that less voids are formed when higher molecular weight polymers are used as membranes, leading to films with lower water sensitivity.[41]

Table 5.6 shows the average particle sizes of latices prepared with copolymers of different molecular weights and the static contact angle of the films made from those latices. The hydrophobicity of the surface of the final films remained largely unaffected as the

molecular weight is changed. Contact angles of all the films made with copolymers having different molecular weights varied between 107-109º. This indicates that changing the molecular weight of the copolymer had no significant effect on the hydrophobicity of the films' surface.

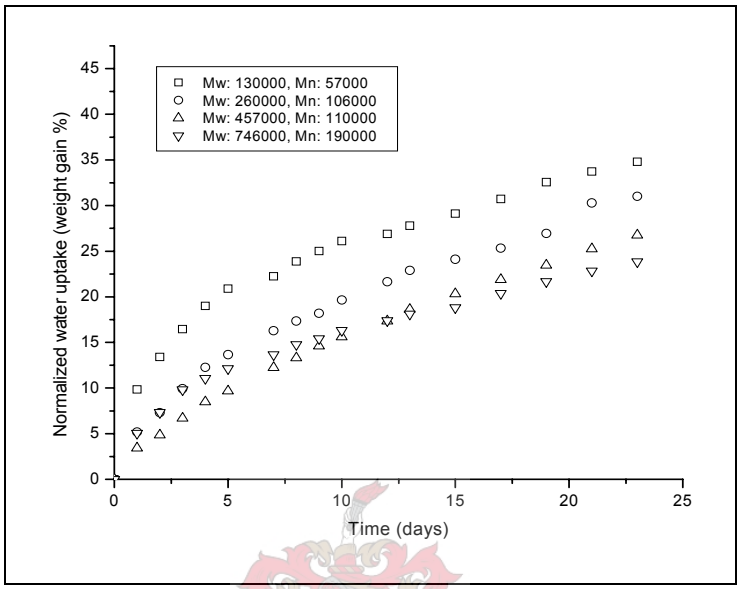

Figure 5.15: Influence of the molecular weight - Water uptake vs. time.

Table 5.6: Average particle size of the latices made with copolymers that have different molecular weight and static contact angle of the films made from those latices.

Paraffin wax (wt%)	**Average particle size (nm)**	$\overline{M}_n$ (g/mol)	$\overline{M}_w$ (g/mol)	**Static contact angle (º)**
10	127	190000	746000	108
10	125	110000	457000	107
10	121	106000	260000	108
10	126	58000	165000	108
10	131	57000	130000	109

The effect of the molecular weight on the migration of surfactant towards the films' surface was also studied. As shown in Figure 5.16, conductivity results showed that changes in the molecular weight had a slight impact on the migration of surfactant towards the film surfaces. Water conductivity (in which polymer films with different molecular weight were immersed) decreased slightly with the increased molecular weight polymer. This can be

attributed to the fact that surfactant migration is less pronounced in films with high molecular weight polymer. This indicates that the higher molecular weight resulted in more chain entanglements, leading to a reduction in the migration of surfactant towards the film surfaces.

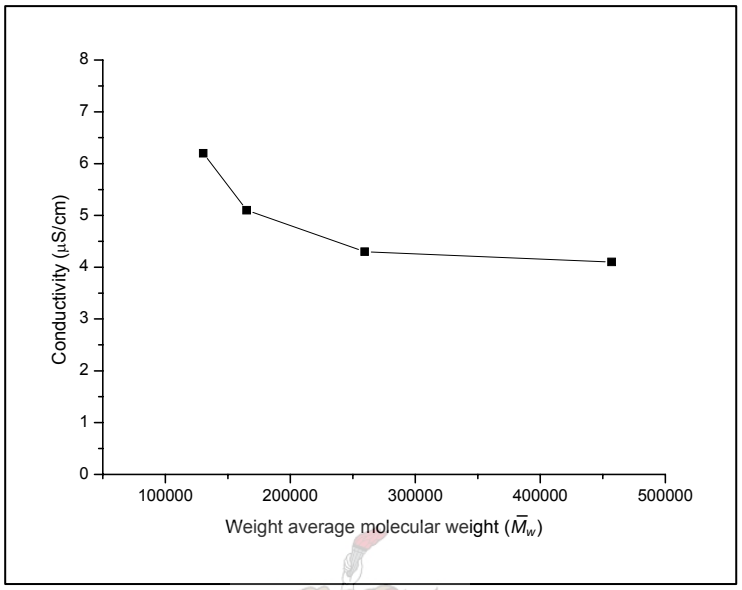

Figure 5.16: Influence of the molecular weight of the copolymer shell-Conductivity vs. molecular weight.

Molecular weight of the polymer was also expected to have a large impact on the permeation of water vapour molecules through the final polymer films. As indicated earlier, the permeation rate of water vapour through polymer membranes is a function of both the solubility of the vapour as well as the rate of diffusion through a polymer. Both diffusion and solubility coefficients are influenced by the interaction between polymer chains, and hence, the molecular weight of the polymer.[42] Longer polymer chains result in greater chain entanglement, reducing the chain mobility, and resulting in reduced diffusion and consequently lower permeability through the polymer.

Figure 5.17 shows the effect of the weight average molecular weight ($\overline{M}_w$) on MVTR values for the copolymer with a T_g of 8.5 ºC. It was found that the MVTR decreased as the chain length of the copolymer increased. This confirms the initial deduction, namely that longer polymer chains result in lower permeability due to chain entanglements.

The molecular weight is also expected to affect the fundamental properties, such as the morphology of the polymeric membranes. Jung *et al.*[41] studied the effect of molecular weight of polymeric additives (poly(vinylpyrrolidone) (PVP)) on morphology and permeation

properties of polyacrylonitrile (PAN) membranes. They found that the top PVP layers are thicker as higher molecular weight PVP is added, thus less voids were formed, leading to lower water permeability. In addition, the molecular weight can affect the free volume of the polymer, which in turn can influence the permeability properties of the polymer.[43] The longer the polymer chains are, the smaller the free volume will be, leading to a tighter polymer structure, thus restricting the permeation of a penetrant.[44]

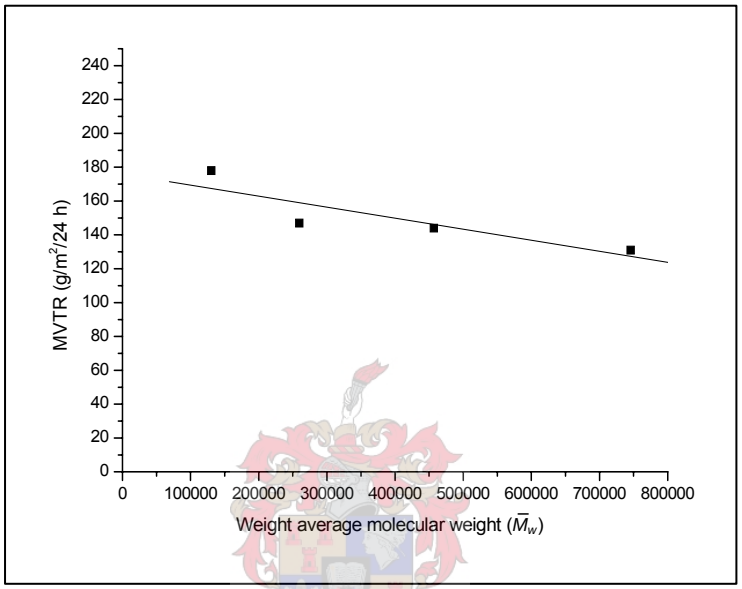

Figure 5.17: Influence of the molecular weight of the copolymer shell - MVTR vs. molecular weight.

5.1.4 Influence of the amount of Veova-10 monomer

It has been reported that Veova monomers can offer a variety of beneficial properties to polymers prepared using these monomers. The inclusion of such monomers in these polymer systems introduces very good alkali resistance, UV resistance and hydrophobicity to the polymer films.[45] In this study, Veova-10 monomer was used to enhance the performance of acrylate polymers in terms of their water resistance. Latices were prepared using 10 wt% of paraffin wax as the core of the particles while the shell was made from the copolymer containing MMA, BA and Veova-10. KPS (0.0133 g) was used as the initiator and the polymerization was carried out at 85 ºC. The amount of Veova-10 monomer was varied from 10, 20, 30, 40, 50 and 60 wt% relative to the total amount of monomers. The ratio of the other two monomers (MMA and BA) was kept constant (1:1) in all experiments. This was done in an attempt to study the effect of Veova-10 monomer (most hydrophobic monomer) on the hydrophobicity and water permeability properties of the resultant films.

Monomer conversion, which was determined by a gravimetric method, is shown in Figure 5.18. All polymerization reactions continued to relatively high monomer conversion, averaging between 84-97%. It was found that the rate of polymerization as well as monomer conversion decreased significantly as the amount of Veova-10 monomer increased. Thus longer reaction times with less monomer conversion were observed when higher amounts of Veova-10 monomer were used. This was attributed to the low water solubility of Veova-10 (7.5×10^{-4} wt%)[46] and its effect on initiation, radical entry and particle formation.

Balic[47] found that these monomers have low polymerization rates and long inhibition periods. He attributed this to the extremely low water-solubility of the monomer in the aqueous phase. The low water-solubility of the monomer retards the formation of oligomeric radicals of sufficient length to enter the polymer particles.

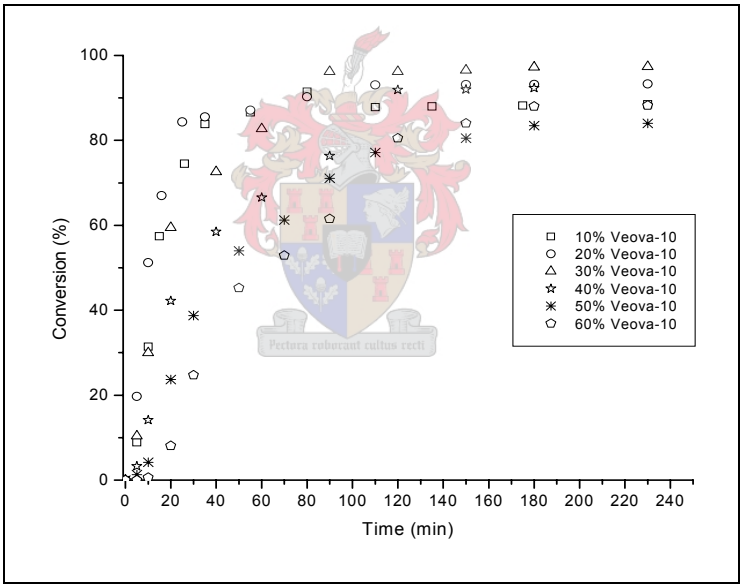

Figure 5.18: Gravimetric conversion curves of the miniemulsion polymerization of different amounts of Veova-10 with MMA-BA in the presence of 10% of paraffin wax.

The effect of Veova-10 monomer on the rate of polymerization can also be due to the differences in the propagation rate coefficients (k_p) of Veova-10 compared to MMA and BA monomers.[48] As seen from Table 5.7, the average sizes of the particles changed slightly when the amount of Veova-10 monomer was increased. This suggests that the rate of polymerization was influenced by the differences in k_p and not particle size.

As expected, the water uptake of the resultant films decreased significantly with increasing amounts of Veova-10 in the copolymers (See Figure 5.19). Independent of the T_g of the copolymer shell, water uptake measured about 52% mass increase at 23 days for the film containing 10 wt% Veova-10, decreasing to about 10% mass increase for the film containing 60 wt% of Veova-10. In addition, as the amount of Veova-10 increased, the rate of water uptake of the films decreased significantly.

Table 5.7: Average particle size of the latices prepared using different amounts of Veova-10 monomer.

Amount of Veova-10 monomer (wt%)	MMA:BA weight ratio (wt%)	Theoretical T_g of the resultant copolymer (°C)	Average particle size (nm)
10	45:45	6.0	122
20	40:40	4.9	123
30	35:35	3.9	127
40	30:30	2.9	124
50	25:25	1.9	135
60	20:20	0.9	135

The positive influence of Veova-10 incorporation into the acrylic copolymers in terms of the water resistance is expected due to the highly branched structure of Veova monomers.[49] Thus a decrease in the water uptake with increasing Veova-10 content is expected due to the increase in the copolymer hydrophobicity by the substitution of Veova-10 for the acrylic monomers.

These results agreed well with the data reported by Slinckx and Scholten,[50] who studied the effect of incorporating Veova-9 monomer into MMA/BA copolymers. A big influence in terms of water resistance of MMA/BA acrylic copolymer films was observed. Their results showed that incorporating Veova-9 into the final copolymers led to a better latex performance in terms of water resistance than that of the conventional MMA/BA copolymer films. Independent of the T_g, the copolymer compositions that were investigated led to a significant improvement in the water resistance and decreased absorption of water in the final films. Water uptake was reduced from 60% (when 0 phm of Veova-9 was used) to about 10% weight ratio (when 60 phm of Veova-9 was used).

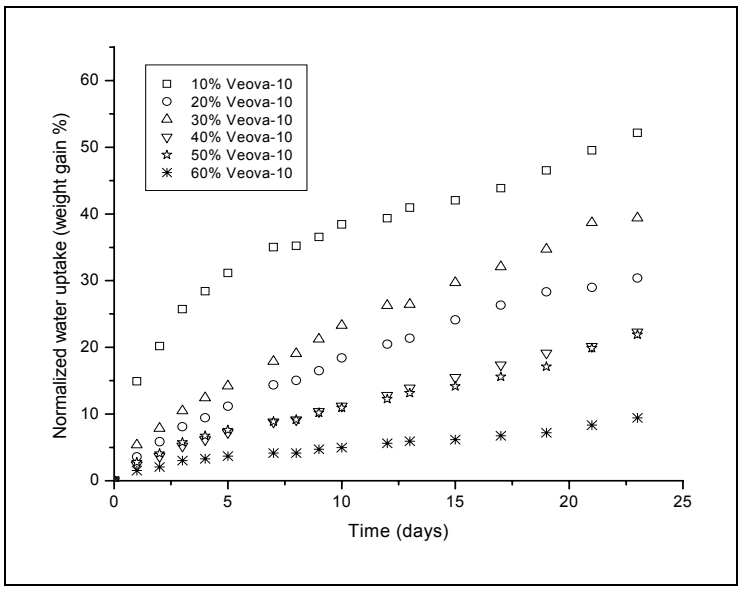

Figure 5.19: Water absorption measured as water uptake vs. time of the films prepared with different amount of Veova-10.

In addition to the improved water resistance, a significant decrease in surfactant migration (obtained from conductivity measurements) with increasing amounts of Veova-10 monomer in the final films also occurred. Water conductivity decreased as the amount of Veova-10 monomer increased in the copolymer (see Figure 5.20). This was attributed to the fact that surfactant migration to the surface was hindered by the increased amount of Veova-10 in the copolymer, leading to better barrier properties of the final films. Veova-10 is a highly branched monomer which can prevent surfactant migration towards the surface of the films.

The effect of Veova-10 monomer on the hydrophobicity of the final polymer films can also be seen from the static contact angle results. Table 5.8 shows the static contact angles of the films made with different Veova-10 amounts. Hydrophobicity of the surface of the films increased slightly with increasing amounts of Veova-10 monomer in the copolymer. A contact angle (θ) of about 106° was recorded for the film that contained 10% Veova-10 while the film containing 60% Veova-10 exhibited a higher contact angle of about 110º.

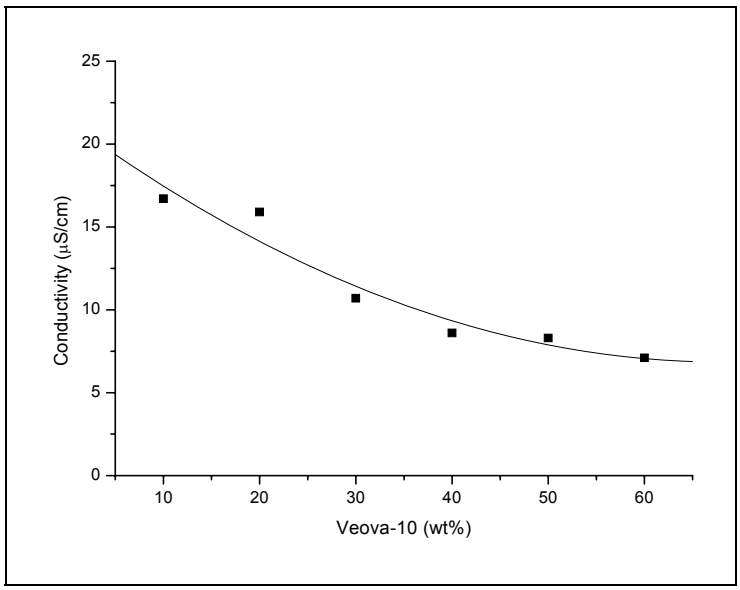

Figure 5.20: Variation of the amount of Veova-10 - Evolution of the conductivity vs. time.

Table 5.8: Static contact angles (average of 10 measurements) of films made with different amounts of Veova-10 monomer.

Veova-10 (wt%)	MMA:BA weight ratio (wt%)	Contact angle (º)
10	45:45	106
20	40:40	108
30	35:35	109
40	30:30	109
50	25:25	109
60	20:20	110

Furthermore, Veova-10 had a big impact on the water vapour permeation in the final films prepared. This is to be expected since this monomer forms polymers which have a branched structure that imparts hydrophobic and steric hindrance effects to reduce the penetration of water molecules between the polymer chains.[51] MVTR results showed that water vapour penetration decreased significantly as the amount of Veova-10 increased (see Figure 5.21).

MVTR measured about 223 g/m^2/24 h for the film made from 10% Veova-10, while another film made with 60% Veova-10 in the copolymer showed an MVTR value of about 147 g/m^2/24 h. The highly hydrophobic structure of Veova-10 monomer resulted in a reduction of the water vapour solubility in the polymer film. In addition, due to the highly branched structure of Veova-10, water diffusion was decreased.

Thus, higher amounts of Veova-10 resulted in lower MVTR values as a result of the combined effect of a reduction of both diffusion and solubility coefficients.[33]

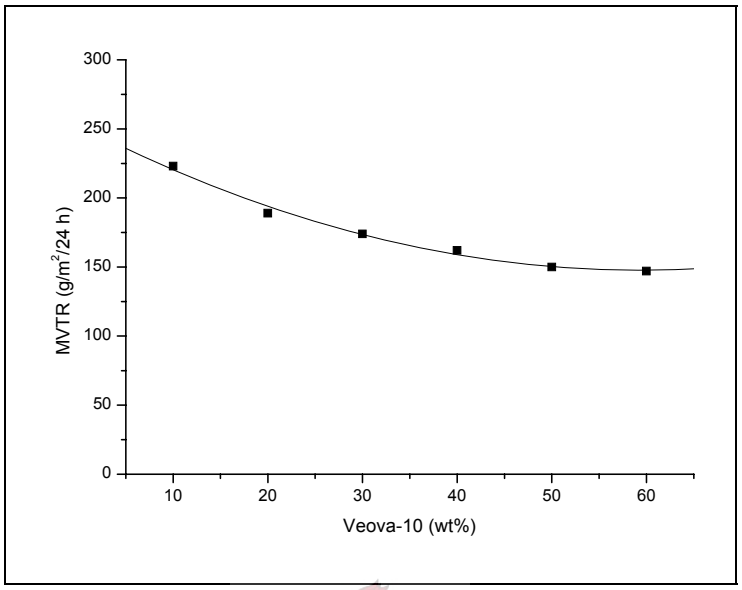

Figure 5.21: Influence of the amount of Veova-10 - MVTR vs. Veova-10 amount (wt%).

5.1.5 Influence of the degree of crosslinking in the copolymer shell

The effect of crosslinking in the polymeric shell on the hydrophobicity and barrier properties of the final films was investigated. Latices with different degrees of crosslinking were prepared. The core of the particles was made from 10 wt% paraffin wax while the shell was mainly made from MMA/BA/Veova-10 copolymer. To obtain different degrees of crosslinking in the copolymer shell, different amounts of a difunctional monomer, EGDMA, were used. Monomer conversion was obtained gravimetrically for all reactions and results are shown in Figure 5.22.

It was found that all polymerizations proceeded to high final monomer conversion (~92-99.5%) and with a low amount of coagulation (<0.5% relative to latex weight). From Figure 5.22 it can be seen that adding different amounts of the crosslinking agent had little effect on the rate of polymerization. In addition, adding the crosslinker had no significant effect on the average particle size of the latices produced (see Table 5.9), which was consistent with the data reported in the literature.[34] As seen in Table 5.9, the hydrophobicity of the films' surfaces remained largely unaffected by increasing the degree of crosslinking in the copolymer shell. Contact angles of 108º-110º were recorded for all polymer films produced.

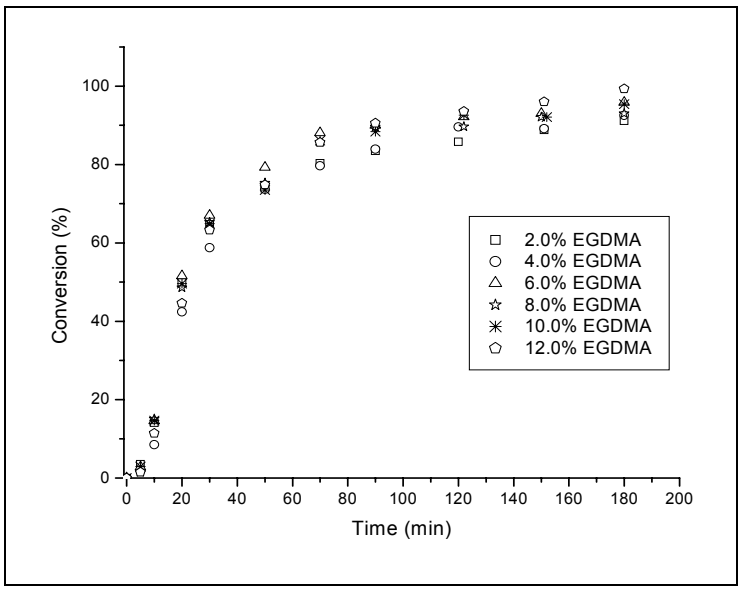

Figure 5.22: Gravimetric conversion curve of the miniemulsion polymerizations of Veova-10 with MMA-BA in the presence of different amounts of EGDMA.

Table 5.9: Averages particle size of latices made from using different amounts of EGDMA and static contact angles (average of 10 measurements) of the films prepared from those latices.

Amount of EGDMA (wt%)	Average particle size (nm)	Contact angle (º)
2	122	109
4	121	109
6	122	108
8	130	111
10	137	110
12	140	110

On the other hand, changing the degree of crosslinking in the copolymer shell significantly affected the water uptake rates of the resultant films. Figure 5.23 shows the water uptake of films made with copolymers that had different degrees of crosslinking. Water uptake decreased from an 18% mass increase to about an 8% mass increase as the degree of crosslinking in the copolymer shell increased from 2% to 12%. It can be also seen that films with higher amounts of crosslinking led to lower water uptake rates, while the films containing a lower degree of crosslinking had higher water uptake rates. This indicates that changes in the degree of crosslinking in the copolymer shell had a significant effect on the water uptake due to a decrease in water diffusion in the final films produced. This agreed

well with data reported by Qiao *et al.*,[51] who studied the effect of crosslinking on the water sensitivity of poly(vinyl acetate) emulsion adhesives. It has been shown that crosslinking the polymer chains internally with monomers which copolymerize with vinyl acetate can form a network in the polymer, resulting in higher molecular weights and improved water resistance of the adhesive films.

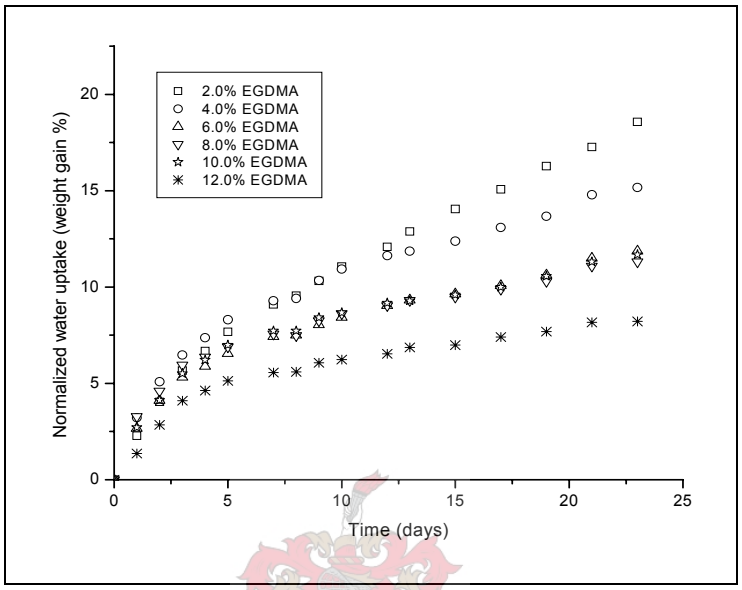

Figure 5.23: Water uptake vs. time for wax-polymer core/shell latex films made with different degrees of crosslinking in the shell.

Crosslinking should generally reduce water permeability in polymers due mainly to a reduction in water diffusivity, however this may not always be the case. In a review article Sangaj and Malshe[52] report that higher amounts of crosslinking should generally be used to decrease water permeability in polymers. They attributed this to the small size of water vapour molecules. Thus a very high degree of crosslinkage is required to reduce their ease of passage between chains. However, higher levels of crosslinking could prevent complete coalescence of particles during film formation,[53] thus channels and voids may be found in the resulting films.

In this study, the MVTR test showed that water vapour permeability increased significantly as the degree of crosslinking in the copolymer increased (see Figure 5.24). This was attributed to the fact that a higher degree of crosslinking resulted in the presence of channels and voids in the final film structure, caused by the improper coalescence of particles during film formation. Thus higher MVTR values and lower barrier properties were observed for latices with higher degrees of crosslinking.

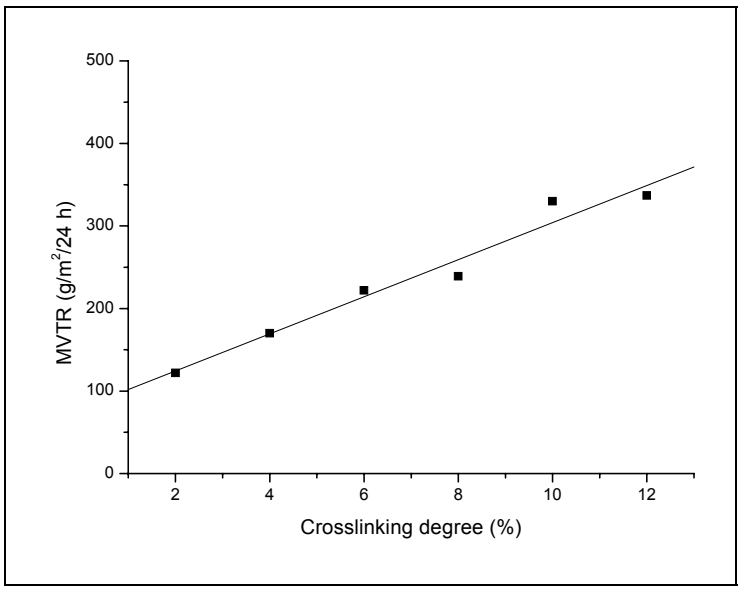

Figure 5.24: Influence of the degree of crosslinking - MVTR vs. degree of crosslinking in the copolymer.

Similarly, an increase in the conductivity of the water in which the films were immersed occurred as the degree of crosslinking increased (see Figure 5.25). This indicated that surfactant migration is more pronounced when high degrees of crosslinking in the polymer films were used. This was also attributed to the fact that as the degree of crosslinking in the copolymer films increased, channels and voids are found, which resulted in a higher migration of surfactant molecules towards the films' surface. On immersion into water, the surfactant is washed out, leading to an increase in the conductivity of the water in which the films were immersed.

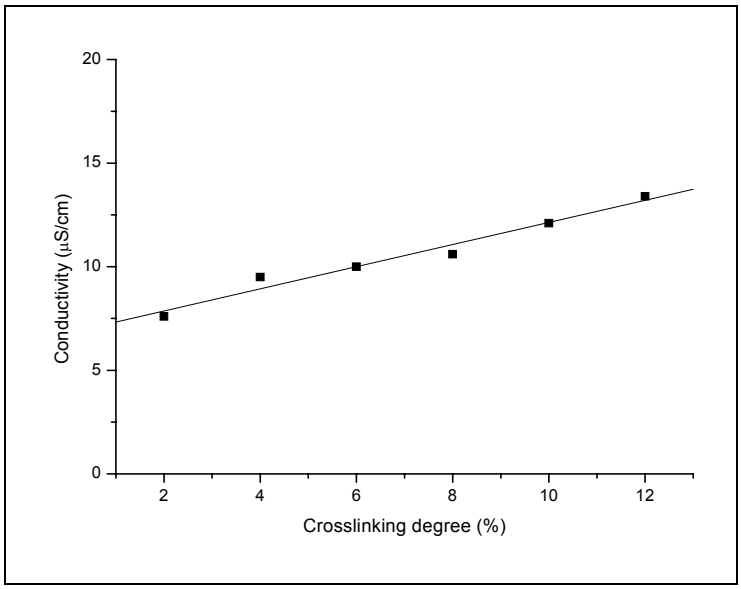

Figure 5.25: Influence of the crosslinking degree on conductivity of water in which the films were immersed.

5.2 References

(1) Luo, Y.; Zhou, X. *Journal of Polymer Science: Part A: Polymer Chemistry* **2004**, *42*, 2145-2154.

(2) Mateo, J.; Cohen, I. *Journal of Polymer Science: Part A* **1964**, *2*, 711-730.

(3) Bechthold, N.; Landfester, K. *Macromolecules* **2000**, *33*, 4682-4689.

(4) Ugelstad, J.; El-Aasser, M.; Vanderhoff, J. *Journal of Polymer Science: Polymer Letters Edition* **1973**, *11*, 503-513.

(5) Lim, M. -S.; Chen, H. *Journal of Polymer Science: Part A: Polymer Chemistry* **2000**, *38*, 1818-1827.

(6) Chern, C. -S.; Liou, Y. -C. *Journal of Polymer Science: Part A: Polymer Chemistry* **1999**, *37*, 2537-2550.

(7) Smith, W.; Ewart, R. *Journal of Chemical Physics* **1948**, *16*, 592-599.

(8) Smith, W. *Journal of the American Chemical Society* **1948**, *70*, 3695-3702.

(9) Smith, W. *Journal of the American Chemical Society* **1949**, *71*, 4077-4082.

(10) Harkins, W. *Journal of the American Chemical Society* **1947**, *69*, 1428-1444.

(11) Behrend, O.; Schubert, K. *Ultrasonics Sonochemistry* **2000**, *7*, 77-85.

(12) Asua, J. *Progress in Polymer Science* **2002**, *27*, 1283-1346.

(13) Chern, C.; Chen, T. *Colloid and Polymer Science* **1997**, *275*, 546 - 554

(14) Lim, M.; Chen, H. *Journal of Polymer Science: Part A: Polymer Chemistry* **2000**, *38*, 1818-1827.

(15) Miller, C.; Venkatesan, J.; Silebi, C.; Sudol, E.; El-Aasser, M. *Journal of Colloid and Interface Science* **1994**, *162*, 11-18.

(16) Antonietti, M.; Landfester, K. *Progress in Polymer Science* **2002**, *27*, 689-757.

(17) van Zyl, A. ; de Wet-Roos, D.; Sanderson, R.; Klumperman, B. *European Polymer Journal* **2004**, *40* (12), 2717-2725.

(18) Butler, L.; Fellows, C.; Gilbert, R. *Journal of Applied Polymer Science* **2004**, *92*, 1813-1823.

(19) Wang, X.; Sudol, E.; El-Aasser, M. *Journal of Polymer Science: Part A: Polymer Chemistry* **2001**, *39*, 3093-3105.

(20) Adamson, A. *Physical Chemistry of Surfaces*. John Wiley & Sons, Inc.: New York, 1982; pp 433-460.

(21) Aramendia, E.; Barandiaran, M.; Grade, J.; Blease, T.; Asua, J. *Langmuir* **2005**, *21*, 1428-1435.

(22) Roulstone, B.; Wilkinson, M.; Hearn, J. *Polymer International* **1992**, *27*, 43-50.

(23) Amalvy, J.; Unzue, M.; Schoonbrood, H.; Asua, J. *Journal of Polymer Science: Part A: Polymer Chemistry* **2002**, *40*, 2994-3000.

(24) Butler, L.; Fellows, C.; Gilbert, R. *Industrial & Engineering Chemistry Research* **2003**, *42*, 456-464.

(25) Tzitzinou, A.; Jenneson, P.; Clough, A.; Keddie, J.; Lu, J.; Zhdan; Treacher, K.; Satguru, R. *Porogress in Organic Coatings* **1999**, *35*, 89-99.

(26) Zhao, C.; Holl, Y.; Pith, T.; Lambla, M. *Colloid & Polymer Science* **1987**, *265*, 823-829.

(27) Kientz, E.; Holl, Y. *Colloids and Surfaces A: Physicochemical and Engineering Aspects* **1993**, *78*, 255-270.

(28) Kientz, E.; Dobler, F.; Holl, Y. *Polymer International* **1994**, *34*, 125-134.

(29) Evanson, K.; Thorstenson, T.; Urban, M. *Journal of Applied Polymer Science* **1991**, *42*, 2297.

(30) Keddie, J. *Materials Science and Engineering* **1997**, *21*, 101-170.

(31) Juhue, D.; Lang, J. *Colloids and Surfaces A: Physicochemical and Engineering Aspects* **1994**, *87*, 177.

(32) Holmberg, K.; Jonsson, B.; Kronberg, B.; Lindman, B. *Surfactants and Polymers in Aqueous Solution*. Second ed.; John Wiley & Sons Ltd.: England, 2003; pp 227-259.

(33) Delassus, P. *Barrier Polymers*, In *The Wiley Encyclopedia of Packaging Technology*, Brody, A.; Marsh, K., Eds.; John Wiley & Sons, Inc.: New York, 1997; pp 71-77.

(34) Tiarks, F.; Landfester, K.; Antonietti, M. *Langmuir* **2001**, *17*, 908-918.

(35) Despond, S.; Espuche, E.; Cartier, N.; Domard, A. *Journal of Applied Polymer Science* **2005**, *98*, 704-710.

(36) Stauffer, T.; Venditti, R.; Gilbert, R.; Kadla, J. *Journal of Applied Polymer Science* **2002**, *83*, 2699-2704.

(37) Schuman, T.; Wikstrom, M.; Rigdahl, M. *Progress in Organic Coatings* **2004**, *51*, 228-237.

(38) Hagenmaier, R.; Baker, R. *Journal of Agricultural and Food Chemistry* **1994**, *42*, 899-902.

(39) Hagenmaier, R.; Shaw, P. *Journal of Agricultural and Food Chemistry* **1991**, *39*, 1705-1708.

(40) Glinel, K.; Prevot, M.; Krustev, R.; Sukhorukov, G.; Jonas, A.; Hohwald, H. *Langmuir* **2004**, *20*, 4898-4902.

(41) Jung, B.; Yoon, J.; Kim, B.; Rhee, H. -W. *Journal of Membrane Science* **2004**, *243*, 45-57.

(42) Mills, N. *Plastics Microstructure Properties and Applications*. Edward Arnold: 1986; pp 225-226.

(43) Mondal, S.; Hu, J.; Yong, Z. *Journal of Membrane Science* **2006**, *280*, 427-432.

(44) Lee, W. *Polymer Engineering and Science* **1980**, *20*, 65-69.

(45) Vandezande, G.; Smith, O.; Bassett, D. *Vinyl Acetate Polymerization*, In *Emulsion Polymerization and Emulsion Polymers*, Lovell, P.; El-Aasser, M., Eds.; John Wiley & Sons Ltd.: New York, 1997; pp 593-587.

(46) Wu, X.; Hong, X.; Cordeiro, C.; Schork, F. *Journal of Applied Polymer Science* **2002**, *85*, 2219-2229.

(47) Balic, R. PhD thesis, University of Sydney: Sydney, Australia, 2000.

(48) Brink, M.; Papers, M.; Herk, A.; German, A. *Polymer Reaction Engineering* **2001**, *9* (2), 101-133.

(49) Bassett, D. *Journal of Coatings Technology* **2001**, *73*, 42-55.

(50) Slinckx, M.; Scholten, H. *Surface Coatings International* **1994** *77* (3), 107-112.

(51) Qiao, L.; Easteal, A.; Bolt, C.; Coveny, P.; Franich, R. *Pigment and Resin Technology* **2000**, *29* (3), 152-158.

(52) Sangaj, N.; Malshe, V. *Progress in Organic Coatings* **2004**, *50*, 28-39.

(53) Zosel, A.; Ley, G. *Macromolecules* **1993**, *26*, 2222-2227.

CHAPTER 6

CONCLUSIONS AND RECOMMENDATIONS

6.1 Conclusions

The overall objective of this research was to prepare hydrophobic core/shell latex particles using different materials, including an oil (HD) and two different waxes (paraffin and microcrystalline wax) as the core of the particles, for use in barrier coatings. Latex particles with the desired core/shell morphology were successfully synthesized using a miniemulsion process as a one-step nanoencapsulation technique. Particles with liquid (formed by the oil HD) or hard (formed by the wax) cores were prepared. The shell of the particles was mainly made from three relatively hydrophobic monomers, namely MMA, BA and Veova-10.

Particle morphology was determined using two different methods: TEM and AFM. TEM was used to directly visualize the particles at the nanometer level to obtain their particle morphology and size. Particle size was also measured using a dynamic light scattering technique, the results of which showed good agreement with TEM results. AFM was used to monitor the drying and film formation process of the synthesized core/shell latices. Results showed that AFM is a powerful tool to study the film formation behaviour of core/shell latices, revealing their particle morphology and gave an idea of how rough or smooth the resultant films were.

A second objective of the study was to investigate the effect of different factors on the hydrophobicity and barrier properties of the resulting films obtained from the synthesized core/shell latices to water and water vapour molecules. This included investigating the effect of (i) the amount of surfactant used in the miniemulsion formulation, (ii) the wax/polymer ratio for both waxes, (iii) the amount of Veova-10 monomer (the most hydrophobic monomer used), (iv) the molecular weight of the resulting copolymer shell and (v) the degree of crosslinking of the copolymer shell.

Results showed that all the above-mentioned factors had a big influence on the hydrophobicity and barrier properties of the final latex films produced from the synthesized core/shell latices to water and water vapour.

It was found that water sensitivity of the final films is greatly affected by the amount of surfactant used in the miniemulsion formulation. An increase in the surfactant concentration led to a significant decrease in the barrier properties of the final films prepared. Higher water uptake and MVTR values were observed when high amounts of surfactant were used. Hydrophobicity of the films' surface was also decreased as the surfactant concentration increased, which was mainly due to the migration of surfactant molecules towards the film-air interface. Surfactant migration was confirmed using conductivity measurements. In addition, by changing the surfactant concentration it was possible to synthesize a wide variety of particle sizes. Core/shell particles with a particle size of 94 nm could be synthesized by increasing the surfactant concentration from 0.5% to 3.0% (wt% to the monomer).

It was also shown that the presence of wax materials as the cosurfactant in the miniemulsion polymerization of MMA, BA and Veova-10 monomers, could significantly improve the hydrophobicity and barrier properties of the resulting films in comparison to films containing the standard cosurfactant (HD). Hydrophobicity and barrier properties of the final films increased dramatically when the wax materials were used instead of HD in the miniemulsion formulation. Relatively small amounts of wax (~10-20 wt% relative to monomer) were sufficient to induce a significant increase in the overall hydrophobicity of the latex films' surface. However, the hydrophobicity of the films' surface remained largely unaffected by the increased amount of both paraffin and microcrystalline wax. Similar contact angle values were recorded for all latex films that were prepared with different amounts of wax (ranging from 10-50 wt% relative to monomer).

In contrast, the amount and type of wax used in the miniemulsion formulation was found to affect the affinity and barrier properties of the resultant films to water and water vapour molecules. Water uptake of the final films decreased considerably as the amount of both paraffin and microcrystalline wax was increased in the miniemulsion formulations. This was due to the highly hydrophobic nature of the waxes.

MVTR also decreased as the amount of both paraffin and microcrystalline wax increased. However, paraffin wax led to films with lower MVTR values than films made with microcrystalline wax. This was due to the fact that paraffin wax has a higher hydrophobicity and crystalline content than microcrystalline wax.

It was also found that changing the molecular weight of the copolymer shell had no significant effect on the hydrophobicity of the films' surface. However, water sensitivity (measured as water uptake and MVTR) was considerably affected by changing the molecular weight of the shell. It was found that water uptake decreased as the molecular weight of the copolymer shell increased. In addition, MVTR decreased as the molecular weight increased. This was attributed to the effect of molecular weight on the chain entanglement and free volume of the polymer chains.

Changing the amount of the most hydrophobic monomer used in the miniemulsion formulation (Veova-10) had a significant effect on the hydrophobicity and barrier properties of the final films. Increasing the amount of Veova-10 monomer led to an increase in the hydrophobicity and barrier properties of the resultant films. Higher contact angles and low MVTR values were observed when higher amounts of Veova-10 were used.

Changing the degree of crosslinking in the shell had no effect on the hydrophobicity of the films' surfaces. On the other hand, water uptake was slightly decreased as the degree of crosslinking increased. Increasing the degree of crosslinking in the copolymer shell was expected to increase the barrier properties of the resultant films. However, MVTR values of the final films were increased significantly (low water sensitivity) when the degree of crosslinking was increased. This was attributed to the fact that a higher degree of crosslinking resulted in the presence of channels and voids in the final film structure, caused by the improper coalescence of particles during film formation. Thus higher MVTR values and lower barrier properties were observed for latices with higher degrees of crosslinking.

6.2 Recommendations for future work

As mentioned in Chapter 2, many different high shear dispersion devices such as sonifiers and high-pressure homogenizers can be used for a miniemulsification process. In this study, the initial dispersion of the hydrophobic components was established by ultrasonication of the latex sample. This led to the formation of latex particles with the desired core/shell morphology. However, this is usually associated with some disadvantages, such as excessive heat generated during sonication and limited latex sample quantities with broad polydispersities can be obtained. Future work could focus on the use of high-pressure homogenizers such as a Microfluidizer, where larger latex sample quantities with narrow polydispersities can be easily handled without heat build-up.[1]

Other factors such as the effect of T_g on the permeation properties to water and water vapour molecules of the final core/shell latex films should also be investigated. Furthermore, sorption equipments such as dynamic mass sorption can be used to determine the absorption isotherms and kinetic data of the synthesized core/shell latices. These isotherms can be classified into different types according to the porosity of the film and the interaction between the polymer films and the penetrant, such as water and water vapour molecules.[2] This will give more information to explain the permeation properties of the resultant polymer films to water and water vapour.

Pectora roborant cultus recti

6.3 References

(1) Tang, P.; Sudol, E.; Silebi, C.; El-Aasser, M. *Journal of Applied Polymer Science* **1991**, *43*, 1059-1066.

(2) Comyn, J. *Polymer permeability*. Elsevier Applied Science Publishers Ltd.: 1986.

Appendix 1: Typical DSC scans for paraffin and microcrystalline waxes

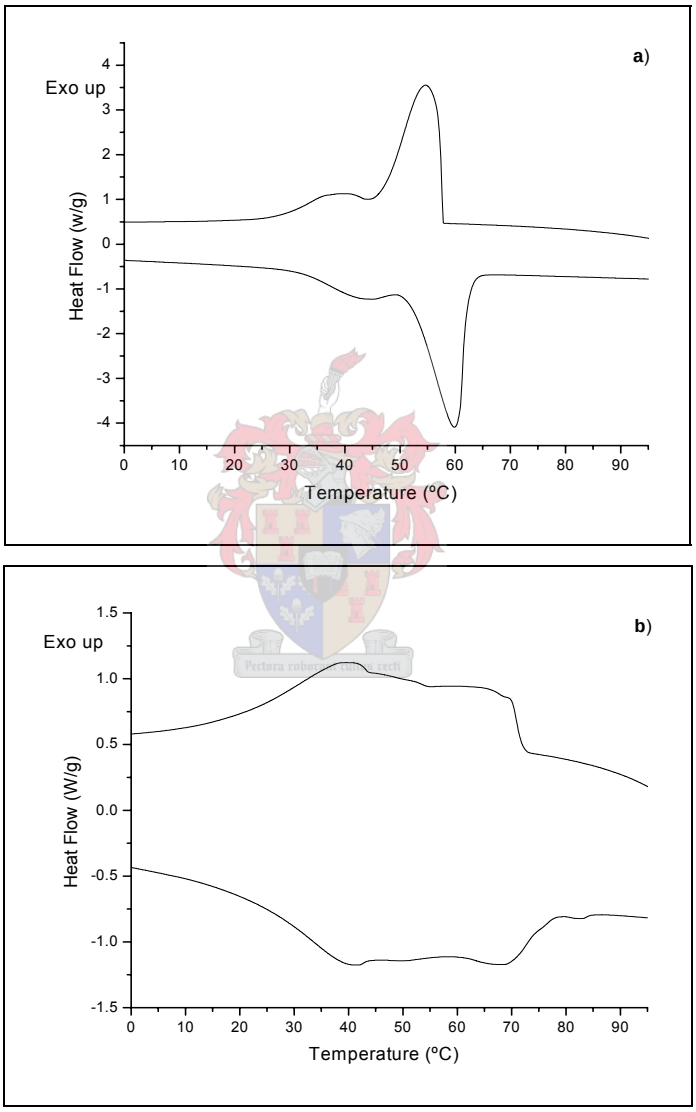

Figure A.1: DSC thermographs for a) paraffin wax and b) microcrystalline wax.

Appendix 2: Moisture vapour transmission rate (MVTR) test

The MVTR test is used to determine the amount of moisture vapour that passes through a standard paperboard in 24 h under specified conditions of temperature and relative humidity.

Apparatus:

- Humidity cabinet set at 30 ºC and 90% relative humidity.
- Moisture resistant glass vessel of 84 mm diameter, open at the top, and equipped with a screw-on open lid with a rubber seal.
- A balance (accurate to two decimal places).
- Silica gel with a colour indicator.

Procedure:

- Silica gel was dried in an oven at 110 ºC for 2 h.
- 100 g of the dried silica gel was added to the glass vessel.
- A round disc sample was cut and fitted in the lid of the vessel.
- The lid with the sample was screwed onto the vessel.
- The vessel was weighed and the weight was recorded (A).
- The sample was left in the humidity cabinet for 24 h at 30 ºC and 90% relative humidity.
- The vessel was weighed again after 24 h and the weight was recorded (B).
- The open area of the vessel was calculated in m^2.
- The MVTR was calculated by means of the following equation:

$$MVTR = \frac{B - A}{Area}$$

MVTR: Moisture vapour transmission rate ($g/m^2/24$ h)

A: Weight of jar prior 24 h exposure (g)

B: Weight of jar after 24 h exposure (g)

Area: Area of the circle (m^2)

Appendix 3: Glass transition temperature of the synthesized MMA/BA/Veova-10 copolymer obtained by DMA

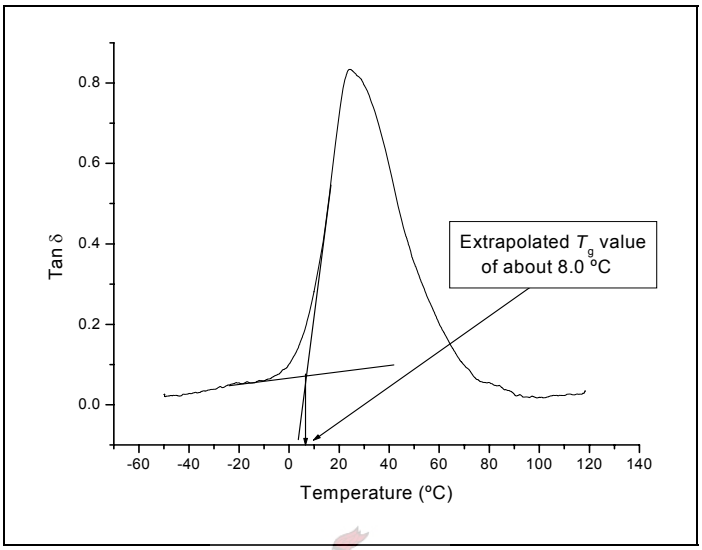

Figure A.3: Tan δ vs. temperature curve of the synthesized MMA/BA/Veova-10 copolymer.